UNIVERSITY OF SOUTHAMPTON

Faculty of Natural and Environmental Sciences

School of Chemistry

The Role of Colloidal phase in the Measurement of Pollutants in Natural Waters

by

Natthakarn Ketkoom

Thesis for the degree of Doctor of Philosophy

October 2011

UNIVERSITY OF SOUTHAMPTON

ABSTRACT

FACULTY OF NATURAL AND ENVIRONMENTAL SCIENCES

SCHOOL OF CHEMISTRY

Doctor of Philosophy

THE ROLE OF COLLOIDAL PHASE IN THE MEASUREMENT OF POLLUTANTS IN NATURAL WATERS

BY Natthakarn Ketkoom

The components of natural water can be divided into three categories: dissolved, colloidal and particulate phases. The colloids are small particles with at least one dimension between 1.0 nm and 1.0 μm (IUPAC); they do not sediment when suspended in "solution". The small size of colloidal particles causes this fraction to have a large surface area with potential to bind significant amounts of trace metals and organic pollutants and also allows colloids to migrate over long distances potentially increasing the spread of the contaminants.

To better understand the behaviour of colloidal matter in natural waters, engineered spherical silica colloids of known size were made and chemically labelled so that the colloids can be sensitively tracked through the fractionation process of analytical filtration. The labels used to date have included the toxic metalloid arsenic and the fluorescent compound Rhodamine B, which had also been used to improve sensitivity.

The behaviour of engineered labelled colloidal sols has been investigated during the preliminary filtration study in the laboratory. Artificial colloidal sols of the silicas in water were investigated to see how their filtration, employing a sequential filtration of a water sample through 1.6 (or 8 μm) and 0.1 μm cut-off filters, influenced a measurement of arsenic. The content of the filters after filtration were investigated by scanning electron microscopy and analysed for arsenic using atomic absorption spectroscopy. *Ca.* 50% and 65% of the silica particles were found on the large pore filters (1.6 μm and 8.0 μm filter), providing evidence of the aggregation and clogging effects on the fibre filter.

The analysis of the Tamar estuary water samples revealed substantial amounts of arsenic, attributed to drainage from mining activities. Colloidal arsenic was found along with dissolved and particulate arsenic in freshwater. However, the saline water samples showed the arsenic content to be distributed mainly in the particulate and dissolved fractions. A suggested explanation of this phenomenon is that aggregation of colloids took place in the presence of saline water and therefore most of the colloidal arsenic was collected with the particulate fraction. Finally, a study of Southampton Water and Dart waters was performed by adding engineered colloidal particles to explore the aggregation of colloids in water of different salinity. Unfortunately, experimental problems prevented a definite verification of the influence of salinity in this case.

Contents

List of figures

Section **Page number**

Chapter 3

Section **Page number**

Chapter 4

Section **Page number**

List of tables

DECLARATION OF AUTHORSHIP

I, Natthakarn Ketkoom

declare that the thesis entitled

The role of colloidal phase in the measurement of pollutants in natural waters

and the work presented in the thesis are both my own, and have been generated by me as the result of my own original research. I confirm that:

- this work was done wholly or mainly while in candidature for a research degree at this University;
- where any part of this thesis has previously been submitted for a degree or any other qualification at this University or any other institution, this has been clearly stated;
- where I have consulted the published work of others, this is always clearly attributed;
- where I have quoted from the work of others, the source is always given. With the exception of such quotations, this thesis is entirely my own work;
- I have acknowledged all main sources of help;
- where the thesis is based on work done by myself jointly with others, I have made clear exactly what was done by others and what I have contributed myself;
- none of this work has been published before submission, or [delete as appropriate] parts of this work have been published as: [please list references]

Signed: ……..

Date:…….

Acknowledgements

Many people have been a part of my Ph.D. study, as friends, teachers, and colleagues. Dr. Alan G Howard, first and foremost, has been one of these. He is actively involved in the work of all his students, and clearly always has their best interest in mind. Thank you for pushing me. Thanks especially to Prof. John Owen for acting as my observational advisor, I am also thankful to him for reading my reports, commenting on my views and helping me understand and enrich my ideas. I also wish to express gratitude to several past and present members of research community and staff of University of Southampton, particularly from School of Chemistry, all very helpful anytime it was needed.

The generous support from Royal Thai Government is greatly appreciated. They granted me the scholarship for the whole Ph.D. study in United Kingdom. Without their support, my ambition to study abroad can hardly be realised. Furthermore, I would especially like to thank Department of Science Service, Ministry of Science and Technology, the organiser which allow me to spend my work time, studying in abroad.

I would like to express my special thanks to Dr. Francesco Giustiniano and Dr. Orawan Pinprayoon as their kindly being my proof-readers. Some Thai friends, particularly of ‘Ice-house’ mates 07-09, they have made my time in Southampton enjoyable, made a grey sky a brighter blue and helped me overcome setbacks and stay focused on my graduate study. I greatly value their friendship and I deeply appreciate their belief in me. Ph.D. is not just studying but means a lot with their companies.

Most importantly, none of this would have been possible without the love and patience of my family. My immediate family, to whom this thesis is dedicated to, has been a constant source of love, concern, support and strength all these years. I would like to express my heart-felt gratitude to my family. My special appreciation goes to my parent, Siriwon (Mom) KETKOOM and Supaluk (Dad) KETKOOM, my sister and brother in law who always care, support and love spiritually throughout my life.

Abbreviations

AAS	atomic absorption spectroscopy
As	arsenic
As^{+3} or As(III)	trivalent arsenite
As^{+5}or As(V)	pentavalent arsenate
As-Si	arsenic labelled silica
C_{12}TMABr	n-dodecyltrimethylammonium bromide
CFF	cross flow filtration
CT	cryogenic trap
DL	detection limit
DLS	dynamic light scattering
DTC	dithiocarbamate
DTC-Si	bis-dithiocarbamate modified silica
EDL	electrical double layer
El	electrical
ETM	estuarine turbidity maxima
FFF	field flow fractionation
Fl	flow
Fl-FFF	flow field-flow fractionation
g	gram
GF-AAS	graphite furnace atomic absorption spectroscopy
Gr	gravitational
HA	mixed cellulose esters
HDPE	high-density polyethylene
HG	hydride generation
L or l	litre
LS	light scattering
MF	mixed cellulose acetate and nitrate
mg	milligram
mL or ml	millilitre
mM or mmol	milimolar
MPTMS	3-mercaptopropyltrimethoxysilane

ng	nanogram
nM or nmol	nanomolar
ppb	part per billion (in this thesis µg l^{-1})
ppm	part per million (in this thesis mg l^{-1})
ppt	part per tillion (in this thesis ng l^{-1})
PCS	photon correlation spectroscopy
PSD	particle size distribution
QD	quantum dot
RhB	Rhodamine B
S	sieve or plain type filter
Sd-FFF	sedimentation field-flow fractionation
SEM	scanning electron microscopy
SiSH-Rh	Rhodamine labelled-thiol modified silica
SH-Si	thiol modified silica
Sd	sedimentation
SD	standard deviation
TEA	tetraethylamine
TEM	transmission electron microscopy
TEOS	tetraethoxysilane
TFF	tangential flow filtration
TMOS	tetramethoxysilane
TMZ	turbidity maximum zone
Th	thermal
TP	tortuous path or depth type filter
UV	ultra-violet
v/v	volume per unit volume
V_A	attractive van der Waals force
V_R	repulsive electrical double layer force
V_T	total interaction energy
w/v	weight per unit volume
Z-6094	N-[3-(trimethoxysilyl)propyl]ethylenediamine
µm	micrometre
µg	microgram

Chapter 1 The colloidal phase

1.1 Introduction

1.1.1 Motivation

Natural water contains many substances and these can be categorised according to their particle sizes. The three main categories are (1) the dissolved phase, (2) the colloidal phase, and (3) the particulate phase. By convention, the dissolved and particulate phases are often isolated by filtration of the water through a membrane having pore size diameter of 0.45 µm. The dissolved phase is assumed to be the portion that has passed through the membrane whilst the particulate phase is the portion retained on the filter. As a result of its field-portability, simplicity, and low cost, filtration is widely used, even though it is recognised that colloidal particles are included in both the operationally defined "dissolved" and "particulate" fractions. The presence of colloids can cause major operational difficulties when distinguishing between dissolved and particulate matter. The size distribution of aquatic colloids varies in a continuous manner over the nano (10^{-9}) to micro (10^{-6}) metre size range (see section 1.2).

Fractionation by filtration has been observed to be subject to error in the measurement of trace metals in filtered water samples [1-5]. Filters and membranes of different pore sizes can in principle be used to accomplish a sequential size fractionation of colloids and macromolecules [6-8]. It could also be used to determine the extent to which trace elements (particularly metals) are associated with various size categories of colloids [9-13]. Such a sequential size fractionation technique needs to be applied with caution as a number of factors may cause erroneous results.

1) Particles larger than the size of a pore are retained, but many smaller particles (sometimes 10-1,000 times smaller than the pore size) may also be retained.

2) Aggregation or coagulation occurs in the bulk sample and in the filter. This increases with the flow rate used for filtration.

3) Colloidal particles interact with the filter materials (glass, cellulose nitrate, polycarbonates etc.) on filter walls and with the retained particles.

After filtration, colloidal particles can be present either suspended in the dissolved phase or aggregated to the particulate phase, depending on their sizes and filtration characteristics [8, 14, 15]. Inorganic substances such as As, Pb, Cd, which are common water pollutants, tend to be present within the particles and colloidal phases that exist in natural waters [16-18]. The results of analysis of these inorganic substances may be affected by their attachment to the particulate phases [19-21].

This thesis records a study of the influence of the colloidal particles in natural waters on the measurement of inorganic pollutants. Engineered-colloidal silica particles were selected to model natural colloidal particles and arsenic was chosen as a representative water contaminant that is often associated with the colloidal phase and that can be accurately measured in the laboratory.

1.1.2 The areas of the project

The main aim of this study was to investigate how the presence of natural colloidal matter in waters affects the measurement of inorganic pollutants. The study was divided in two sections. Artificial colloidal particles (silica) with bound contaminant were first produced and characterised in the laboratory. These colloidal particles were then employed to study the effect of the filtration procedure on the determination of contaminants in natural and artificial water systems.

The specific objective of this investigation were:

- To produce fluorescent and arsenic labelled particles lying in the size range of 100-1,000 nm diameters (assuming spherical structure).
- To investigate the influence of the size of the colloidal particles on the analytical measurement of the 'dissolved' and 'particulate' phases, in procedures employing filtration as the separation technique.
- To measure the particulate, colloidal and dissolved arsenic fractions in the Tamar estuary and rivers in Devon and Cornwall. The concentrations of colloidally associated arsenic were measured and the fractionation of arsenic by the commonly used method of membrane filtration was investigated.

1.1.3 Organisation of the thesis

This chapter covers theoretical aspects and literature involving the study of colloidal dispersions, interactions between particles and the general properties of colloidal particles in natural waters.

Chapter 2 describes the synthesis of sub-micron silica particles, the modification of their surface and their morphological characterisation by scanning electron microscopy and dynamic light scattering techniques.

Chapter 3 investigates how the man-made particles behave during the conventional filtration method commonly employed in analytical measurement. Different types of filter were investigated.

Chapter 4 describes the measurement of arsenic in the colloidal fraction of waters from the Tamar estuary. It includes all the analytical methodology used in the sampling, separation and determination of arsenic concentrations. Known sizes of labelled-fluorescent particles were added into the water samples to investigate their behaviour during filtration.

Chapter 5 summarises the research findings and also includes suggestions for future work that could further develop the research done here.

1.2 Description of colloidal particles

The topic of "natural colloids in the environment" has been the subject of many and varied studies. These have included the adsorption of contaminants onto colloidal particles, their coagulation and attachment and their role in the transport of reactive elements, of radionuclides and other pollutants through the environment [22], [23], [24]. Many familiar substances in the environment are colloids; in our surroundings these include clays, natural waters, mist and smoke. Additionally, new forms of colloid-containing materials are continually being produced by industrial processes such as those employed for the manufacture of synthetic paints, foams, pastes, etc. Colloids in natural waters are ubiquitous; they are present in relatively large concentrations in fresh surface waters, in ground waters, in oceans and in sediment pore waters. Because of their role in human life, it is therefore important to understand the physicochemical properties of colloids, to better identity their interactions within the environment. For this study, the colloidal suspensions in natural waters are of particular interest.

Natural waters contain a wide variety of particles ranging from dissolved, through colloidal to larger particulates. In most analytical procedures, these have to be separated (usually by pre-filtering through membranes with 0.45 μm pore sizes). Matter larger than 0.45 μm is often defined as 'particulate' while the term 'dissolved' is used for the particles that pass through the filter. In this case, the colloidal matter remains in either or both fractions. C**olloidal particles** are usually defined on the basis of their size; according to the International Union of Pure and Applied Chemistry (IUPAC), they are "generally a small size of matter that have, at least in one direction, a dimension roughly between 1 nm and 1 μm"[25] (Figure 1).

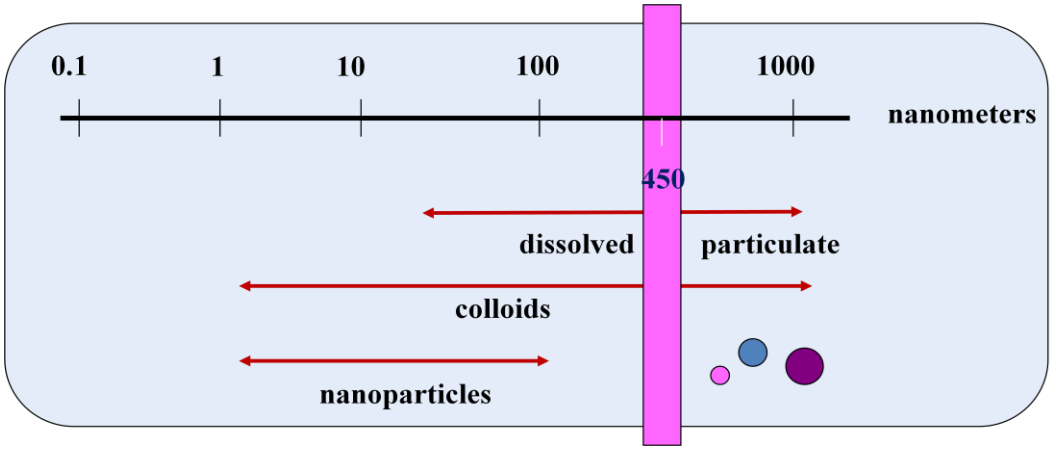

Figure 1 Size domains of component phases in waters.

In aquatic systems, the size of particulate matter determines its properties. Small light particles may be kept in a stable suspension in which units are dispersed evenly throughout the solvent. Whilst much larger than the molecules of the solvent, these units are still small enough to be dispersed and maintain a homogenous appearance; this is called **a colloidal dispersion** or **colloidal system**. A colloidal system is therefore a two phase system formed by a material, such as a gas, liquid or solid, dispersed in another material called the continuous phase (or dispersion medium). In nature, the dispersing media are mainly water or air and the dispersed materials are mainly solids of biological or mineral origins. The distinguishing feature of all colloidal systems is the relationship between the dispersed particles and the continuous phase. Table 1 lists examples of various types of such colloids. Among these are the sol dispersions (solid dispersed in liquid), emulsions (liquid dispersed in liquid) and aerosols (liquid dispersed in gas). A further means of classification is as lyophilic (solvent loving) and lyophobic (solvent hating). When the dispersion medium is water, the terms hydrophilic or hydrophobic are also used. This research focuses on colloidal dispersions of solid particles in a liquid.

The colloid, in which one substance is dispersed in another, can be maintained and transported in an environment for long periods. In addition, the potential for adsorption on high surface area submicron range particles plays a major role in the transport of contaminants.

Table 1 types of colloidal dispersion *.

Continuous phase	Dispersed Phase	Technical name	Examples
Gas	Liquid	Aerosol	Fog, mist
Gas	Solid	Solid aerosol	Smoke
Liquid	Gas	Foam	Whipped cream
Liquid	Liquid	Emulsion	Mayonnaise (oil dispersed in water)
Liquid	Solid	Sol, dispersion	Blood, painting ink
Solid	Gas	Foam	Pumice, plastic foams
Solid	Liquid	Gel	Jelly, opal (mineral with liquid inclusions)
Solid	Solid	Solid sol	Ruby glass

** The nomenclature is adapted from Ostwald [26]*

1.2.1 Special properties of colloidal particles

1.2.1.1 Charged surfaces properties

To understand the behaviour of colloidal materials in aquatic systems, their characteristic surface chemistry and the interactions between particles must first be understood. The size of the colloidal particle is of fundamental importance as the parameter determining many of the general properties of these materials. Particles with diameters in the sub-micrometer range are of particular interest because of their ability to adsorb contaminants due to their large specific surface areas and high surface free energies.

It is more common for charged surfaces or particles to interact across a solution that already contains electrolyte ions. The ion distribution adjacent to an isolated surface in contact with an electrolyte solution (Figure 2) shows that there is an accumulation of counter ions (ions of opposite charge to the surface charge) and a depletion of co-ions[27]. In the locality of a charged colloidal particle there is a balance between the electrical forces which tends to attract counter ions and repel co-ions. Some ions are bound to the surface by electronic and van der Waals forces strongly enough to overcome thermal agitation; this is the so-called *Stern layer*. Others ions form an aqueous atmosphere close to the surface known as the *diffuse electric double layer*. This will be described more detail in the following section. Understanding the properties of the double layer is important as it governs the interaction between two surfaces in a colloidal suspension.

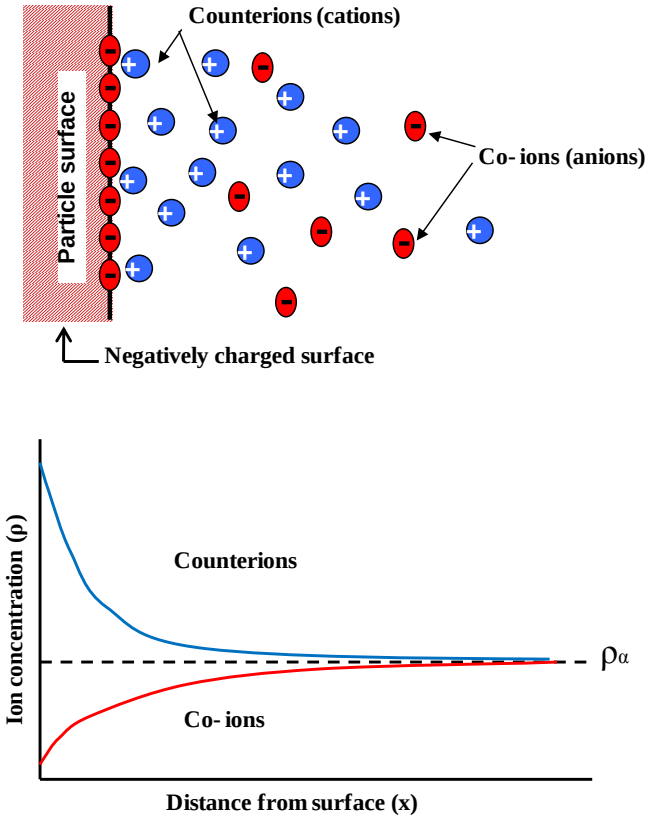

Figure 2 Graphic representation of an ionic distribution in an aqueous electrolyte. x is the distance, ρ is the ionic concentration of ions in the bulk and ρ_α is the ionic concentration at distance, x=α. The diagram is from Ref.[27]

The particle surfaces can develop an electric charge in two principal ways: 1) the charge may arise from chemical reactions at the surface that result in ionisation leaving behind a charged surface. This depends on the pH of the medium; 2) a surface charge may be established by adsorption of hydrophobic species, ions or surfactants onto the particle surface. The adsorption can occur because of acid-base interaction, hydrophobic bonding, and hydrogen bond formation or London van der Waals interactions. Since the surfaces of colloidal particles often carry an electrical charge, attractive and repulsive forces between the particles are established. For example if an electric field is applied, the particles accumulate near the negative electrode, the net charge on the particles is positive. Colloids containing particles with the same charge are typically stable because of repulsion between charges of the same sign.

Many suspended and colloidal solids encountered in waters, sediments and soils have a surface charge that is strongly affected by pH [28] (Figure 3). At neutral pH most suspended solids typically encountered in natural waters are negatively charged[29, 30] as indicated by negative values for their electrophoretic mobility[31, 32]. Puls et al.[33] suggested that the adsorption of negatively charged organic and inorganic species onto the surface of iron oxide, a natural water colloid, significantly enhanced the colloidal stability. Such negatively charged components include quartz, feldspars, clay minerals and natural organic matter.

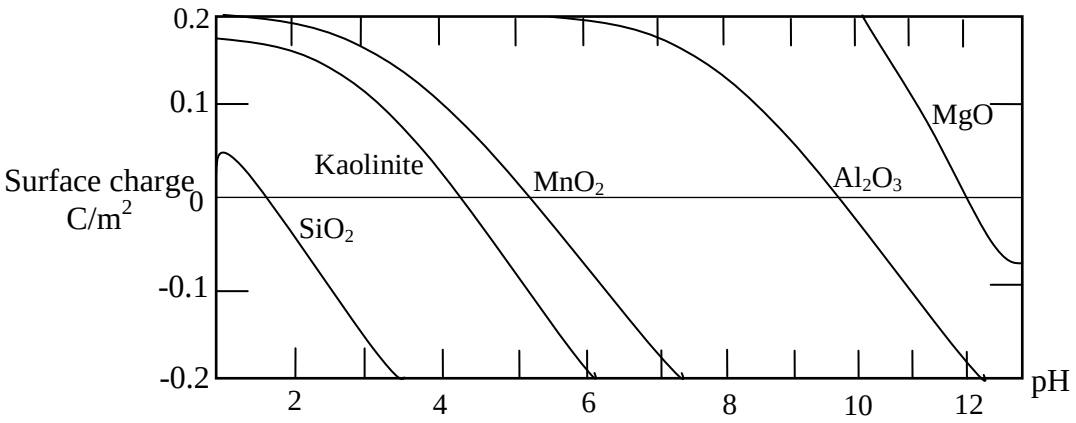

Figure 3 Effect of pH on charge. These simplified curves are based on results by different investigators whose experimental procedures are not comparable and may depend upon solution variables other than pH. The curves are meant to exemplify trends only.

Natural colloidal phases, in fact, consist typically of a mixture of mineral, organic and microbiological materials; it has been observed that the suspended particles are coated with natural organic matter (NOM). This can cause the adsorbed NOM to dominate the surface properties of the natural particles and to have an effect on colloidal stability [34], therefore affecting the transport of colloidal matter in aquatic systems. In this study, silica particles were used as a model for colloidal particles in natural waters and the surface groups on the particles were negatively charged.

1.2.1.2 Interactions and Stabilities

In order to analyse the behaviour and stability of colloids, the basic interparticle electrostatic forces have to be considered. There are two types of interactions to be considered: the electrostatic interaction between two particles and the double layer repulsive interaction. The electrostatic effects result from ionised groups and are usually repulsive forces counteracting attraction due to van der Waals interactions. In this section, the interaction between two particles in the system is considered so that the stability of the whole system can be predicted by looking at the form of the colloidal pair potential.

Most of colloid science is concerned with maintaining the dispersed state of colloids, otherwise called colloidal stabilisation. The instability of a colloidal system either results from a tendency to aggregate or a tendency to sediment under the action of gravity. A stable colloidal system is one in which the particles resist accumulation, flocculation or aggregation and exhibit a long life (many years). There are two possibilities that may prevent aggregation during a collision. One is that the electrical charges on the particles repel one another when they approach. This mechanism is called '*electrostatic stabilisation*'. Another possibility is called '*steric stabilisation*' in which, if the particles are coated with an absorbed layer (e.g. a polymer which physically hinders two particles from approaching each other), their close approach is prevented. Therefore the particles will remain stable in dispersion if they have a

common repulsion. The stability of a colloidal suspension is therefore established by the balance between van der Waals attractive forces that promote aggregation and electrostatic repulsive forces that drive particles apart. To maintain the stability of the colloidal system, the repulsive forces must be dominant. The potential energy curve as a function of intermolecular separation [35] is illustrated in Figure 4. Repulsive interactions dominate at short distances whereas at a longer range, attractive forces govern. It can be seen that repulsive interactions are important when particles are close to each other.

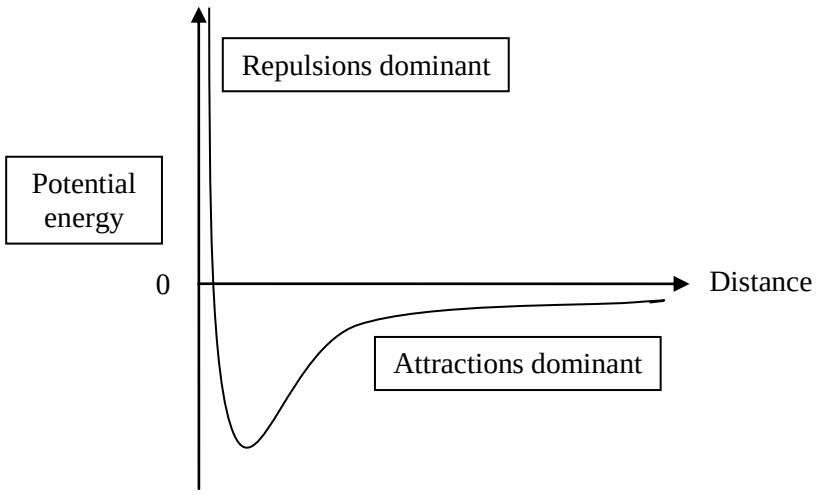

Figure 4 Typical curve of potential energy versus separation of two particles.

The stabilisation originating from attractive (van der Waals) and repulsive (electric double layer: EDL) forces have been described by the extended DLVO theory since the 1940s; DLVO theory (named after Derjaguin and Landau, Verwey and Overbeek) has proven to be a very useful tool to describe the stability of colloids [36]. The theory explains the phenomena of colloidal suspension, adsorption and many other effects.

According to the theory 'the total interaction energy profile' (V_T) is calculated by addition of 'the repulsive EDL force' (V_R) and 'attractive van der Waals forces' (V_A). This can be written as:

$$V_T = V_A + V_R \quad (1)$$

According to the DLVO model, the stability of a system is represented by a potential energy versus between particle distance diagram (Figure 5). The graph shows a state where the attractive forces (van der Waals) are working against the repulsive forces (e.g. electrostatic charge repulsion). An activation energy is required to get particle-particle attachment in either the primary or secondary minimum. A shallow so-called secondary minimum may cause an aggregation that is easily counteracted by stirring[28]. The interaction energy between particles of the same material (V_R) is an exponential function of the distance between the particles. This occurs within a range that is the order of the thickness of the double layer ($1/\kappa$) and V_A decreases as an inverse power of the distance between the particles [37]. Figure 5 shows the two possible types of potential energy curve. $V_T(1)$ shows a repulsive energy maximum whilst $V_T(2)$ shows that the repulsion side does not predominate over van der Waals attraction at any inter-particle distance.

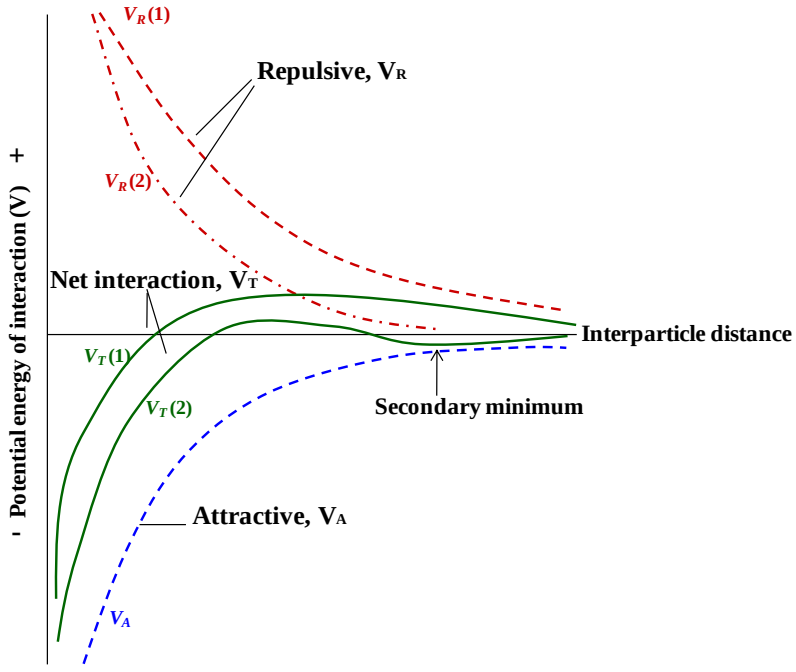

Figure 5 A simplified graph summarising the DLVO interaction energies and the resulting sum function. Total interaction energy curves. $V_T(1) = V_R(1) + V_A$ shows a repulsive energy maximum whilst $V_T(2) = V_R(2) + V_A$ shows that the repulsion potential energy dose not predominate over van der Waals attraction at any inter-particle distance. This figure is adapted from Stumm W.[28]

1.2.1.2.1 The electric double layer surrounding the particles

The formation of the Electric Double Layer (EDL) is a phenomenon playing a fundamental role in colloid stability. In this phenomenon positive colloidal particles gain a negative electric charge when negatively charged ions of the continuous phase are adsorbed on the particle surface. A negatively charged particle attracts positive counter ions to surround the particle. The EDL is the layer surrounding a particle of dispersed phase and includes the ions adsorbed on the particle surface and a film of oppositely charged counter ions from the continuous phase. Figure 6 demonstrates the resulting electrical double layer that forms around a negatively charge colloid and leads to its stabilisation. The particle charge is surrounded by a more or less diffuse ion atmosphere, which forms an electric double layer with the surface charge (Figure 7). Most of the surface is neutralised by the strongly bound counter ions in the Stern layer. The remaining charge is distributed by the diffuse layer of counter ions enlarging out into the dispersion media. The EDL is therefore electrically neutral.

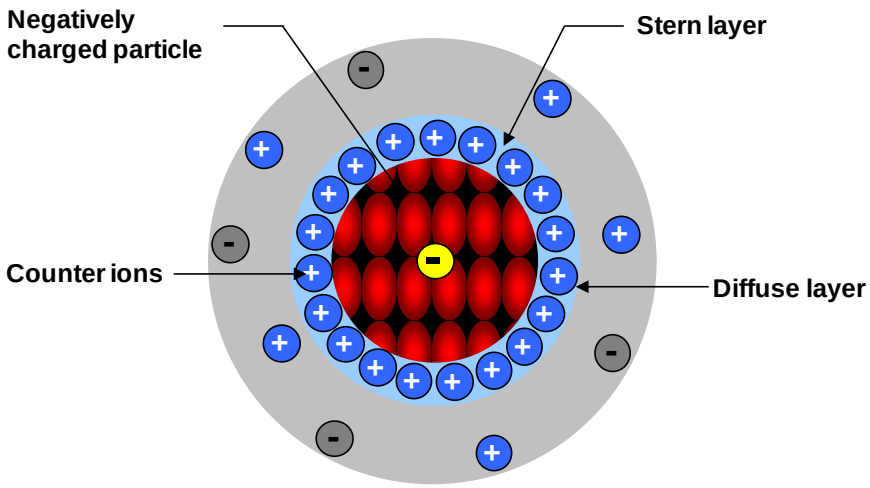

Figure 6 The Electric Double Layer (EDL) consists of three regions; surface charge (commonly negative), Stern layer (charge opposite to the surface charge) and diffuse layer (continuous phase close to the particles).

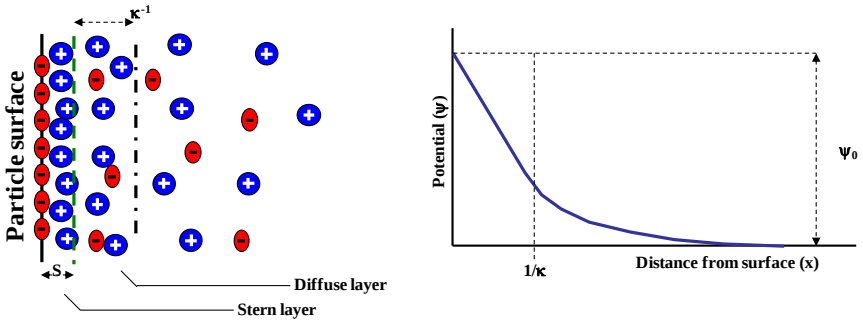

Figure 7 Schematic representation of a diffuse electric double layer. Where κ is the inverse of the double layer thickness, $1/\kappa$, the surface potential be ψ_0 and S is Stern layer.

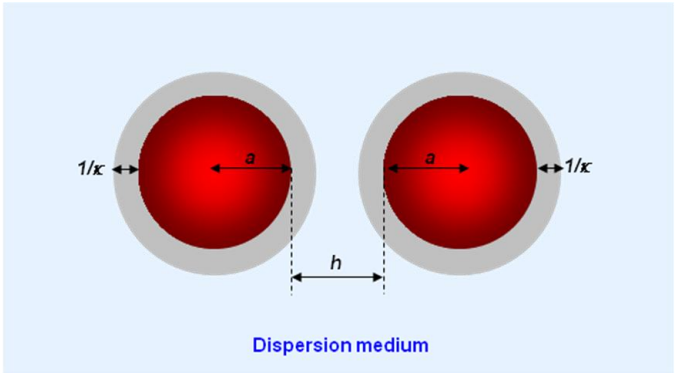

Figure 8 The interaction between two spherical particles of radius a in liquid medium.

When two like-charged particles approach with a surface-surface separation of h (Figure 8), their electrical double layers will start to overlap, resulting in an electronic repulsive force. For a system in which two spherical particles of radii a_1 and a_2 are considered, it is possible to obtain analytical expressions for the calculation of the repulsive interaction energy between the two particles [37] as below:

$$V_R = 2\pi \in a\psi_d^2 [\exp(-\kappa h)] \qquad (2)$$

Where two spherical particles of radius a have a diffuse layer potential ψ_d, there is a small electric double layer overlap (such that $\exp[-\kappa h] \ll 1$) and $\in$ is the permittivity of the dispersion medium or dielectric constant ($\in$ water = 78.5 at 25 ^{o}C).

At high ionic strengths the colloids aggregate due to screening of the charge on the colloids by the electric double layer. Two particles can now approach each other more closely and start to be affected by attractive forces.

1.2.1.2.2 Van der Waals-London attractive forces

Attractive van der Waals forces between colloidal particles can be considered to result from London dispersion interactions between particles (Figure 9). The range of the interaction is comparable with the radii of colloidal particles. The attractive force between two colloidal particles can be calculated.

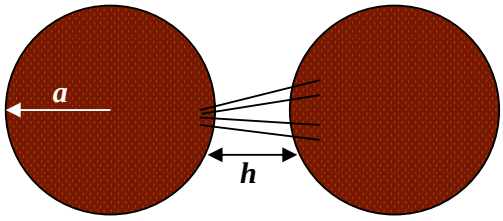

Figure 9 London forces between atoms in two adjacent colloidal particles.

The potential energy of attraction (V_A) between two spherical particles is given by the Hamaker expression (Equation 3).

$$V_A = -\frac{A}{12}\left[\frac{1}{x^2+2x} + \frac{1}{x^2+2x+1} + 2\ln\left(\frac{x^2+2x}{x^2+2x+1}\right)\right] \qquad (3)$$

Where $x = h/2a$ and if the two particles are of the same materials, A is the Hamaker constant given by:

$$A = (\sqrt{A}_{\text{particle}} - \sqrt{A}_{\text{medium}})^2 \qquad (4)$$

Where $A_{particle}$ is the Hamaker constant of the particles and A_{medium} is that of the dispersion medium. For two spherical particles of radius a, in which the interparticle separation is small ($h \ll 2a$):

$$V_A = -Aa/12h \quad (5)$$

The Hamaker constant determines the effective strength of the van der Waals interaction between colloid particles. It varies between materials and a selection of typical values is given in Table 2.

Table 2 values of Hamaker constant *.

Materials	A / 10^{-20} J
Water	3.3-6.4
Silica	50
Silica (fused)[#]	6.5
Quartz	11.0-18.6
Metals (Au, Ag, Pt, etc.)[#]	~40
Hydrocarbon	4.6-10.0

[*]Taken from Ref.[37], [#]Taken from Ref.[38]

1.2.1.3 The movement of colloidal particles

The rate of particle movement depends on the frequency of collisions and on the efficiency of particle contacts. Brownian motion, discovered by the botanist Robert Brown in 1827, describes the random movement of particles suspended in a fluid. An explanation of this effect can be based on the kinetic-molecular theory of matter. The motion is caused by the bombardment of the particles by the surrounding molecules in the solvent. This motion is called Brownian movement. This helps in providing stability to colloidal sols by not allowing them to settle. For this reason, particles can be prevented from aggregating (or coagulating) for long periods, although it must be emphasised that they are still thermodynamically unstable. Nonetheless, the colloidal particles can settle under the influence of gravity at a very slow rate. This section gives some background on the kinetics of aggregation and settling of colloidal particles.

1.2.1.3.1 Aggregation

Aggregation occurs in a sol when the particles have little or no repulsive forces between them. This is often referred to as flocculation or coagulation. Different charges on the surface of the particles can enhance particle-particle interaction resulting in the possibility of a self-organisation to give **colloidal aggregates**.

The processes important to aggregation are mainly particle collisions, and attachment resulting in aggregation with accompanied settling. Once destabilised, aggregation of a colloidal suspension can occur by a number of mechanisms that bring unstable particles into contact. The particle-particle collisions, which lead to unstable colloids in aqueous media, originate from three fundamental processes:

- perikinetic conditions induced by Brownian motion of the particles
- orthokinetic conditions from hydrodynamic motion
- agglomeration by differential settling: particles of different gravitational settling velocities may collide.

The processes of perikinetic, orthokinetic or differential settling are illustrated in circle cartoons in Figure 10. Dotted arrows indicate the graph relating to each process. Perikinetic aggregation (Brownian motion) is the dominant mechanism for the small particles but when particle sizes exceed 1 μm orthokinetic and differential settling become more important [39]. After the initial interactions, the particle-particle, particle-cluster or cluster-cluster may cause aggregation processes [39]. Such aggregates form when the attraction between two particles in contact is so strong that they stick together permanently. Aggregation can occur as homo-aggregation or hetero-aggregation. Homo-aggregation refers to the aggregation of particles of the same type and whilst hetero-aggregation refers to the aggregation of dissimilar particles. Dispersants can be used to aid in the control of agglomeration.

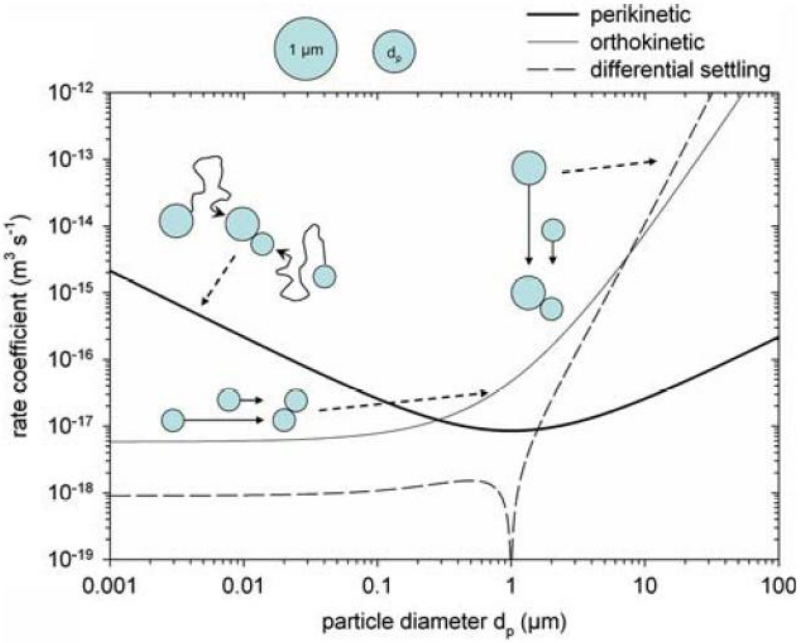

Figure 10 The three collision mechanisms and associated rate coefficients for the aggregation of 1 µm particles of diameter d_p; Temperature is 12 ^oC, particle density 2.6 g ml^{-1}, and shear rate $35s^{-1}$. "With kind permission from Springer Science+Business Media: <Ecotoxicology/ The ecotoxicology and chemistry of manufactured nanoparticles, 17(4), 2008, 287-314, Richard D. Handy, figure 1, copyright notice displayed with material>."

1.2.1.3.2 Settling of a suspension

Colloids usually remain suspended because their gravitational settling rate is less than 10^{-2} cm s^{-1}. Under simplifying conditions (spherical particles), Stokes' law gives the settling velocity[28], Vs

$$Vs = \frac{g}{18}\,(\rho_s - \rho d^2)/\eta \qquad (6)$$

where g is the gravity acceleration (9.81 m s^{-1}), $\rho_s$and ρ are the mass density (g cm^{-3}) of the particle and of water, respectively, η is the absolute viscosity (at 20^{o}C, $1.0x10^{-2}$ kg m^{-1} s^{-1}) and d is the diameter of the particle (cm). Note that Vs is proportional to the square of the particle diameter.

The larger a particle, the faster it will settle due to the force of gravity. Also, the smaller the particle, the greater is the Brownian velocity. Taking into account Brownian velocity and the effects of gravitational settling, for example, researchers consider that colloidal particles larger than 200 nanometers have a low Brownian velocity and colloidal particles smaller than 600 nanometers have a slow settling velocity[40]. Chang and Wang [41] suggested that the stability of suspensions can be decreased by increasing the gravitational forces by centrifugation.

In summary, colloidal stability is influenced by many factors such as inter-particle interactions and surface chemistry. Brownian motion limits the settling rates of particles in the colloidal size range, while larger particles (of micron size) sediment as a result of the gravitational effect. The colloidal particles can be removed from the medium either by settling, if they aggregate, or by filtration if they attach to the materials through which the sol passes. This study was mainly focus on the behaviour of colloidal particles during filtration.

1.2.2 Types of colloids in the aquatic environment

In this section the main groups of natural colloids will be discussed. As previously described, both ‘dissolved’ and ‘colloidal’ fractions exist in the environment. A variety of compounds, such as silicate clays, oxides/hydroxides, carbohydrates, phosphates and metal sulphides, exist as colloidal particles or macromolecular compounds in the hydrosphere. Natural aquatic colloids typically contain both inorganic and organic components. Figure 11 shows a comparison of the sizes of colloid particles.

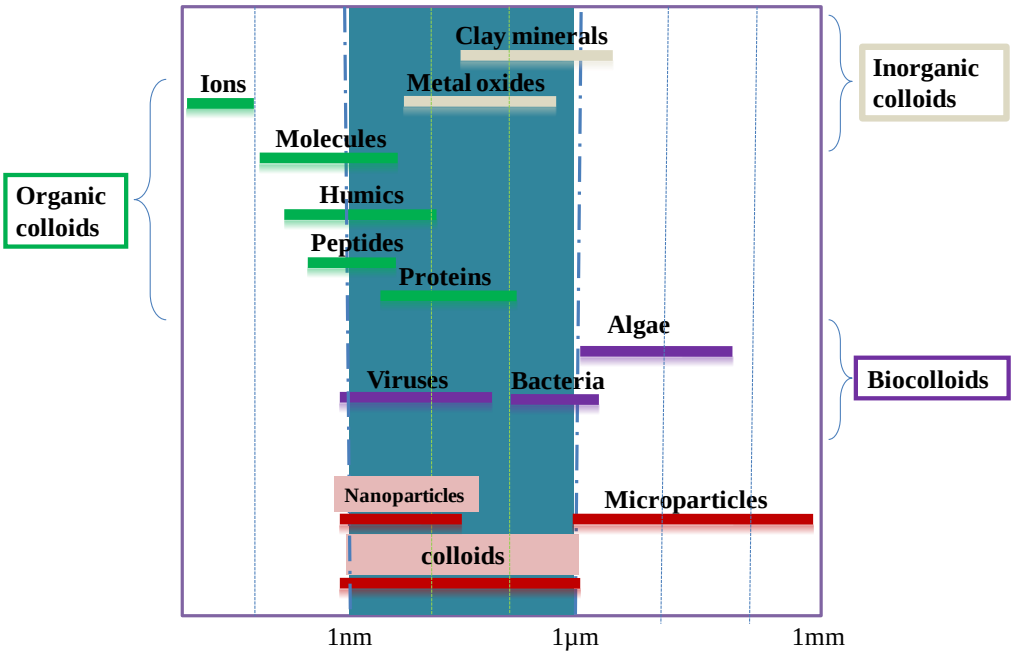

Figure 11 Size domains and typical representatives of natural colloidal particles and nanoparticles. The diagram is adapted from Christian, P.[42] , Kretzschmar, R.[43] and Lead JR.[44]

There are many potential sources of inorganic colloidal particles in natural surface waters; the most relevant are particles in soils and subsurface waters released by changes in solution chemistry and the formation of solid phases by chemical precipitation [10, 45, 46]. In addition, human activities, such as waste disposal and groundwater pumping, can bring about changes in water chemistry and create conditions that favour the formation of colloids. The inorganic colloids more commonly found in oxic waters include aluminosilicates (clays), silicas and oxides of Fe, Mn, Al and Si [47]. Calcium carbonate is also present in aquatic systems but is generally found in the larger size fraction. There are two important characteristics of inorganic colloids[48]

- their irregular shape and physico-chemical heterogeneity;
- the large average size of the particle e.g. with particle size up to 1 µm.

Colloidal organic compounds are mostly of biological origin. As shown in Figure 11, biological material such as viruses and bacteria fall into the colloidal size range. Such ‘biocolloids’ can pose serious health hazards if they occur in drinking water wells.

Microbial contamination of groundwater has been identified as a primary cause of waterborne disease out-breaks. The humic substances (HS) and macromolecules such as proteins and polysaccharides are also included. Organic colloids are reported in oceans and lakes[6], and play an important role in the aquatic systems.

1.3 Occurrence of colloidal particles in environmental systems

Colloidal particles found in environmental systems, e.g. natural waters and soils, can originate from diverse natural processes, such as erosion, volcanic dust, chemical and physical perturbations [6, 49, 50] or industrial processes. Such particles can be formed in the environment during natural processes taking place over millions of years. Atmospheric colloids are released from combustion processes such as soot, waste dumps, fly ash and fine dust. Indeed, the emission of by-products in technological processes, for example during the production of polymers, surfactants, dyes and pigments can be one of the main sources by which colloidal particles are released into the atmosphere.

Non-reacting colloidal particle from larger sources can be induced in many ways such as sudden changes in pH, ionic strength and temperature. Amirtharajah and Raveendran[51] studied the detachment of colloidal latex particles from a packed column containing glass beads as collector grains. They suggested that the detachment efficiency of these particles was higher with lower ionic strength waters. McCarthy and Zachara[29] reported that colloidal particles may be generated through perturbations in the hydrogeochemistry when the ionic strength of groundwater is decreased. Nocito-Gobel and Tobiason[52] investigated the effect of ionic strength on model colloid (polystyrene spheres) deposition and release from silica sand packed column studies in the laboratory. Results indicated that model colloids deposition on silica bed media increases with increasing the ionic strength of the solutions. With

decreasing the ionic strength led to the release of colloidal particles from the sand surface. Jódar-Reyes et al.[53] studied the colloidal stability of polystyrene particles in water under a wide range of ionic surfactant concentrations. Those authors found that high surfactant concentrations induced an instability of the dispersion that caused particle aggregation. Furthermore, García-García S. et al.[54] observed that pH, ionic strength and temperature affected on the stability of colloidal montmorillonite particles in aqueous dispersions. Results suggested that increasing the pH increases the negative charge on the colloidal particles and thus increases the surface potential that resulting in slower aggregation kinetics[55]. The effective repulsion between the charged colloidal particles is decreased by increasing the ionic strength, results in faster aggregation kinetics. The collision frequency and the kinetic energy of the colloidal particles can be increased by increasing the temperature, resulting in faster aggregation kinetics. Bond aging effects were also observed, as the lower release rates from a collecting surface of colloidal particles to waters were found for particles that were attached for longer to a substrate [56].

1.3.1 Engineered nanoparticles and their effects on living organisms in the environment

The term '*engineered nanoparticles*' is used here to refer to colloidal particles having sizes below 100 nm and originating from industrial processes. With the increasing use of products containing engineered nanoparticles, it is inevitable that significant amounts will be released, accidentally or intentionally, into environmental systems such as soils and natural waters (Figure 12).

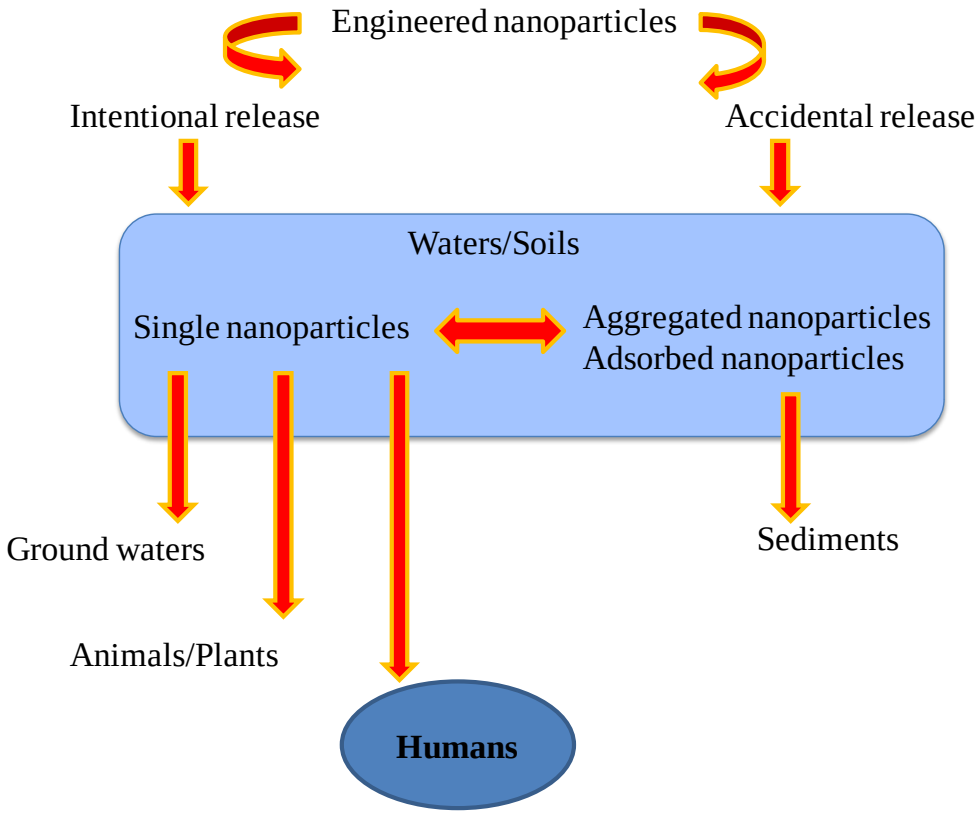

Figure 12 pathways of nanoparticles released into the environmental systems and humans. The diagram is adapted from Nowack, B. And Bucheli, T.[57]

Humans come in contact with these engineered nanoparticles either directly through exposure to air, soil or water, or indirectly by consuming plants or animals which are contaminated by nanoparticles. The cellular accumulation and uptake of nano-scale materials has been shown for a number of organisms. Organisms living in an environment containing nanoparticles will include them within their bodies, mainly via the gut [58]. Nanoparticles can enter into cells by diffusing through the cell membranes, adhesion and endocytosis [59]. Particle interactions with biological systems and their toxicity principally depend on properties such as size, concentration, solubility, chemical and biological properties, and stability [57,[60],[57, 61].

A literature review of ecotoxicological studies of organisms exposed to nanoparticles has highlighted various steps by which nano-sized materials are taken up [39, 62, 63]. The first step involved the association of nanoparticles onto the exterior surface of the organism. The next step involved the movement of nanomaterials across the

membrane. This step could happen by dissolution of hydrophobic nanoparticles into the lipidic double layer, or by endocytosis in the case of hydrophilic particles. Zhu et al. [64] reported that a factor governing nanoparticle toxicity is the duration of exposure. They found that $nTiO_2$ caused minimal toxicity to *Daphnia magna* (water fleas) during a 48 h exposure time, but caused high toxicity when the exposure time was extended to 72 h. Moreover, upon chronic exposure to $nTiO_2$ for 21d, water fleas displayed severe growth retardation and mortality, as well as reproductive faults. These results agree with those obtained by Casals et al. [65] who reported that the presence of nanoparticles inside the cells or inside the body for long periods of time, even at non-toxic concentrations, may have deleterious effects. It followed that the long-term exposure of aquatic organisms to engineered nanoparticles may alter their growth cycles, both at the individual and population level, resulting in severe alterations to the aquatic ecosystems [66, 67].

Some researchers have investigated the toxicity of engineered nanoparticles to microbes in the environment. For example, Tong et al. [68] tested the effects of C_{60} fullerene on a soil microbial community and reported little effect after 30-days exposure to 1 mg C_{60} g^{-1} of soil. In contrast, C_{60} in suspension has been shown to have toxic effects on bacterial cultures in the laboratory. Quantum dots (QDs) are engineered semiconductor nanocrystals containing transition metals such as cadmium, selenium and tellurium (as in CdSe, CdTe, CdSeTe, CdS), zinc (as in ZnSe and ZnS), and others (InAs, PbSe). The uptake of QDs by *E.Coli and Bacillus subtilis* has been reported [69]. QD uptake may lead to the accumulation of potentially toxic metals in the cells, where they may persist for a long time and cause cellular damage[70]. In addition, the interaction of nanoparticles with DNA in the nucleus or in the cytoplasm during mitosis induces gene damage or blocks gene repair, ultimately leading to cancer [65].

1.4 The impact of colloidal particles in natural waters

Associations of sub-micrometer particles with pollutants influence pollutant transport through natural waters. This section will discuss reports involving the behaviour of colloidal particles in natural waters.

1.4.1 The association of pollutants with colloidal particles

Amongst all the components of natural waters, the colloidal phase has the highest specific surface area (>10 m^2/g) and it can be associated with large quantities of adsorbed environmental contaminants. A number of investigations have demonstrated the strong adsorptive capabilities of colloid species[71-73],[74],[10],[11]. For example, Benoit and Rozan [75] reported that speciation may be dominated by colloids and particles, resulting in extremely low amounts of trace metals being in true solution in natural waters. The extent of binding of metals to colloid and/or large particles is dominated by pH, colloidal particle type, concentration, and reaction time. Dahlqvist et al. [10] reported that a considerable amount of colloidally bound Ca has been detected in water samples from Amazonian rivers and the Kalix River, a sub-arctic boreal river, using several analytical techniques. Moreover, the concentration distribution of colloidally associated Ca reached a maximum during winter conditions. As to the major elements, significant quantities of Al and Fe were found to be associated with particles in the range 0.4-1.0 μm (from some U.S.A. rivers)[76].

As a result of having a large surface for binding, many of the inorganic colloids are especially effective at adsorbing pollutants (e.g radionuclides and metals) through either ion exchange or surface reactions [77-79]. Van de Weerd et al. [80] reported that colloidal particles of clay minerals and iron oxides are strong sorbents of radionuclides and other toxic contaminants, as a consequence of their high specific surface area. Li, Yang and Jen [77] supported the role of colloids in the migration of

radionuclides by using transport equations for colloids and radionuclides. The concentration of mobile radionuclides was found to increase due to the high sorption/partition coefficient of radionuclides associated with colloids. In summary, the binding of pollutants to colloids has been shown to be an effective carrier for the migration of contaminants in natural water systems.

1.4.2 Transport of colloidal particles

As a result of the special properties of colloidal particles e.g. high surface areas and near permanent suspension, they are effective adsorbants of dissolved trace contaminants. Indeed, many researchers [81-84] now believe colloidal materials may be the principal means of transport for organic materials, radioisotopes, and some heavy metals in natural waters, as mentioned in Section 1.4.1.

A number of studies have involved the introduction of tracers into an aquifer system or in laboratory testing. Many contaminants readily sorb on immobile surfaces and become trapped in the subsurface, thus presenting little danger as far as natural waters are concerned (Figure 13). However, if colloidal particles are present (Figure 13B) the contaminants may strongly associate with them, increasing their mobility. As a result the colloidal particles do not sediment but instead remain as a solid phase in suspension.

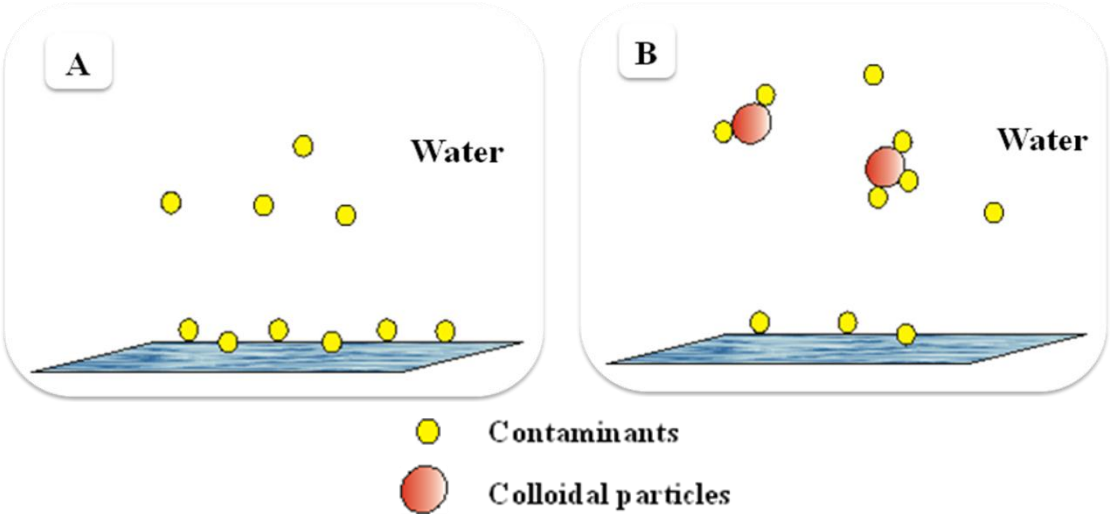

Figure 13 Comparison of two and three-phase aqueous systems. A) two-phase (a dissolved phase and an adsorbed immobile phase); B) three-phase. The third phase in B) is constituted by the colloidal particles, shown here with adsorbed contaminant molecules which are therefore made mobile. The drawing is adapted from Honeyman[85].

Laboratory experiments and field studies have demonstrated that colloids can carry and enhance the spread of potentially toxic substances in natural waters [77, 86, 87], which is of environmental concern [88-91]. Colloid-facilitated transport may increase the distances travelled by pollutants and pathogens. Colloidal trace metals are commonly found in riverine and estuarine waters. Some researchers reported the presence of metals associated with colloidal particles acting as carriers in estuaries[92] and the influence of such interactions on the mobility of pollutant-colloidal particles in rivers[93]. Ryan and Elimelech[30] mentioned that the first criteria on colloid-associated contaminant transport is that colloids must be present in sufficient amount to sorb a significant amount of the contaminant. The movement of colloidal particles in water flowing through porous media enhances the transport of chemical contaminants [94]. However, the migration distance of pollutants associated with colloids can be greater than estimated from laboratory results. The investigation of Penrose et at.[95] reported the transport of plutonium associated with colloidal particles (25 to 450 nm in size). They suggested that the detectable amounts of plutonium can be found 3.4 kilometres away from the source at the Los Alamos National Laboratory.

These results were similar to those of Kersting[83], which found that plutonium associated with colloids with sizes in the range of 7 nm to 1 μm had migrated 1.3 kilometres in 30 years by means of colloid-assisted migration in groundwater.

Environmental physicochemical parameters such as ionic strength, pH, temperature and pressure can affect colloidal mobilisation. Remobilisation of colloids occurred when the ionic strength of the background electrolyte solution was reduced. The mobility of colloids also increased with increasing pH and increasing flow rates. Solutions of higher ionic strength do not however mobilise colloids[96] due to the increasing of aggregation kinetic[54]. Most of the studies of mobile colloids have focused on groundwater, and there are to date few studies on colloid-bound trace metals in other natural waters. For such reasons further understanding of colloid behaviour in the laboratory is essential for predicting the potential for colloid-facilitated transport in a given natural water. Within this thesis, the composition of aquatic natural colloidal matter, its properties and morphology were investigated and reported using several analytical methods, such as fractionation, determinations of metal content, and microscopic observations of the colloidal components (Chapter 3 and 4).

1.5 Analytical techniques for the study of colloidal particles in natural waters

1.5.1 Size fractionations of colloids

Unfortunately, the colloid size range is not well served by convenient methods for separation and size analysis. Complications arise from the heterogeneity of natural colloids, their low concentrations, the broad size distribution, and their tendency to

form aggregates. These combine to make it particularly difficult to measure their sizes and size distributions accurately [97].

Knowledge of how the number of particles, total mass, specific element content etc., vary as a function of the particle size, provides useful information for sample characterisation. These functions require specific detection systems coupled with techniques which enable us to either determine the physical dimensions of colloidal particles found in aqueous suspensions (e.g. electron microscopy) or to size-fractionate the sample (e.g. filtration). Such techniques include size-fractionation, ultrafiltration, field flow fractionation, scanning and transmission electron microscopy, as well as photon correlation spectroscopy.

There are a number of techniques suitable for the fractionation and sizing of colloidal particles analysis. The most common separation methods are based on differences in the particle size, density, mass or a combination of these. Size-fractionation of environmental colloids is generally the first step in their characterisation. Filtration is the most commonly used method of size-fractionation. In principle the separation is based simply on size whilst in practice there are a number of complications associated with the formation of a cake layer (an increase in colloid concentration directly above the membrane surface). These problems may result in fractionation occurring over a different size range than would be expected from the nominal pore size of the filter. Furthermore, the actual size range separated may alter over the course of the filtration [1, 98, 99]. However, these problems can be reduced by the use of appropriate filters and filtration conditions, particularly flow rates.

Ultrafiltration usually requires an initial prefiltration step at a pore size of 0.45 µm [100, 101]. Recently ultrafiltration has been performed in cross-flow filtration (CFF) [102-104] or tangential flow filtration (TFF). This approach has attracted attention due to its time-efficient processing of large volumes of natural water and minimum alteration of colloidal matter. CFF enables the processing of large volume samples (10–1,000 L,

depending on the system) to recover colloids. CFF membranes are usually made of regenerated cellulose[105] or polysulfone[106] and are often used in the study of estuarine waters, seawaters and river waters. Filtration using this system may offer certain advantages over traditional ultrafiltration, such as increased flow rate [107]. However, it is doubtful whether cross-flow filtration can be used at significantly higher flow rates than the classical filtration without cake formation above the membrane surface leading to errors in the size discrimination [108]. The accumulation of material on the membrane surface, known as fouling, can disturb the quantitative measurements of compounds associated with colloids[109]. It constitutes the main limitation of this technique.

Field flow fractionation (FFF) is a family of separation methods used in the separation and characterisation of colloidal materials. The techniques of FFF include sedimentation (Sd)[110], flow (Fl)[111], thermal (Th)[112], electrical (El)[113] and gravitational (Gr) FFF[114]. Moreover, they can be employed coupled with various detectors [110, 111, 115] such as ultra-violet (UV), fluorescence, differential refractive index (RI) and atomic spectrometre. Such couplings enhance the gathering of the information needed. Flow field-flow fractionation (Fl-FFF) is the most widely used technique and is applicable to macromolecules, particles and colloids ranging from 0.001 μm (approximately 1,000 molecular mass) up to at least 50 μm in diameter. It has taken an important place among the different separative tools because of its high resolution, its capability to fractionate over a wide range of size and the lower interactions with the analytical system in comparison to chromatography. Sedimentation field-flow fractionation (Sd-FFF), which belongs to the chromatographic-like field flow-fractionation (FFF) family of separation techniques, was used for characterising complex samples, because of its high resolution (fractionating power) [110, 116]. Contado et al. [110] demonstrated that Sd-FFF can be indirectly interfaced with graphite furnace atomic absorption spectroscopy (GF-AAS) to produce element composition data of A1, Fe across the size distribution of colloidal samples. Beckett et al.[116] used Sd-FFF with exponentially decaying fields

either to fractionate and give particle size information or to characterise the colloidal particles present in natural waters.

1.5.2 Characterisation of colloidal particles

Filtration and ultracentrifugation can be used to characterise a size distribution, but results yield classes of size rather than a real particle size distribution (PSD). In addition, the determination of the physical dimensions of colloidal particles in aqueous suspensions has also been proven difficult. Scanning and transmission electron microscopy (SEM and TEM) are direct methods used to characterise particles and obtain length, width, and area. Particle size distributions have also been determined using photon correlation spectroscopy (PCS) and light scattering (LS) techniques.

The use of SEM and TEM for determining the size, morphology, associations and composition (when used with a specific probe) of submicron particles is well documented [109, 117-119]. These techniques allow observation of fine structures at the near nanometre level. PCS yields a weighted average size distribution of the sample, contrarily to TEM which allows determination of single particle sizes[120]. PCS is based on the instantaneous changes in light scattering caused by the Brownian motion of submicron particles. A highly coherent, monochromatic laser is focused on a very small volume of a sample. Particles present within the focused volume scatter light at an intensity which is proportional to their concentration. Large particles scatter much more light than small particles. LS measurements yield relative estimates of the total particulate content of suspensions. LS is a function of both particle size and concentration; for this reason, LS cannot be used as an accurate measure of particulate concentration when the size of the particles in fractionated samples is decreasing[121].

Therefore, filtration is best used simply to reduce the polydispersity of natural particles before applying other methods of particle size analysis. When filtration is used, filtration conditions and flow rate need to be optimised in order to obtain an accurate fractionation. This can be done by analysing the filtrate and retentate as a function of filtration conditions and analysis of the retained material on the membrane by either scanning or by transmission electron microscopy (SEM or TEM). TEM is particularly useful for comparing (1) the size of the colloids with the nominal membrane pore size and (2) the degree of aggregation on the membrane surface with the degree of aggregation of colloids in the bulk solution. However, it might be time consuming but may be the only way to reliable measure the size of particles.

Throughout the present work, the literature concerning the effects of colloidal size of particles with the natural systems and the difficulty of their analysis are discussed. A brief discussion is given of the relevant artefacts that may result from sampling, pre-filtration, filtration and analysis as a result of the unstable nature of colloidal fractions and the trace metals associated with them. Understanding the colloidal particles properties (which act as the pollutant carrier) and behaviour of colloidal particles requires a precise analysis and an understanding of the distribution of pollutants between the dissolved and particulate phases of a water sample. This thesis includes an investigation of the behaviour of colloidal particles during analytical measurement. This is to gain a better understanding of the role of natural and man-made colloidal particles in pollutant transport in the environment.

1.6 References

[1] A. J. Horowitz, K. A. Elrick and M. R. Colberg, *Water Research* **1992**, *26*, 753-763.

[2] R. W. Sheldon, *Limnol. Oceanogr.* **1972**, *14*, 441-444.

[3] L. G. Danielsson, *Water Research* **1982**, *16*, 179-182.

[4] D. P. H. Laxen and I. M. Chandler, *Analytical Chemistry* **1982**, *54*, 1350-1355.

[5] S. Karlsson, A. Peterson, K. Häkansson and A. Ledin, *Science of the Total Environment* **1994**, *149*, 215-223.

[6] J. Buffle, K. J. Wilkinson, S. Stoll, M. Filella and J. Zhang, *Environmental Science & Technology* **1998**, *32*, 2887-2899.

[7] J. Buffle and G. G. Leppard in *Characterization of Aquatic Colloids and Macromolecules. 2. Key Role of Physical Structures on Analytical Results*, *Vol. 29* **1995**, pp. 2176-2184.

[8] G. E. M. Hall , G. F. BonhamCarter, A. J. Horowitz, K. Lum, C. Lemieux, B. Quemerais and J. R. Garbarino, *3rd International Symposium on Environmental Geochemistry* (Krakow, Poland) **1994**, pp. 243-249.

[9] S. R. Aston, I. Thornton, J. S. Webb, B. L. Milford and J. B. Purves, *Science of the Total Environment* **1975**, *4*, 347-358.

[10] R. Dahlqvist, M. F. Benedetti, K. Andersson, D. Turner, T. Larsson, B. Stolpe and J. Ingri, *Geochimica Et Cosmochimica Acta* **2004**, *68*, 4059-4075.

[11] W. X. Wang and L. D. Guo, *Environmental Science & Technology* **2000**, *34*, 4571-4576.

[12] T. Baumann, P. Fruhstorfer, T. Klein and R. Niessner, *Water Research* **2006**, *40*, 2776-2786.

[13] T. Kanti Sen and K. C. Khilar, *Advances in Colloid and Interface Science* **2006**, *119*, 71-96.

[14] Y. Ran, J. M. Fu, G. Y. Sheng, R. Beckett and B. T. Hart, *Chemosphere* **2000**, *41*, 33-43.

[15] C. Gueguen and J. Dominik, *Applied Geochemistry* **2003**, *18*, 457-470.

[16] S. W. Karickhoff, *Journal of Hydraulic Engineering* **1984**, *110*, 707-735.

[17] H. R. Rogers, *Colloids and Surfaces A: Physicochemical and Engineering Aspects* **1993**, *73*, 229-235.

[18] F. L. L. Muller, *Marine Chemistry* **1996**, *52*, 245-268.

[19] M. A. Morrison and G. Benoit, *Environmental Science & Technology* **2001**, *35*, 3774-3779.

[20] A. Gomez-Gutierrez, E. Jover, J. M. Bayona and J. Albaiges, *Analytica Chimica Acta* **2007**, *583*, 202-209.

[21] J. R. Lead, J. Hamilton-Taylor, W. Davison and M. Harper, *Geochimica Et Cosmochimica Acta* **1999**, *63*, 1661-1670.

[22] L. E. Schemel, B. A. Kimball and K. E. Bencala, *Applied Geochemistry* **2000**, *15*, 1003-1018.

[23] J. G. Oswald and M. Ibaraki, *Journal of Contaminant Hydrology* **2001**, *52*, 213-244.

[24] O. S. Pokrovsky and J. Schott, *Chemical Geology* **2002**, *190*, 141-179.

[25] *IUPAC Manual of Symbols and Terminology, Appendix 2, Part I, Colloid and Surface Chemistry Pure Appl. Chem.* **1972**, *31*, 578.

[26] W. Ostwald, *Z. Phys. Chem. (Leipzig)* **1907**, *34*, 295.

[27] J. Israelachvili, *Intermolecular and surface forces*, Academic press and imprint of Elsevier, **1991**, p.

[28] W. Stumm, *Chemistry of the solid-water interface: Processes at the mineral-water and particle-water interface in natural systems*, John Wiley & Sons, Inc., New York, **1992**, p.

[29] J. F. McCarthy and J. M. Zachara, *Environmental Science & Technology* **2002**, *23*, 496-502.

[30] J. N. Ryan and M. Elimelech, *Colloids and Surfaces a-Physicochemical and Engineering Aspects* **1996**, *107*, 1-56.

[31] J. Gerritsen and S. W. Bradley, *Limnol. Oceanogr.* **1987**, *32*, 1049-1058.

[32] R. A. Neihof and G. I. Loeb, *Limnol. Oceanogr.* **1972**, *17*.

[33] R. W. Puls, C. J. Paul and D. A. Clark, *Colloids and Surfaces a-Physicochemical and Engineering Aspects* **1993**, *73*, 287-300.

[34] A. I. Schäfer, U. Schwicker, M. M. Fischer, A. G. Fane and T. D. Waite, *Journal of Membrane Science* **2000**, *171*, 151-172.

[35] I. W. Hamley, *Introduction to soft matter, Polymers, Colloids, Amphiphiles and Lipid Crystals*, John Wiley & Sons, Ltd. , Chichester, England, **2003**, p.

[36] B. V. Derjaguin and L. Landau, *Acta Physicochim. URSS* **1941**, *14* 633.

[37] D. J. Shaw, *Introduction to Colloid and Surface Chemistry; 3 ed.*, Butterworths: London, **1980**, p.

[38] T. Cosgrove, *Colloid Science: Principles, Methods and Applications*, Blackwell Publishing, Oxford, UK, **2005**, p.

[39] R. Handy, F. von der Kammer, J. Lead, M. Hassellöv, R. Owen and M. Crane, *Ecotoxicology* **2008**, *17*, 287-314.

[40] B. Ulén, *Water, Air, & Soil Pollution* **2004**, *157*, 331-343.

[41] Y.-I. Chang and M.-C. Wang, *Colloids and Surfaces A: Physicochemical and Engineering Aspects* **2004**, *251*, 75-86.

[42] P. Christian, F. Von der Kammer, M. Baalousha and T. Hofmann, *Ecotoxicology* **2008**, *17*, 326-343.

[43] R. Kretzschmar, M. Borkovec, D. Grolimund, M. Elimelech and L. S. Donald in *Mobile Subsurface Colloids and Their Role in Contaminant Transport, Vol. Volume 66* Academic Press, **1999**, pp. 121-193.

[44] J. R. Lead. and K. J. Wilkinson., *Environmetal colloids and particles: Behaviour, Separation and Characterisation* **2006**, *John Wiley, Chichester, UK*, 1-15.

[45] A. Gunnars, S. Blomqvist, P. Johansson and C. Andersson, *Geochimica Et Cosmochimica Acta* **2002**, *66*, 745-758.

[46] J. M. Martin, M. H. Dai and G. Cauwet, *Limnology and Oceanography* **1995**, *40*, 119-131.

[47] M. L. Wells, *Nature* **1998**, *391*, 530-531.

[48] M. Filella and J. Buffle, *Colloids and Surfaces A: Physicochemical and Engineering Aspects* **1993**, *73*, 255-273.

[49] O. Gustafsson and P. M. Gschwend, *Limnology and Oceanography* **1997**, *42*, 519-528.

[50] K. J. Wilkinson, J. C. Negre and J. Buffle, *Journal of Contaminant Hydrology* **1997**, *26*, 229-243.

[51] A. Amirtharajah and P. Raveendran, *Colloids and Surfaces A: Physicochemical and Engineering Aspects* **1993**, *73*, 211-227.

[52] J. Nocito-Gobel and J. E. Tobiason, *Colloids and Surfaces A: Physicochemical and Engineering Aspects* **1996**, *107*, 223-231.

[53] A. B. Jódar-Reyes, A. Martín-Rodríguez and J. L. Ortega-Vinuesa, *Journal of Colloid and Interface Science* **2006**, *298*, 248-257.

[54] S. García-García, S. Wold and M. Jonsson, *Applied Clay Science* **2009**, *43*, 21-26.

[55] A. M. L. Kraepiel, K. Keller and F. M. M. Morel, *Journal of Colloid and Interface Science* **1999**, *210*, 43-54.

[56] M. Weiss, Y. Lüthi, J. Ricka, T. Jörg and H. Bebie, *Journal of Colloid and Interface Science* **1998**, *206*, 322-331.

[57] B. Nowack and T. D. Bucheli, *Environmental Pollution* **2007**, *150*, 5-22.

[58] A. P. Roberts, A. S. Mount, B. Seda, J. Souther, R. Qiao, S. Lin, P. C. Ke, A. M. Rao and S. J. Klaine, *Environmental Science & Technology* **2007**, *41*, 3025-3029.

[59] J. S. Kim, T.-J. Yoon, K. N. Yu, B. G. Kim, S. J. Park, H. W. Kim, K. H. Lee, S. B. Park, J.-K. Lee and M. H. Cho, *Toxicol. Sci.* **2006**, *89*, 338-347.

[60] S. Diegoli, A. L. Manciulea, S. Begum, I. P. Jones, J. R. Lead and J. A. Preece, *Science of the Total Environment* **2008**, *402*, 51-61.

[61] S. Iyer, Y. Kievsky and I. Sokolov, *Skin Research and Technology* **2007**, *13*, 317-322.

[62] R. D. Handy, R. Owen and E. Valsami-Jones, *Ecotoxicology* **2008**, *17*, 315-325.

[63] A. P. Klaine SJ, Batley GE, Fernandes TF, Handy RD, Lyon DY, Mahendra S, McLaughlin MJ, Lead JR., *Environmental Toxicoloy and Chemistry* **2008**, *27*, 1825-1851.

[64] X. Zhu, Y. Chang and Y. Chen, *Chemosphere 78*, 209-215.

[65] E. Casals, S. Vázquez-Campos, N. G. Bastús and V. Puntes, *TrAC Trends in Analytical Chemistry* **2008**, *27*, 672-683.

[66] J. R. Lead. and K. J. Wilkinson., *Environ. Chem.* **2006**, *3*, 159-171.

[67] B. Seredynska-Sobecka, A. Baker and J. R. Lead, *Water Research* **2007**, *41*, 3069-3076.

[68] Z. Tong, M. Bischoff, L. Nies, B. Applegate and R. F. Turco, *Environmental Science & Technology* **2007**, *41*, 2985-2991.

[69] F. B. Kim S, Eisler HJ, Bawendi M., *J. Am Chem Soc.* **2003**, *125*, 11466-11467.

[70] M. R. Kloepfer JA, Nadeau JL. , *Appl Environ Microbiol* **2005**, *71*, 2548-2557.

[71] M. Baalousha and J. R. Lead, *Environmental Science & Technology* **2007**, *41*, 1111-1117.

[72] K. A. Howell, E. P. Achterberg, A. D. Tappin and P. J. Worsford, *Environ.Chem.* **2006**, *3*, 199-207.

[73] O. S. Pokrovsky, B. Dupre and J. Schott, *Aquatic Geochemistry* **2005**, *11*, 241-278.

[74] B. P. Jackson, J. F. Ranville, P. M. Bertsch and A. G. Sowder, *Environmental Science & Technology* **2005**, *39*, 2478-2485.

[75] G. Benoit and T. F. Rozan, *Geochimica Et Cosmochimica Acta* **1999**, *63*, 113-127.

[76] M. A. Morrison and G. Benoit, *Journal of Environmental Quality* **2005**, *34*, 1610-1619.

[77] S. H. Li, H. T. Yang and C. P. Jen, *Nuclear Technology* **2004**, *148*, 358-368.

[78] R. Kretzschmar and T. Schafer, *Elements* **2005**, *1*, 205-210.

[79] H. Meier, E. Zimmerhackl and G. Zeitler, *Geochemical Journal* **2003**, *37*, 325-350.

[80] H. van de Weerd, A. Leijnse and W. H. Van Riemsdijk, *Journal of Contaminant Hydrology* **1998**, *32*, 313-331.

[81] S. B. Kim and M. Y. Corapcioglu, *Journal of Contaminant Hydrology* **2002**, *59*, 267-289.

[82] L. C. D. Anderson and K. W. Bruland in *Biogeochemistry of arsenic in natural waters: the importance of methylated species, Vol. 25* **1991**, pp. 420-427.

[83] A. B. Kersting, D. W. Efurd, D. L. Finnegan, D. J. Rokop, D. K. Smith and J. L. Thompson, *Nature* **1999**, *397*, 56-59.

[84] D. Grolimund, M. Borkovec, K. Barmettler and H. Sticher, *Environmental Science & Technology* **1996**, *30*, 3118-3123.

[85] B. D. Honeyman, *Nature* **1999**, *397*, 23-24.

[86] M. X. Guo and J. Chorover, *Soil Science* **2003**, *168*, 108-118.

[87] Y. G. Chen, K. N. Zhang and C. B. Huang, *Journal of Central South University of Technology* **2005**, *12*, 168-172.

[88] C. Shani, N. Weisbrod and A. Yakirevich, *Colloids and Surfaces A: Physicochemical and Engineering Aspects* **2008**, *316*, 142-150.

[89] H. M. Anawar, J. Akai, T. Yoshioka, E. Konohira, J. Y. Lee, H. Fukuhara, M. T. K. Alam and A. Garcia-Sanchez, *Environmental Geochemistry and Health* **2006**, *28*, 553-565.

[90] D. Vignati and J. Dominik, *Aquatic Sciences* **2003**, *65*, 129-142.

[91] R. W. Puis and R. M. Powell, *Environmental Science & Technology* **1992**, *26*, 614-621.

[92] G. Benoit, S. D. Oktaymarshall, A. Cantu, E. M. Hood, C. H. Coleman, M. O. Corapcioglu and P. H. Santschi, *Marine Chemistry* **1994**, *45*, 307-336.

[93] J. M. Ross and R. M. Sherrell, *Limnology and Oceanography* **1999**, *44*, 1019-1034.

[94] K. T. Valsaraj and I. Sojitra, *Colloids and Surfaces a-Physicochemical and Engineering Aspects* **1997**, *121*, 125-133.

[95] W. R. Penrose, W. L. Polzer, E. H. Essington, D. M. Nelson and K. A. Orlandini, *Environmental Science & Technology* **1990**, *24*, 228-234.

[96] M. H. Baik and S. Y. Lee, *Journal of Industrial and Engineering Chemistry 16*, 837-841.

[97] J. Buffle and G. G. Leppard in *Characterization of Aquatic Colloids and Macromolecules. 1. Structure and Behavior of Colloidal Material, Vol. 29* **1995**, pp. 2169-2175.

[98] R. Saindon and T. M. Whitworth, *Aquatic Geochemistry* **2006**, *12*, 365-374.

[99] G. F. BonhamCarter, A. J. Horowitz, K. Lum, C. Lemieux, B. Quemerais and J. R. Garbarino, *Applied Geochemistry* **1996**, *11*, 243-249.

[100] M. Waeles, V. Tanguy, G. Lespes and R. D. Riso, *Estuarine, Coastal and Shelf Science* **2008**, *80*, 538-544.

[101] M. Pédrot, A. Dia, M. Davranche, M. Bouhnik-Le Coz, O. Henin and G. Gruau, *Journal of Colloid and Interface Science* **2008**, *325*, 187-197.

[102] R. Liu and J. R. Lead, *Analytical Chemistry* **2006**, *78*, 8105-8112.

[103] A. Wilding, R. X. Liu and J. L. Zhou, *Journal of Colloid and Interface Science* **2005**, *287*, 152-158.

[104] M. L. Wells, G. J. Smith and K. W. Bruland, *Marine Chemistry* **2000**, *71*, 143-163.

[105] A. Wilding, R. Liu and J. L. Zhou, *Journal of Colloid and Interface Science* **2005**, *287*, 152-158.

[106] L. Sigg, H. Xue, D. Kistler and R. Sshönenberger, *Aquatic Geochemistry* **2000**, *6*, 413-434.

[107] S. B. Moran and K. O. Buesseler, *Journal of Marine Research* **1993**, *51*, 893-922.

[108] J. Buffle, D. Perret and M. Newman, *The use of filtration and ultrafiltration for size fractionation of aquatic particles, colloids and macromolecules.*, Lewis Publishers, Boca Raton, **1992**, p.

[109] F. J. Doucet, L. Maguire and J. R. Lead, *Talanta* **2005**, *67*, 144-154.

[110] C. Contado, G. Blo, F. Fagioli, F. Dondi and R. Beckett, *Colloids and Surfaces A: Physicochemical and Engineering Aspects* **1997**, *120*, 47-59.

[111] L. J. Gimbert, K. N. Andrew, P. M. Haygarth and P. J. Worsfold, *TrAC Trends in Analytical Chemistry* **2003**, *22*, 615-633.

[112] P. M. Shiundu, P. S. Williams and J. C. Giddings, *Journal of Colloid and Interface Science* **2003**, *266*, 366-376.

[113] Y.-T. Lin, M. Sung, P. F. Sanders, A. Marinucci and C. P. Huang, *Separation and Purification Technology* **2007**, *58*, 138-147.

[114] S. Rasouli, P. Blanchart, D. Clédat and P. J. P. Cardot, *Journal of Chromatography A* **2001**, *923*, 119-126.

[115] L. J. Gimbert and P. J. Worsfold, *Journal of Chromatography A* **2009**, *1216*, 9120-9124.

[116] R. Beckett, G. Nicholson, B. T. Hart, M. Hansen and J. Calvin Giddings, *Water Research* **1988**, *22*, 1535-1545.

[117] D. Perret, M. E. Newman, J.-C. Nègre, Y. Chen and J. Buffle, *Water Research* **1994**, *28*, 91-106.

[118] F. J. Doucet, L. Maguire and J. R. Lead, *Analytica Chimica Acta* **2004**, *522*, 59-71.

[119] J. R. Lead, W. Davison, J. Hamilton-Taylor and J. Buffle, *Aquatic Geochemistry* **1997**, *3*, 213-232.

[120] M. Filella, J. Zhang, M. E. Newman and J. Buffle, *Colloids and Surfaces A: Physicochemical and Engineering Aspects* **1997**, *120*, 27-46.

[121] I. P. Chung and D. Dunn-Rankin, *Journal of Aerosol Science* **1995**, *26*, 166-167.

Chapter 2

Synthesis, modification and characterisation of colloidal silicas

2.1 Introduction

This chapter describes the synthesis, characterisation and surface modification of sub-micron size silica particles having mean particle diameters between 100 and 1,000 nm.

2.1.1 Sub-micron silicas and their surface functionalisation

Silica particles have been developed to have specific pore or surface properties to suit their applications. These properties include pore size and shape, pore volume fraction, pore distribution as well as pore connection [1-3]. Several approaches have been used to synthesise sub-micron silicas. One of the best known is the Stöber method [4]. In 1968, Stöber and co-workers introduced the method for the synthesis of spherical monodisperse silica nanoparticles with diameters ranging from 50 nm to 2 μm. The method described by Stöber has since been used in many studies [5-7].

Two types of silica are discussed in this study; microporous silica and mesoporous silica. Microporous silica particles are those having pore size diameters less than or about 2 nm, whilst mesoporous silica particles have pore size diameters between 2 and 80 nm. Mesoporous silicas with uniform, controllable pore sizes and large internal surface areas have been developed [8] for applications in catalysis, membrane

filtration and separation technologies [9-14]. Theses silicas can be in a powder form with particle size ranging from 0.1 to 100 μm. They can also be in a monolithic form having size as large as 100 mm. Mesoporous silica can have a large specific area, reaching as large as 1,600 $m^2 g^{-1}$. Mesoporous silicas can be synthesised under acid or base conditions in the presence of surfactant templates. Silicas with a uniform pore size of about 1.22 nm could, for example, be synthesised in the presence of the surfactant, dodecyldimethybenzylammonium chloride under either under acidic or basic pathways[15]. The concentration of surfactant and other conditions (such as solvent choice, temperature, etc.) play important roles in changing the silica pore size and morphology[8]. A number of reviews of the synthesis and characterisation of these materials can be found in the literature [16-18].

Other approaches to synthesise silica particles with controlled size, size distribution and morphology have been reported. For instance, Mueller et al. [19] synthesised silica particles in methane/oxygen diffusion flames. The particles produced by this method were not agglomerated and the mean particle size was found to be 44-78 nm. Liou [20] obtained silica particles having an average particle size of 60 nm using the decomposition of rice husks in air. Jal et al. [21] synthesised silica particles by dissolving silica gel in sodium hydroxide solution over 2 days and then adding concentrated sulfuric acid to the alkaline silicate solution until the pH reached 7.5-8.5. The particles produced by this method had a mean diameter of 50 nm and the surface area was found to be 560 $m^2 g^{-1}$.

A number of works have reported the chemical modification of silica surfaces [17, 22, 23]. This is a convenient method for combining silicas with an organic molecule to alter their physical and chemical properties [24, 25]. In general, functionalisation of these materials can be carried out by two different approaches[26]. The first approach involves grafting the surface of the silica by reacting their surface silanol groups with, for example, an organoalkoxysilane compound carrying additional functional groups. The second approach consists of the simultaneous co-condensation (within the

synthesis medium) of an alkoxysilane precursor with a compound chosen to functionalise the material during the silica formation step. The modified silica particles are usually used for applications such as catalysis, analytical pre-concentration and for the removal of heavy metals from contaminated waters [27, 28]. Modification of silicas with chelating groups has been used for the enrichment of contaminants from seawater [29] and natural waters[30, 31]. The method has also been optimised to synthesise dye doped silica nanoparticles by covalently attaching organic fluorescent dye molecules to the silica matrix [6, 32-34].

To remove heavy metal ions from aqueous solutions, the surface of mesoporous silica needs to be functionalised by a chelating agent that has a selective reactivity for the target metal ion. The chelating ligand should be covalently bound since the physically adsorbed chelating ligand can be easily leached from the solid. Silicas functionalised with thiol groups [35-37] have been shown to be effective in removal of toxic metal ions from water and the used absorbents can be regenerated through a simple acid washing [38-40]. For example, Feng et al.[38] reported that thiol-functionalised mesoporous silicas were extremely efficient in removing mercury and other heavy metals from both aqueous and nonaqueous waste streams, with distribution coefficients up to 340,000. Nooney et al.[41] also found that these materials are effective in the removal of mercury and silver ions from aqueous solutions, with a mercury capacity of up to 1.26 mmol g^{-1}. Liang et al.[42] found that thiol-modified silicas had high capacities for Pb^{2+} and Cd^{2+}. The capacities were found to be 130 mg/g for Pb^{2+} and 39 mg/g for Cd^{2+}. Thiol-functionalised silica has also been successfully used for the enrichment of arsenite, lead, copper and zinc ions from natural waters[30].

Other metals have been found to be efficiently adsorbed on silica modified with organic chains containing one or more amine groups [43-45]. One of the earliest modifications of silica, reported by Leyden and Luttrell [46], was the functionalisation of silica surfaces with amine groups. Monoamine, diamine and triamine ligands were incorporated into mesoporous silicas by grafting[47] and co-condensation[48]. In

addition, multi amine-functionalised materials have been used in anion removal by copper-loaded amine-silica [49], CO_2 capture [50], and base catalysis in fine chemistry reactions [51]. Sayen and Walcarius [52] reported the modification of mesoporous silica and clay with amine groups. These silica products were used for the determination of Cu(II).

Silica-bound amine groups in which their surfaces have been converted to mono- and bis-dithiocarbamates (DTC) were found to have twice the metal binding capacity of the unconverted anions. Dithiocarbamates were reported to form strong complexes with noble metals and transition elements. For instance, Espinola et al.[53] reported the preparation of a bis-dithiocarbamate ligand anchored on silica gel that exhibited high selectivity for cobalt. Venkatesan et al.[54] subsequently investigated the effect of pH, concentration, time and temperature on the extraction of cobalt(II) on Si–DTC and found that this modified surface contained 0.37 mmol g^{-1} of the ligand sites available for the extraction of cobalt. The sorbent extracted cobalt only when the pH of the aqueous phase was above 7.

In the present work, colloidal silica particles were synthesised in the laboratory and used in the investigation of the behaviour of colloid-bound pollutants in natural waters. Both microporous and mesoporous silicas were prepared and their properties were compared. The synthetic approaches and their analysis are shown in Figure 1.

In this chapter, details of the synthesis and characterisation of micrometer-sized silica spheres with mesoporous structures with various mean particle sizes were also discussed. Monodisperse mesoporous silica spheres with diameters ranging from 0.10 to 1.00 μm were produced. When the desired particle size had been achieved, the silica surfaces were modified with an amine or thiol functionalised linker group to which a fluorescent label could be attached. These silicas were used for the investigation of how particle size affected analytical measurement procedures that employ conventional filtration; this will be described in Chapter 3.

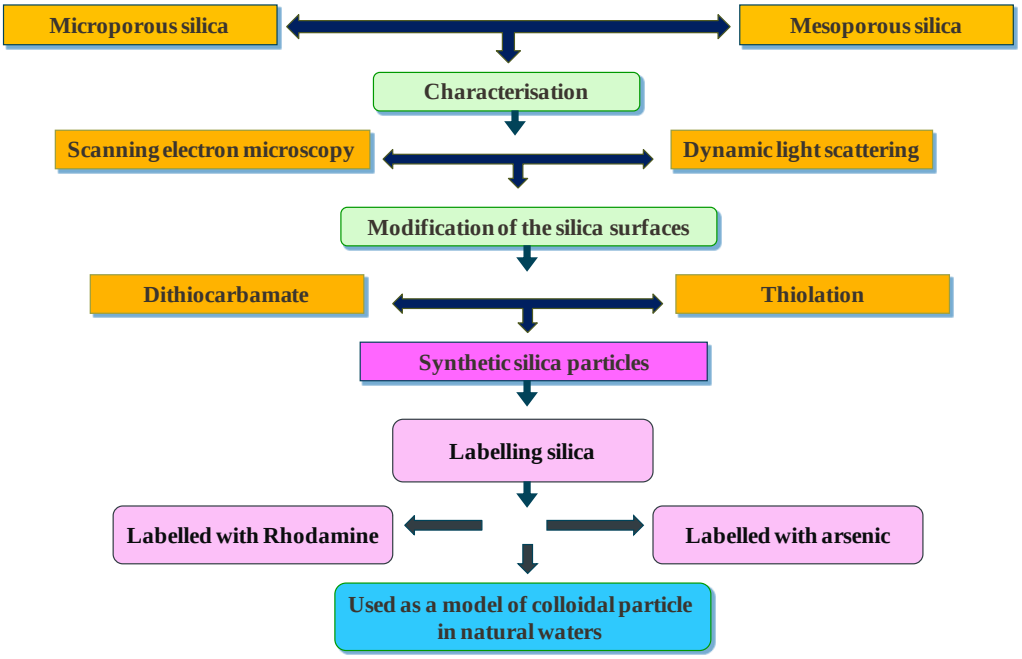

Figure 1 Sub-micron silica synthesis and its characterisation.

2.2 Synthesis, modification and characterisation of silica

2.2.1 Syntheses of silica particles

Two approaches were used to prepare sub-micron sized silica particles. One approach was based on the Stöber method whilst another involved the use of a template such as n-dodecyltrimethylammonium bromide (C_{12}TMABr) surfactant to produce mesoporous silicas.

2.2.1.1 Materials

Tetraethoxysilane (TEOS) (98%), tetramethoxysilane (TMOS), tetraethylamine (TEA) and 3-mercaptopropyltrimethoxysilane (MPTMS, 95%) were obtained from Aldrich (Poole, UK). Ammonium hydroxide (NH_4OH) (SG=0.88, 35% (w/v)), n-dodecyltrimethylammonium bromide (C_{12}TMABr) and ethylene glycol ($C_2H_6O_2$) were purchased from Alfa Aesar (Lancashire, UK). Sodium hydroxide (NaOH) and

reagent grade methanol (MeOH) were purchased from Fisher Scientific (Leicestershire, UK). Water was purified by deionization using the Elga Option 4 system. All glasswares was soaked in hydrochloric acid (5% v/v) overnight and then rinsed well with deionised water before use.

2.2.1.2 Preparation of microporous silicas

Microporous spherical silica particles were produced by the following method[7]: 250 mL of NH_4OH (SG= 0.88) and 250 mL of MeOH were mixed in a 1 L conical flask for 5 minutes using a magnetic stirrer. 5 mL of TEOS was slowly added, whilst continuing vigorously stirring. The reaction was left to proceed at 20 ^oC for one hour. The product was then centrifuged at 3,000 g for 60 minutes and the supernatant was discarded. The obtained silica was rinsed with MeOH typically at least 5 times, discarding the solvent at each stage after centrifugation. Following this step, the silica product was dried at 110 ^oC then kept under continuous vacuum overnight.

2.2.1.3 Preparation of mesoporous silicas

2.2.1.3.1 250 nm sized mesoporous silicas

The 250 nm mesoporous silica particles were obtained using a C_{12}TMABr surfactant template. The synthesis was carried out using the method reported by Yamada and Yano[55] and is described in detail below.

0.42 g of C_{12}TMABr and 0.75 mL of 1M NaOH were dissolved in 22.5 mL of ethylene glycol and 77.5 mL of water. After stirring for 15 minutes, 0.45 mL of TMOS was added into the solution and the mixture was continuous stirred at 20 ^oC. The reaction resulted in the formation of a white precipitate. After leaving the reaction for 8 hours, the white powder was washed with deionised water at least 5 times and dried at 60 ^oC for 72 hours. The white powder obtained was then heated in a muffle furnace at 550 ^oC for 8 hours to remove the organic template.

2.2.1.3.2 Various sizes of mesoporous silicas

Mesoporous silicas with different particle sizes (other than 250 nm) were produced using a two step process, an initial acid catalysis step followed by a second base-catalysed step.

The initial acid catalysis step[17] proceeded as follows. 80 mL of water was placed in a 100 mL beaker and acidified with 1.6 mL of 0.1 M HCl (pH 2.7), while stirring at a moderate rate using a magnetic stirrer and 10 mL of MPTMS (95%) was then added. The MPTMS was initially insoluble and formed an emulsion that gradually disappeared as the MPTMS hydrolysed and became more soluble. The solution was then left to react with stirring for more than 8 hours; a new emulsion phase appeared that was centrifuged to separate it into 2 phases. The aqueous supernatant was separated from the oil and diluted with HCl in water (pH 3.5) to obtain various concentrations (1.5, 3, 5, 10, 50, and 100%) of the supernatant phase.

In the second base-catalysed step, 100 μL of TEA (99%) was rapidly injected into 100 mL aliquots of the supernatant–water mixture, after 8 hours of continuous stirring. Approximately 30 minutes after the addition of TEA, the formed particles were separated from solution by centrifugation at 2000 g for 5 minutes and then washed in ethanol.

2.2.2 Modification of the silica surfaces

Two methods were used to modify silica surfaces. The first method was the thiol modification of pre-formed spherical silica particles. The second method was based on the addition of a diamine functionalised silane (Dow Corning Z-6094) during the formation of the silica.

2.2.2.1 Materials

Tetraethoxysilane (TEOS) (98%), 3-mercaptopropyltrimethoxysilane (MPTMS, 95%), and glacial acetic acid were obtained from Aldrich (Poole, UK). Sodium hydroxide (NaOH) was purchased from Fisher Scientific (Leicestershire, UK). Ammonia hydroxide (NH_4OH) (SG=0.88), n-propanol (C_3H_8O), toluene (C_7H_8) and methanol (MeOH) were reagent grade. Toluene was dried by Dean-Stark distillation. Carbon disulfide (CS_2) was obtained from Rathburn (UK). N-[3-(trimethoxysilyl)propyl]ethylenediamine (Dow Corning (Z-6094)) was supplied by Aldrich (Poole, UK) . Water was purified by deionisation using an Elga Option 4 system.

2.2.2.2 Reagents

Arsenious oxide (As_2O_3) was obtained from Hopkin & Williams Ltd, (London). A 1,000 mg L^{-1} stock solution of As(III) was prepared by dissolving 0.1322 g of As_2O_3 into a beaker with small amount of water and 1 pellet of NaOH. After that, HCl solution was added until a pH of 4 was achieved. The solution was then made up to 100 ml (1,000 mg L^{-1}) with deionised water. Rhodamine B was purchased from Avocado Research Chemical Ltd (Heysham, UK). A 100 mM Rhodamine stock solution was prepared by dissolving 4.7902 g of Rhodamine B (RhB) in 100 ml methanol.

2.2.2.3 Preparation of thiol-modifed silicas

The thiol-modified silica was produced by the following procedure: 25 mL of dry toluene was mixed with 3 mL of MPTMS in a 100 mL round bottom flask. Whilst under gentle and continuous stirring, a known weight of 250 nm sized silicas (*ca.* 1 g) was added, followed by 0.15 mL of glacial acetic acid. The flask was fitted with a water condenser and the mixture was stirred for 2 hours under nitrogen, and then heated at 60 ^{o}C for 2 hours. The product was isolated by centrifugation. Methanol was

added to wash the silica and the mixture was sonicated and then centrifuged to isolate the solid. This washing stage was repeated 2-3 times. The product was dried under continuous vacuum overnight and stored in a glass vial under nitrogen in the dark at a temperature below 4°C. Figure 2 shows a schematic diagram showing the modification of silica with MPTMS.

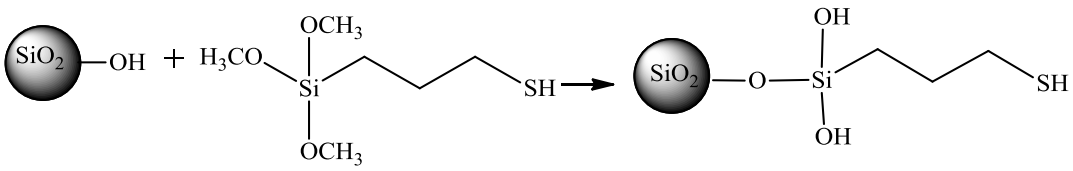

Figure 2 Modification of silica with 3-mercaptoproply-trimethoxysilane.

2.2.2.4 Preparation of dithiocarbamated silicas (DTC)

Two preparation steps were used to produce the DTC silicas. The first step was to produce diamine silicas and the second was to convert diamine silicas to DTC by the addition of carbon disulfide (CS_2).

2.2.2.4.1 Diamine silica

The diamine silica was synthesised using the following procedure (Figure 3). 80 mL of dry toluene (dried by Dean-Stark distillation) was transferred to a 250 mL round-bottom flask fitted with a reflux condenser. *Ca.* 1 g of 250 nm sized silica (dried in an oven at 120°C overnight) was dispersed in the toluene. The mixture was agitated using a magnetic stirrer for 15 minutes and then heated to 90 °C under nitrogen with constant stirring. After the temperature had stabilized, 4 mL of N-[3-(trimethoxysilyl)propyl]ethylenediamine was slowly added to the flask. After 4 hours, the reaction mixture was allowed to cool. It was then centrifuged (3,000 g) and the supernatant removed. The product was rinsed thoroughly with toluene, and dried overnight under vacuum.

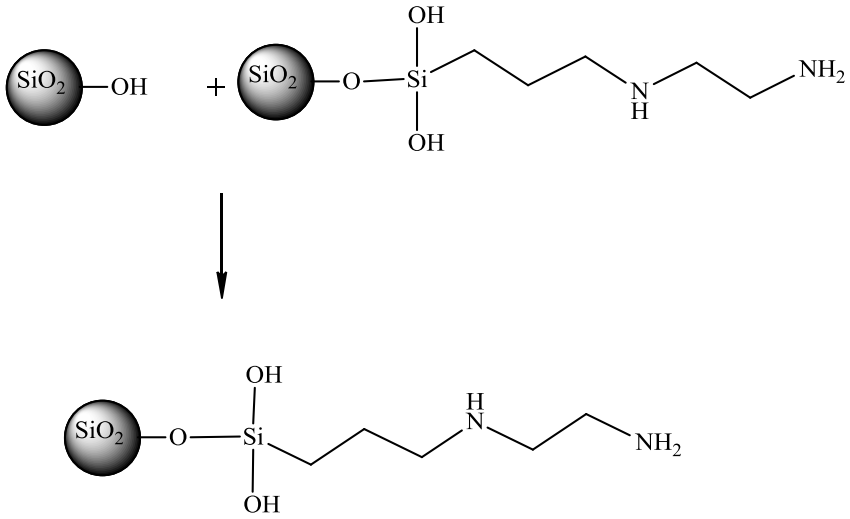

Figure 3 Modification of silica with N-[3-(trimethoxysilyl)propyl]ethylenediamine (Z-6094).

2.2.2.4.2 Bis-dithiocarbamated-silica (DTC-Si)

Figure 4 illustrates the steps involved in the production of the bis-dithiocarbamated silicas. The bis-dithiocarbamated silica was formed [7] by mixing *ca.* 1 g of diamine-silica (prepared as described in Section 2.2.2.3.1) with 20 mL of deionized water, 2 mL of CS_2, 2 mL of n-propanol and 0.5 mL of 0.1 mol l^{-1} NaOH(aq). The mixture was stirred for 15 minutes. The solution was then centrifuged. The supernatant was removed and the solid product was rinsed 4 times with n-propanol and then once with MeOH. The product was dried under vacuum and stored in the dark under nitrogen at 4 °C.

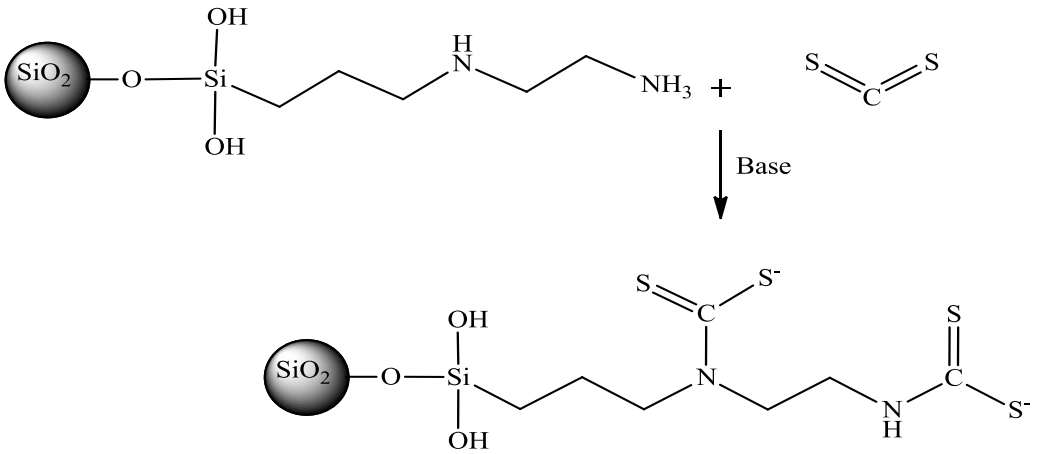

Figure 4 Modification of diamine silica with CS_2.

2.2.2.5 Preparation of the labelled silicas

In the present work, arsenic-labelled, fluorescent-labelled, and Rhodamine B silicas, were prepared.

2.2.2.5.1 Arsenic-labelled silicas

In this section, the synthesis of arsenic-bound modified silicas and the analytical technique employed for the determination of the quantity of arsenic released from silica surfaces are reported. Silica particles were made by binding arsenic (*ca.* 10 mmol g^{-1} arsenic) to the modified silicas (from previous section). The binding of arsenic depends on the pH and redox potential of its environment[56]. The complexation of arsenic by dithiocarbamates was reported to be favoured at pH 4 [57, 58].

Method

Ca. 0.1 g of modified silica (DTC-Si or SH-Si) was added to an aqueous solution of 75 mg of As (III) in pH 4 buffer (1,000 mg L^{-1}), mixed for 30 minutes using sonication, then centrifuged for 1 hour to isolate the particles from the solution. The solid was rinsed at least 5 times with pH4 buffer to remove unbound arsenite. Methanol was used for the final rinse to dry the product. After washing, the product was dried and kept under vacuum.

2.2.2.5.2 Rhodamine-labelled silica

Rhodamine-labelled thiol-modified silicas were prepared using the method described in detail below.

Method

Ca. 0.1 g of thiol- silica was transferred into a 10 mL polypropylene tube and 5 mL of Rhodamine B (100 mM) in methanol was added to the tube. The tube was sonicated for 60 minutes and then centrifuged (at 5,000 g) for 30 minutes. The pink solution was removed and discarded while the pink particles at the bottom of the tube were collected and washed with 10 mL of methanol, followed by sonication and centrifugation in order to get rid of excess Rhodamine. This washing stage was carried out until no significant further release of Rhodamine was visually observed. The pink particles were then dried at 60 ^{o}C in an oven overnight.

2.2.3 Characterisation and analysis of the silica products

To demonstrate whether the syntheses of the modified silicas had been successful, the silica products were examined by scanning electron microscopy (SEM) and light scattering.

2.2.3.1 Particle size and particle morphology

The SEM used was a Philips Co., XL-30 ESEM normally operated at an acceleration voltage of 30 kV, secondary electron imaging (SEI). Two sample preparation methods were used and employed as appropriate.

2.2.3.1.1 Suspended particles

Samples were prepared by mixing of *ca.* 10 mg of silica particles in 10 mL of deionised water that had been pre-filtered through a cellulose nitrate membrane filter (pore size 0.45 μm). The silica dispersion was ultasonicated for 5 minutes. 1 drop of the dispersion was then applied to an acetone-washed glass slide, fitted on an aluminum SEM stub and the samples were allowed to dry at room temperature.

2.2.3.1.2 Gold precoating of the SEM stub

Ca. 0.1 mg of thiol-silica was suspended in 30 mL of deionised water. One drop of the suspension was put onto the gold coated stub and allowed to evaporate.

The sample stub was finally coated with a *ca.* 10 nm thick gold film, using a Hummer 6.2 sputtering system (Anatech Ltd). The following conditions were employed: 5 psi argon gas, current ~15 mA with 6 minutes of coating. The number-average particle sizes were determined by counting at least 200 particles from SEM micrographs.

2.2.3.2 Particle size distribution

Particle size distributions were examined using a dynamic light scattering technique (DLS). The DLS measurements were conducted using a Coulter N4 plus instrument (Coulter Electronics Instruments, Miami, Fl, U.S.A) fitted with a 20 mW He-Ne laser (632.8 nm) and the detector angle was set at a 90° scattering angle. The measurements were performed using dispersions containing a particle concentration of 0.01 wt. % unless otherwise stated. This concentration gives a photon count rate between 10 and 200 kcps (kilocounts per second) as suggested by the instrument manufacturer. During the measurements, the sample temperature was controlled at 20 ± 1 °C. The sample dispersion was prepared as follows: *ca.* 10 mg of silica was mixed in 5 mL of filtered (cellulose nitrate membrane filter, pore size 0.45 μm) deionised water. The dispersion was ultrasonicated for about one hour and then transferred to a glass cuvette. The particle size distribution was then measured.

2.2.3.3 Thiol and copper capacities of the modified silica

2.2.3.3.1 Materials

Rhodamine B and sodium borohydride ($NaBH_4$) were purchased from Avocado Research Chemical Ltd (Heysham, UK). Hydrochloric acid (HCl, 37% w/v) was obtained from Fluka (Gillingham, UK.). Sodium hydroxide (NaOH) and reagent grade methanol (MeOH) were purchased from Fisher Scientific (Leicestershire, UK). Water was purified by deionisation using an Elga Option 4 system. All glassware were cleaned by soaking in 5% (v/v) HCl overnight and then rinsed well with deionised water.

2.2.3.3.2 Reagents

A 100 mM Rhodamine stock solution was prepared by dissolving 4.7902 g of Rhodamine B (RhB) in 100 ml methanol. A series of Rhodamine solutions (0, 5, 50, 100, 200, 400 and 600 nM) were subsequently prepared by diluting the stock solution with 1M methanolic NaOH. The structure of RhB is shown in Figure 5.

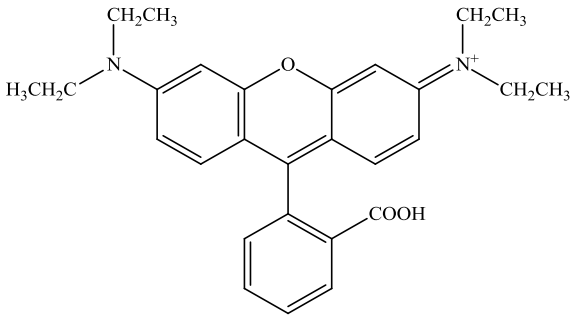

Figure 5 The structure of Rhodamine B (RhB).

A standard copper solution containing 1,000 µg Cu mL^{-1} was prepared by dissolving 3.9292 g of copper (II) sulphate pentahydrate in 1L of deionized water**.**

2.2.3.3.3 The thiol capacity

To determine the thiol-content of the thiol-modified silica, a fluorescence method was employed. The Rhodamine fluorophore was covalently bound to the thiol-modified silica particles and subsequently released by mixing with methanolic NaOH. This fluorescence signal from the released Rhodamine was measured and the thiol capacity of the silica was determined by relating the signal magnitude to a standard Rhodamine B (RhB) calibration curve.

Rhodamine calibration solutions were prepared by dilution of the RhB stock solution in 1M methanolic NaOH. Fluorescence was measured at 543 nm excitation and 564 nm emission using a Perkin Elmer LS-5B spectrometer. The RhB equivalent concentration in the solutions was calculated using by interpretation of the RhB calibration data.

Method

Accurately weighed portions of thiol-silica (*ca.* 50 mg) were transferred into 10 mL polypropylene tubes and 5 mL of Rhodamine B (100 mM in methanol) was added to each tube. The tubes were sonicated for 2 minutes, shaken for a further 60 minutes and then centrifuged (3,000g) for 10 minutes. The supernatant was removed and 10 mL of methanol was added to rinse the Rhodamine-bound silica particles. The mixture was then centrifuged and the supernatant was discarded. This washing stage was repeated until no further release of Rhodamine was visually observed (pink solution). 5 mL of 1M methanolic NaOH was then added to the silica and the mixture was shaken for 5 minutes before centrifugation (8,000 g). The first resulting solution was transferred into a 10 mL flask and the hydrolysis step was repeated using a further 5 mL of methanolic NaOH. The second batch of methanolic NaOH was added to the first and the solution made up to the mark. The Rhodamine was immediately determinated by spectrofluorimetry.

2.2.3.3.4 The copper capacity

To determine whether the synthesis of the diamine and bis-dithiocarbamate silicas had been successful, the silica particles were bound to copper. The copper capacity of the diamine and bis-dithiocarbamate silicas was measured using flame atomic absorption spectroscopy (AAS). The AAS used was a Perkin Elmer 2380 instrument. The conditions employed were those recommended by the instrument manufacturer.

Method

An accurate weight (10 mg) of diamine or DTC-silica was placed in a 10 mL glass tube. 5 mL of Cu (II) (1000 µg mL^{-1}) solution was added to the tube. The mixture was shaken for 5 minutes, left in a water bath at 40°C for 5 minutes, and allowed to cool to room temperature. After being cooled, the tube was centrifuged and the supernatant was discarded. The product was rinsed 5 times with deionised water. For each rinse the water was added to the tube, the tube was then shaken and centrifuged. 10 mL of 6 mol L^{-1} HCl was added to the silica in the tube in order to release the bound copper. The mixture was then centrifuged for 5 min and the acidic solution was transferred to a 100 mL volumetric flask. 10 mL of HCl was again added to the tube; the second acidic solution was transferred to the same volumetric flask. The flask was made up to the mark with deionised water. The copper content of the solution was measured by flame AAS at 324.7 nm.

2.2.3.4 Analysis of arsenic-labelled thiol-modified silica (As-Si)

2.2.3.4.1 The arsenic content of the silicas

The arsenic loaded thiol-silica (SiSH-As) and DTC-silica (SiDTC-As) were analyzed for arsenic content using two digestion methods; 1) dry ashing with a the mixture of magnesium oxide and magnesium nitrate[59] and 2) wet ashing with aqua regia. The arsenic content was then measured by hydride generation atomic absorption

spectroscopy (HG-AAS), with atomization in an electrically heated silica tube and detection at λ=193.7 nm with a Perkin-Elmer 3100 Atomic Absorption Spectrophotometer (using the parameters described in Appendix A).

Method 1 Dry ashing digestion: the method is employed as follows: *ca.* 10 mg of arsenic loaded silica was put into a 10 mL beaker, followed by 1 mL of Mg mixture [2% (w/v) $Mg(NO_3)_2$ and 0.2% (w/v) MgO], and warmed at 130 ^oC for 30 minutes to remove any traces of water. The beaker was then placed in the muffle furnace at 550 ^oC for a further 3 hours. Once the sample had cooled, the ash samples were each dissolved in 5 mL of hydrochloric acid (37% w/v) with the assistance of a hotplate and and diluted with deionised water to 50 mL.

Method 2 Wet ashing digestion: the digestion of the sample in acidic media using a combination of acids such as nitric acid was employed. Aqua regia digestion was employed as follows, *ca.* 50 mg of arsenic loaded silica was put in a 50 mL beaker and 4 mL of aqua regia solution (3.5:10.5 v/v HNO_3:HCl)[60] was added. The mixture was warmed gently for 1 hour and left to cool. After that, the mixture was filtered (Whatman GF/C) and diluted with deionised water in a 50 ml volumetric flask.

Finally, the concentrations of total arsenic in the digests were determined by HG-AAS.

2.2.3.5 Analysis of Rhodamine-labelled thiol-modified silica (SiSH-Rh)

Fluorescence labelling techniques enable measurements with high sensitivity. Most of the methods used for the preparation of fluorescent particles are based on physical adsorption or covalent binding to connect the fluorophores to the solid [34, 61-63]. In theory, fluorescence is detected and identified by changes in the emission and excitation of the spectra. Rhodamine B was attached to 250 nm man-made colloidal

particles. The fluorescence measurement and calibration curve of standard Rhodamine are given in Appendix D.

2.2.3.5.1 The spectra of Rhodamine in different solvents

Four solvents: water, 1M methanolic NaOH, MeOH and aqueous 1M NaOH were chosen for the study of the effect of different solvents on the Rhodamine spectrum. Rhodamine B was investigated through a series of emission experiments in different solvent environments.

Method

The experiment was carried out as follows: 5 mL of an aqueous Rhodamine standard solution (200 nmole dm^{-3}) was put into a glass vial and 5 mL of solvent was added. The mixture was mixed then heated at 80 ^{o}C for one hour. After cooling, the solution was transferred into a volumetric flask and diluted to 25 mL with deionised water. The emission spectrum was then acquired using 543 nm excitation.

2.2.3.5.2 The Rhodamine content of the silica products

To determine whether the Rhodamine bound thiol-silica (SiSH-Rh) had been successfully synthesised, the analysis of the Rhodamine content was carried out using the following method:

Method

An accurate weight of SiSH-Rh (*ca.* 2 mg) was transferred into a 10 mL polypropylene tube and 10 mL of deionised water was added. The tube was sonicated for 30 minutes and then centrifuged for 15 minutes (speed 2,000 g). The supernatant was removed and a second 10 mL aliquot of deionised water was added. The mixture was then repeatedly sonicated and centrifuged with the removal of the supernatant. 5 mL of 1.0M methanolic NaOH was added and the mixture was sonicated for 30

minutes before centrifugation. The pink solution (the first batch) was transferred into a 10 mL flask and the hydrolysis step was repeated using a further 5 mL of methanolic NaOH. This second batch of methanolic NaOH was added to the first and made up to the mark. The Rhodamine was immediately determined by spectrofluorimetry.

2.3 Results and discussion

2.3.1 Size distribution and morphology

2.3.1.1 Microporous silicas

Figure 6a shows a typical SEM micrograph of the microporous silica particles whilst Figure 6b illustrates their particle size distribution. The average particle diameter obtained from SEM was found to be 252.3 nm with SD 12.7 (% CV = 5.0) whilst the diameter determined from DLS was found to be 292.9 ± 23.4 nm (% CV = 8.0). The silica particles are spherical and appear to have a narrow size distribution, as judged by the relatively low coefficient of variation (CV).

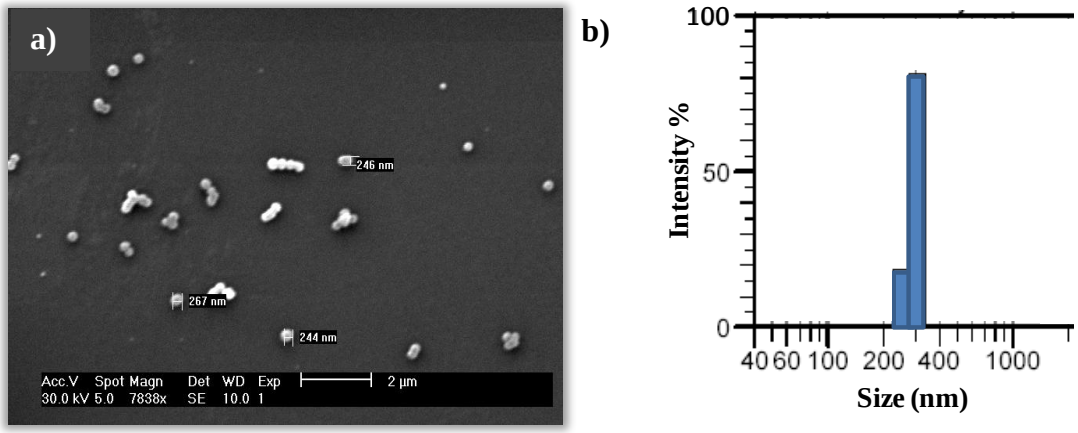

Figure 6 a) SEM micrographs of the microporous silicas, b) their particle size distribution determined by DLS.

The particle size obtained from SEM was slightly smaller than that obtained from DLS for these microporous silica particles. Generally, particle sizes measured by SEM are smaller than the corresponding sizes measured by DLS. The larger sizes by DLS result from the fact that they include the hydrodynamic layer around the particles, whereas the sizes obtained from SEM are the sizes of dehydrated particles [64]. In this work, however, the difference is significant not only because of the difference between hydrated and dehydrated particles, but also because DLS data are heavily weighted to the larger particles. It is also possible that the larger particles measured by DLS were that size due to particle aggregations. Light is scattered more strongly from larger particles. Considering the aggregation of particles, silica particles having small sizes will have a higher thermodynamic surface energy, which drives the silica particles to come close together to obtain a stable state [65]. The particle aggregations should not prevent meaningful interpretation of the synthesis of the microporous silica. The particle sizes determined by the two methods should have been made more comparable by using ultrasonication to disaggregate the silica particles before the DLS size measurement.

Regarding to the size of the silica particle determined using SEM, it can be considered that microporous silica with a diameter of 250 nm had been successfully synthesized.

2.3.1.2 Mesoporous silicas

An SEM image and particle size distribution of the mesoporous silica is shown in Figure 7. The particle size of the mesoporous silicas determined by SEM was found to be 240.4 ± 27.9 nm (%CV = 11.6) (Figure 7A) and 351.9 ± 76.6 nm (%CV = 21.8) (Figure 7B) when measured by DLS. As explained in the previous section, a lack of agreement of particle sizes measured using SEM and DLS is believed to be the result of particle aggregations. This evidence was supported by the SEM micrograph as large clusters of particles can be clearly seen (Figure 8).

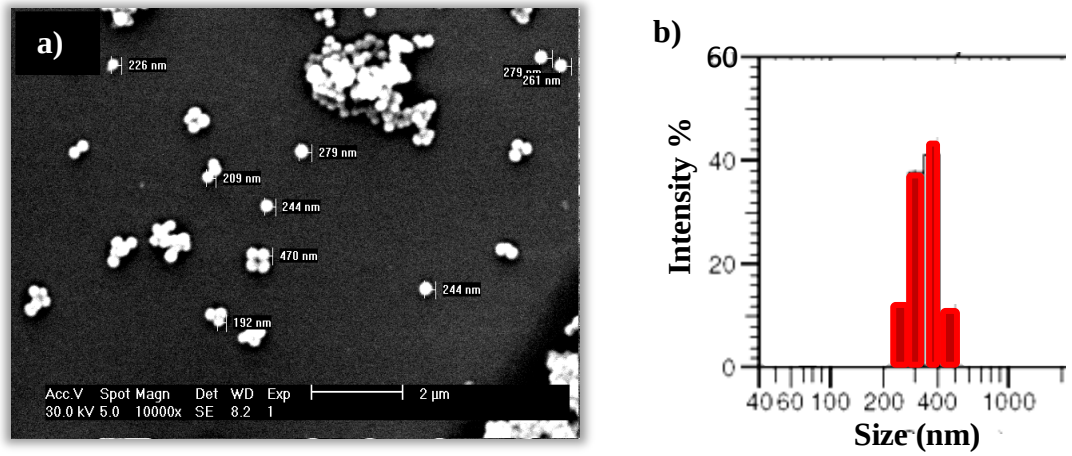

Figure 7 a) SEM micrographs of aggregates of mesoporous silicas and b) particle size distribution obtained by DLS.

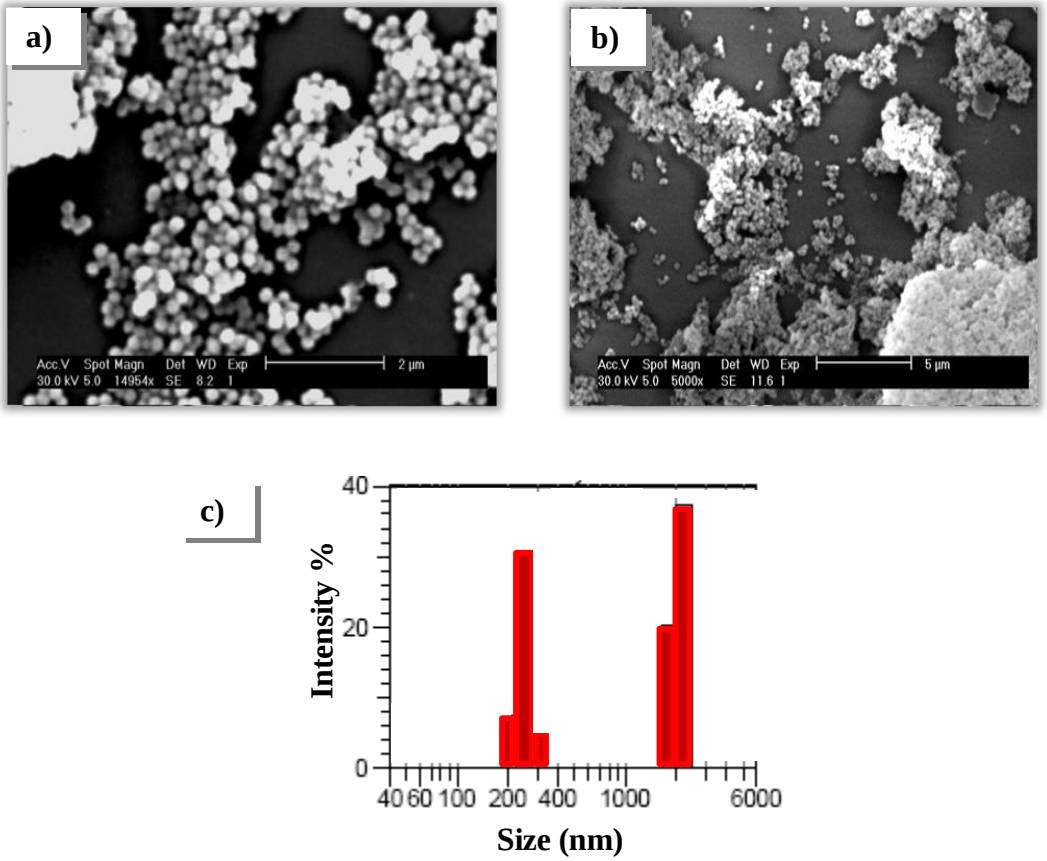

Figure 8 SEM image of the mesoporous silicas; a) high magnification (14,954x), b) low magnification (5,000x) and c) particle size distribution.

The clusters observed in the SEM images (Figure 8) were probably formed during solvent evaporation in the sample preparation process. Particle aggregation during the particle size measurement by DLS led to a bimodal size distribution with the mean diameter of 245 nm (± 27.5 nm) for the first population, whereas the mean diameter of the second population was found to be ca. 2,000 nm (Figure 8c). These results support those obtained by SEM.

Interestingly, the mesoporous silicas were found to aggregate more than the microporous silicas. This may be due to the higher surface area of the mesoporous silicas resulting in the higher surface energy that drives the particles to aggregate more easily.

2.3.2 Various sizes of mesoporous silicas

The tendency of colloidal particles to aggregate was found to be a problem for the SEM investigation. Aggregation of colloidal silicas was usually found, especially for particles with small sizes as shown in Figure 8a) and 8b). To prevent this problem, an ultrasonic treatment of particles in aqueous suspension was employed. The ultrasonic treatment typically enables the separation of most aggregates into isolated individual particles or smaller aggregates. Further efforts to prevent aggregation during SEM characterisation are now reported. Attempts to disaggregate the thiol modified silica particles were performed by using gold pre-coating of the SEM stub (Section 2.2.3.1.2). This method was used for the characterisation of the small silica particles (Figure 9).

SEM micrographs of particles are shown in Figure 9 and Figure 10. These images show the successful synthesis of spherical silica particles with sizes being dependent on the different dilutions of the emulsion phase. As can be seen in Figure 10, using a low dilution (high percentage) resulted in larger silica particle sizes whilst using a high dilution (lower percentage) of emulsion phase lead to the production of particles

of smaller size. As shown in Figure 9A, the size of the silica particles synthesised from the 1.5% dilution of the supernatant phase was found to be approximately 100-170 nm in diameter. As the percentage of emulsion phase increased the particle size was found to increase (size increases form Figure 9A to Figure 10F). At the highest percentage of emulsion phase (minimum dilution of supernatant phase with water) (Figure 10F), the biggest size particles were obtained, with a diameter ranging from 2 to 3 μm. The particle sizes obtained using DLS (Figure 9a-9c and Figure 10d-10f) were found be similar to those obtained using SEM.

In summary, the spherical sub-micron mesoporous silica particles of various sizes ranging from 100-1,000 nm were successfully produced.

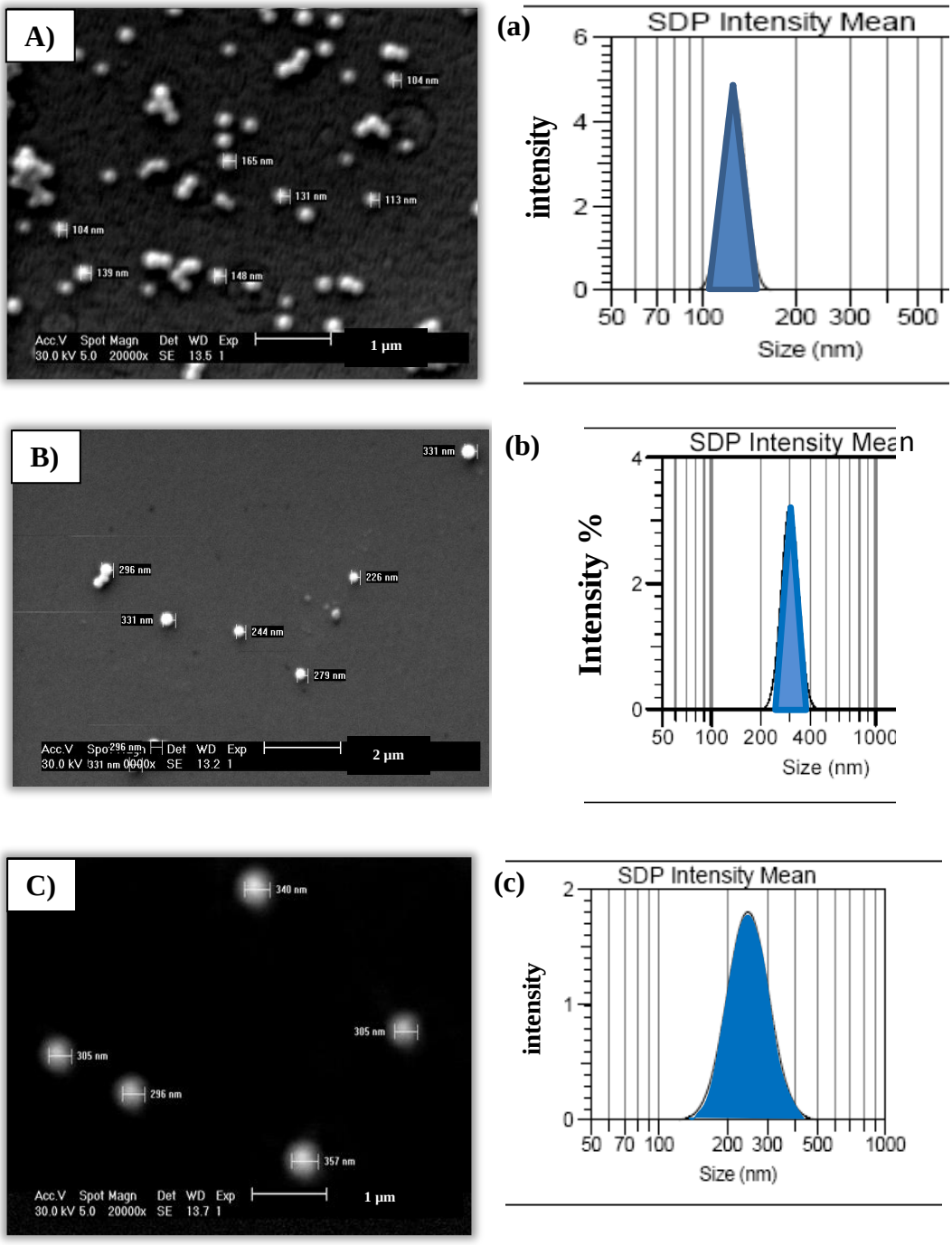

Figure 9 Capital letters (A-C) refer to the SEM micrographs (preparation using the method reported in 2.2.3.1.2) of mesoporous silica formed using the dilution of the supernatant phase (1.5, 3 and 5%) resulting in particles of various sizes: A) 100-170 nm, B) 200-400 nm, C) 300-500 nm. Small letters (a-c) refer to their particle size distributions determined by DLS.

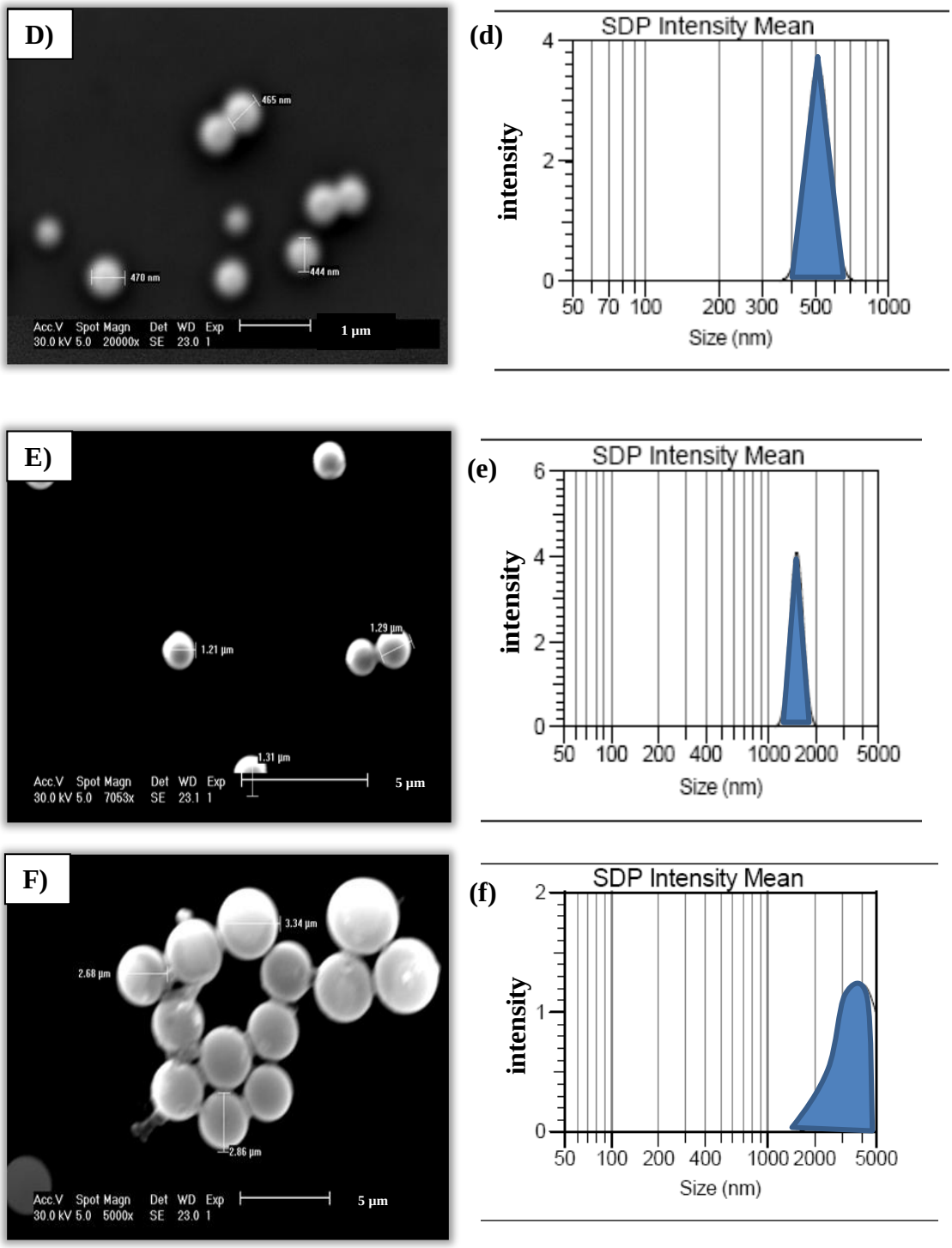

Figure 10 Capital letters (D-F) refer to the SEM micrographs (preparation using the method reported in 2.2.3.1.1) of mesoporous silica formed using the dilution of the supernatant phase (10, 50 and 100%) resulting in particles of various sizes: D) 400-800 nm, E) 1,000-1,500 nm, and F) 2,000-3,000 nm diameter. Small letters (d-f) refer to their particle size distributions determined by DLS.

2.3.3 Thiol capacity of thiol-modified silicas

Rhodamine B (RhB) was bound to the thiol-modified silica particles (Section 2.2.3.3.3) and released and measured by spectrofluorimetry. RhB was chosen because of its high molar extinction coefficient (106,000 M^{-1} cm^{-1} at 542.75 nm in ethanol) and high fluorescence quantum yield. It can therefore be sensitively measured by spectrofluorimetry[66]. This fluorophore was covalently bound to the thiol-modified silica particles as in the proposed [66] reaction scheme shown in Figure 11.

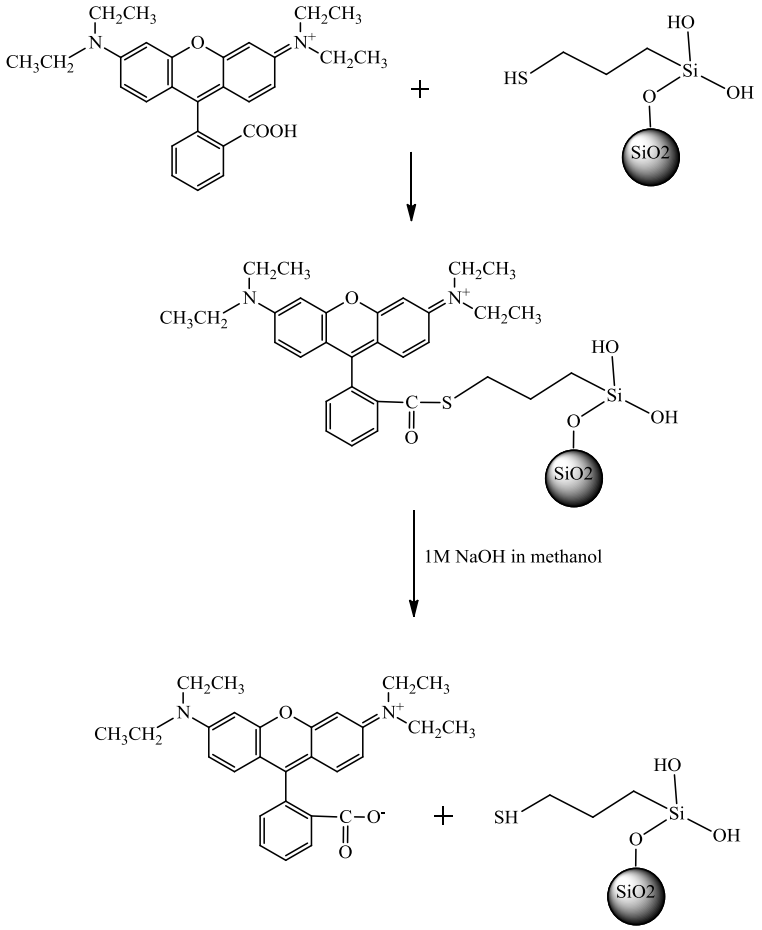

Figure 11 Reaction of Rhodamine B with a thiol modified silica and its release by methanolic sodium hydroxide [66].

The released Rhodamine was related to the thiol content of the modified silica by using the standard calibration curve (Figure 12). Based on the typical weight of silica employed in this study (50 mg), the lowest measurable Rhodamine concentration corresponded to *ca.* 12 nmol of thiol per gram of silica.

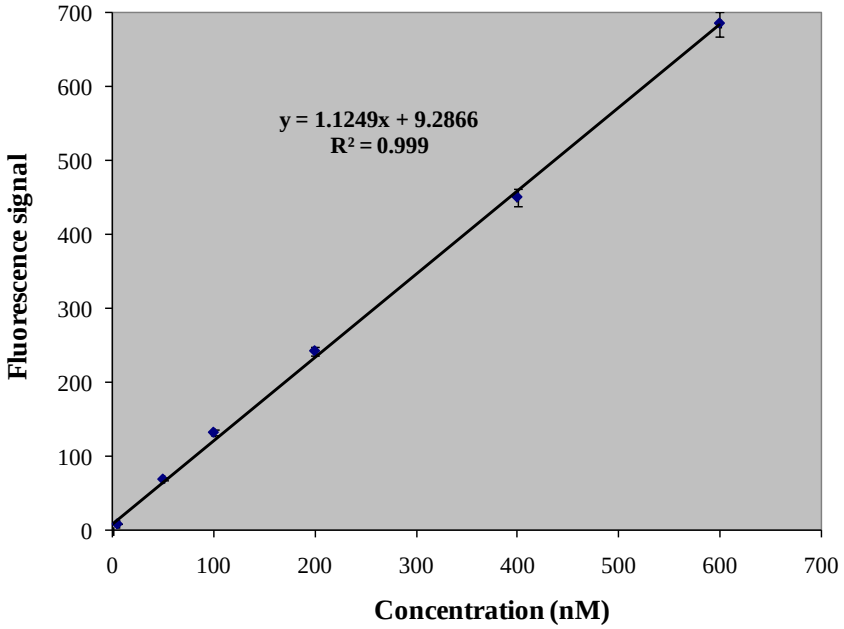

Figure 12 The calibration curve of Rhodamine solutions over the 0-600 nM concentration range.

The Rhodamine content of the thiol-mesoporous silica was found to be 4.70 mmol g^{-1} silica (SD = 0.03, n=5), while the Rhodamine content of the thiol-microporous silica was below the detection limit of the measurement (*ca.* 12 nmol g^{-1}). The Rhodamine contents of microporous and mesoporous silicas are tabulated in Table 1.

Table 1 The thiol-contents of micro and mesoporous silicas.

Thiol functionalised surface	Rhodamine contents mmol g^{-1} silica, ± SD (n=5)
Microporous silica	< 12 nmol g^{-1} silica (detection limit)
Mesoporous silica	4.70 ±0.03

The results from Table 1 support the view that the mesoporous silicas had higher available surface areas and consequently larger binding capacities than the microporous silica. They were considered to be more useful in this study.

2.3.4 Copper capacity of diamine and bis-dithiocarbamate-modified silicas

Microporous and mesporous silicas were surface-modified with the DTC functional group. The capacities of the diamine and bis-DTC modified silicas were measured by saturation of their reactive sites with a concentrated copper (II) solution and then assessing the copper taken onto the silica using AAS (Section 2.2.3.3.4). The copper capacities of the diamine and bis-DTC materials prepared from mesoporous silicas were significantly higher than those of microporous silicas. The diamine and bis-DTC microporous silicas were found to have copper capacities of 0.04 (±0.02) mmolCu g^{-1}Si and 0.07 (±0.03) mmolCu g^{-1} Si, respectively, whilst those of mesoporous silicas were found to be 1.32 and 2.69 mmol g^{-1}, respectively (Table 2).

Table 2 The copper contents of diamine and DTC functionalised silicas.

Silica batches	Copper loading mmol g^{-1} silica, ± SD (n=5)	
	Diamine	Bis-DTC
Microporous	0.04 ±0.02	0.07 ±0.03
Mesoporous	1.32 ±0.02	2.69 ±0.03

Visually the colour of the amino-silica turned from white to blue after copper was added to the suspension, with the degree of colour change corresponding to the copper capacity. The diamine silica turned from white to blue after copper addition whilst the colour of the bis-DTC silica changed from yellow to brownish-yellow. These colours were consistent with those of similar solution phase complexes. It is proposed that the copper loading of the bis-DTC was twice of the diamine silica due to different coordination schemes shown in Figure 13 and Figure 14.

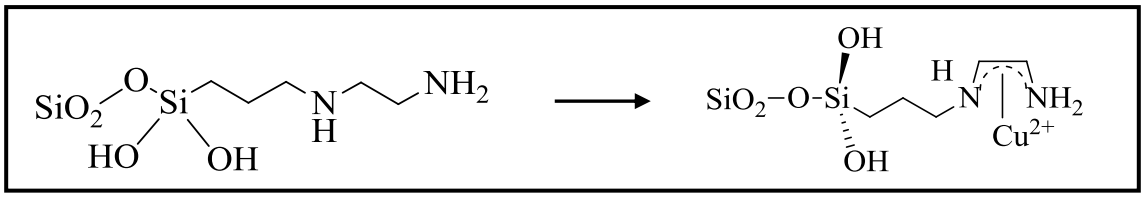

Figure 13 Diamine silica and its chelation of copper (II).

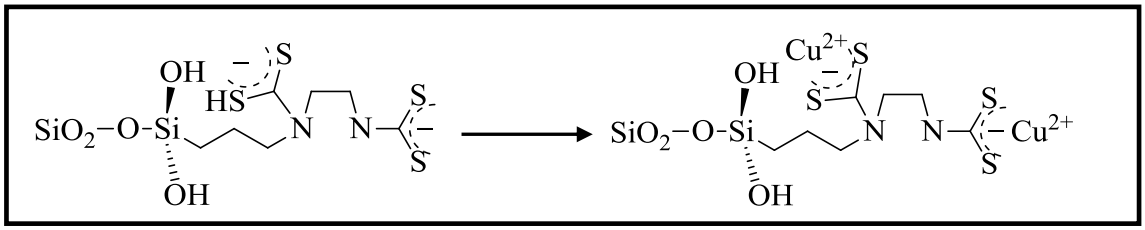

Figure 14 Bis-dithiocarbamate-silica and its chelation of copper (II).

2.3.5 Arsenic labelled silicas

Two types of arsenic-loaded mesoporous silicas were examined for their arsenic contents (thiol and bis-DTC silicas). The arsenic loaded thiol-silica (SiSH-As) and DTC-silica (SiDTC-As) were found to contain 31.08 (±0.07) and 13.68 (±0.30) mg (As) g^{-1} silica (0.42 and 0.18 mmol g^{-1}), respectively. Arsenic capacities of the two modified silicas are compared in Table 3. The arsenic loadings obtained with the mesoporous silica type were considered to be a significant improvement on the loadings found using the microporous silicas (below 9 μg g^{-1}).

Table 3 Comparison of arsenic capacities of modified mesoporous silicas.

Functionalised surface	**Arsenic content (mmol g^{-1}) ***
Thiol-modification	0.42
DTC-modification	0.18

*with the standard deviation (SD) = 0.04, n=5

The arsenic analysis was carried out using two kinds of digestion method (dry and wet ashing). By comparison of the digestion efficiencies it was found that determination of arsenic content using dry ashing with MgO was 28.45 (±2.99) mg As g^{-1} silica, whereas the aqua regia digestion method gave an arsenic content of 19.76 (±1.33) mg As g^{-1} silica (0.38(±0.04) and 0.26 (±0.02) mmol g^{-1}, respectively) (Table 4).

It can be seen that dry ashing with magnesium oxide digestion was slightly more effective in removing arsenic from thiol-silica than wet digestion with aqua regia method. However, the ashing procedure can potentially create problems during the experiments. For example, if hydrochloric acid is used in the digestion process, volatile $AsCl_3$ halides (boiling point 130 ^oC) may be formed, which can result in a lower arsenic concentration than expected. To ensure an accurate measurement of arsenic concentrations in the sample, the wet ashing digestion was used as the sample digestion method in this study.

Table 4 Arsenic capacities and recovery using two digestion methods.

Digestion methods	Capacity mmol As(III) g^{-1} silica, ± SD (n=5)	% Recovery of As(III)
Dry ashing	0.38±0.04	87.44
Wet ashing	0.26±0.02	83.32

2.3.6 Rhodamine labelled silicas

Rhodamine B is a xanthene dye, whose optical properties depends on various factors, such as solvent, concentration, pH value etc [67, 68]. The carboxyl group participates in a typical acid–base equilibrium, with the acid and basic forms being strongly coloured and luminescent. This fluorophore can be covalently bound to thiol-silica [69] and quantitatively released with an appropriate solvent. The effect of solvents on the release of Rhodamine B (RhB) from Rhodamine-labelled thiol-modified silica (SiSH-Rh) was investigated, in order to find the most appropriate solvent to use in this study.

In the present work, four solvents were used: water, sodium hydroxide, methanol and methanolic sodium hydroxide. The spectra of the fluorescent products in these solvents are compared in Figure 15.

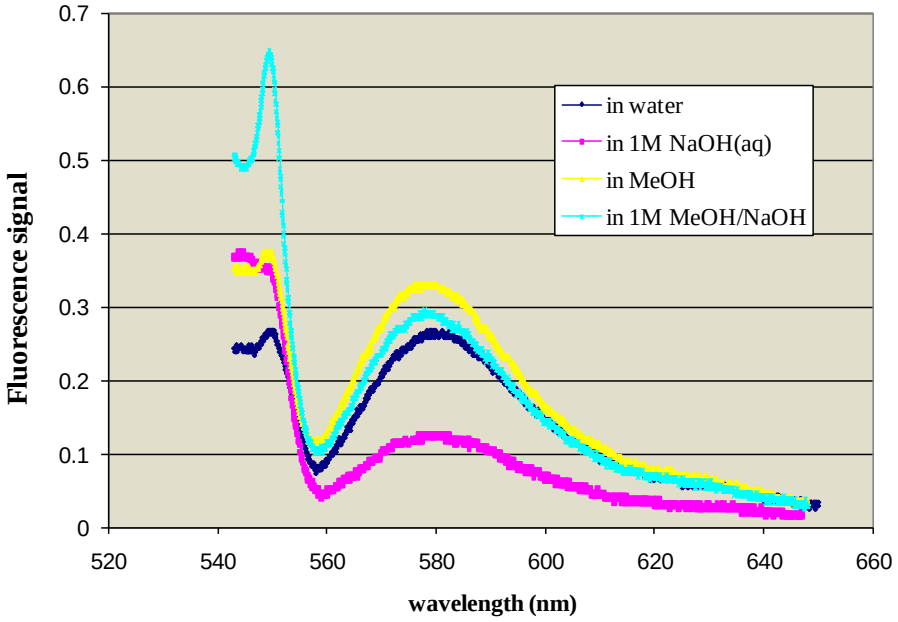

Figure 15 Effect of the solvents on the emission spectra of Rhodamine B (excitation wavelength = 543nm).

From Figure 15, the emission spectra in methanol (MeOH) and 1M methanolic sodium hydroxide (MeOH/NaOH) both exhibit maxima at 580 nm with 543 nm excitation. With MeOH/NaOH the emission intensity was slightly lower than that in pure methanol. The emission maximum in aqueous solutions was shifted to lower wavelength by approximately 5nm. The emission intensity was significantly reduced in aqueous NaOH compared to those of the other solvents.

These results indicated that the solvent environment significantly influenced the emission spectra of Rhodamine. It may be that in the aqueous NaOH solution the Rh carboxylate group is deprotonated leading to a reduced fluorescence yield from its molecule. Methanolic NaOH was chosen as the appropriate medium for the measurement of Rhodamine and therefore for its release from silica in the case of Rhodamine-bound silica.

Rhodamine calibration solutions were then prepared by dilution of the stock solution in 1.0 M methanolic NaOH (described in Section 2.2.3.3.2). All scattering effects from the methanolic NaOH solution were eliminated by filtration before use. RhB labelled silica, a 250 nm thiol-modified silica had a RhB content of 5.04 (±0.05) mmol g^{-1}. Different sizes of RhB labeled particles were also examined (Table 5). The absorption and the fluorescence emission spectra of a standard RhB solution and the RhB released from the SiSH-Rh were measured at room temperature in methanolic NaOH and are shown in Figure 16 and Figure 17, respectively.

Table 5 Comparison of Rhodamine capacities of thiol-mesoporous silicas (SiSH-Rh).

Particle size of SiSH-Rh (nm)	The content of Rhodamine (mmol g^{-1}) *
100	6.51
250	5.04
600	4.42

*with the standard deviation (SD) = 0.05, n=5

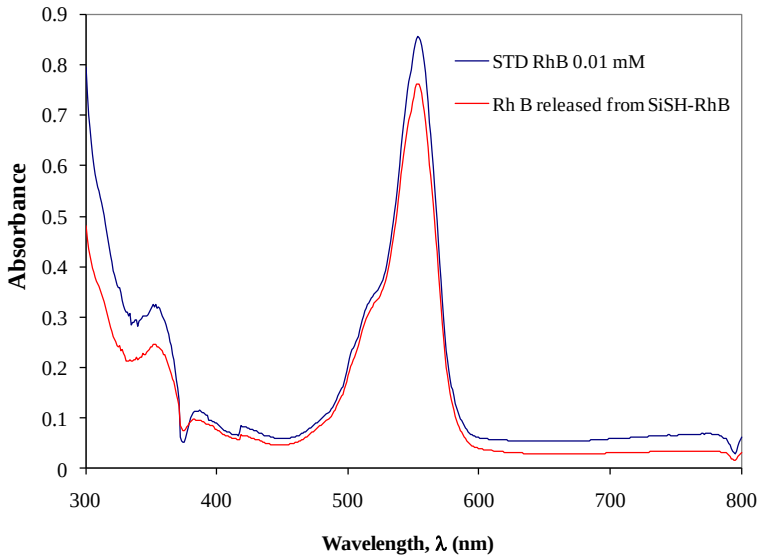

Figure 16 UV absorption spectra of SiSH-Rh and STD RhB (ε = 84,200 cm^{-1} mol^{-1} dm^3) with absorption maximum (λ_{ab}) at 551 nm in methanolic NaOH.

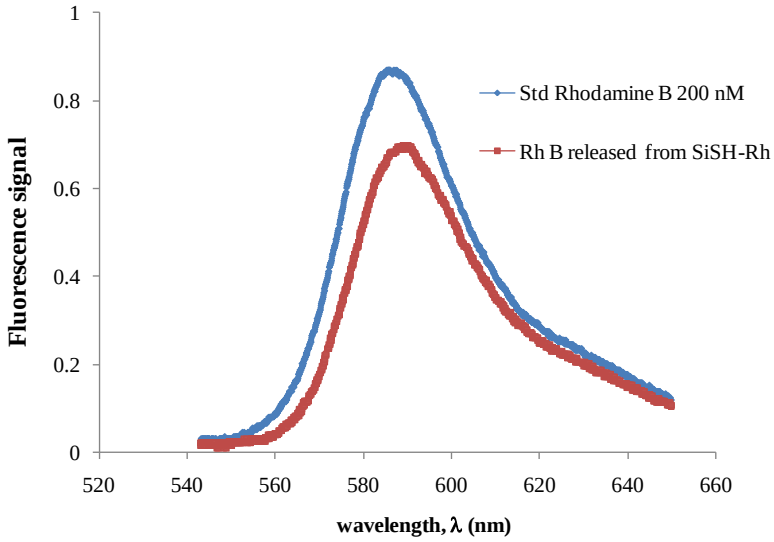

Figure 17 Fluorescence emission spectra of 200 nM standard Rhodamine B and RhB released from silica using 1M methanolic NaOH (aq) digestion.

Figure 16 shows the UV–vis spectra of RhB and the RhB released from SiSH-Rh in methanolic NaOH. The absorption maxima of both molecules appeared at 551 nm. The spectra in Figure 17 were norminalised and only the spectra in the region of 520 nm to 660 nm range were considered. It can be seen from the figure that a broad band in the standard RhB spectrum had a maximum around 585 nm. The Rhodamine B emission spectrum released from the silica surface was found to have a shifted by 2 nm from the standard RhB emission spectrum. This shift was likely to be due to a change in the exact chemical structure of the Rhodamine B as a consequence of its binding to the silica, leading to the shift in the emission spectrum [70].

2.4 Conclusions

In this chapter, the synthesis of microporous and mesoporous sub-micron silicas has been reported. Microporous silica with a mean diameter of 252.3 ± 12.7 nm, was synthesised by adding tetraethoxysilane (TEOS) to a mixture of methanol and ammonium hydroxide. The synthesis of a mesoporous silica with a mean diameter of 240.4 ± 27.9 nm was performed in the presence of a surfactant template (dodecyltrimethyl ammonium bromide).

The silica particle products were characterised using scanning electron microscopy (SEM) and dynamic light scattering (DLS). Under optimal conditions, very uniform spherical silica particles with a desired diameter and narrow particle size distribution were obtained. However, SEM micrographs suggested that particle aggregation had occurred. Attempts to disaggregate particles were introduced successfully by gold coating the SEM stub so that silica thiol groups bound to the gold, preventing their aggregation during solvent evaporation. This technique was then used for further SEM preparations used in particle characterisation.

The silica products were chemically modified either with thiol or diamino (later converted to a dithiocarbamate) functional groups. The loadings of functional groups on the silicas were investigated using Rhodamine B and copper capacity measurements (for thiol and diamine or bis-DTC-silicas, respectively). Rhodamine B measurements suggested that the capacity of the thiol-modified mesoporous silicas (4.70 mmol g^{-1}) was more than 100 times larger than that of the thiol-modified microporous silica ($1.2x10^{-5}$ mmol g^{-1}). In addition, the copper capacity measurements suggested that the bis-DTC microporous silica had surface areas lower than those of the mesoporous silicas (0.07 and 2.68 $mmolg^{-1}$, respectively).

Due to the large surface area and uniform pore structure of the mesoporous silica, this silica was therefore chosen to be used as artificial colloidal particles. Mesoporous

silica particles with diameter 100-1,000 nm had successfully synthesised. It was noticed that the larger surface area of the mesoporous silica particles resulted in larger chemically active surface; this promoted a larger extent of aggregation, which in turn resulted in a broadening of the size distribution.

Later, spherical sub-micron silica of a known size was used as a binder of arsenic and for fluorescent labelling of colloidal materials. The fluorescent dye was attached to the silica surface so that it can be identified and semi-quantified in further experiments. The arsenic loading of the product was found to be 0.42 (±0.04) mmol g^{-1}. Rhodamine B (RhB) labelled silica was successfully prepared by binding onto a 250 nm thiol-modified silica resulting in a RhB content of 5.04 (±0.05) mmol g^{-1}. It has also been shown that the thiol-reactive dye, Rh B, can be strongly associated with active thiol sites. These silicas can be therefore identified using their fluorescence properties.

2.5 References

[1] S. Kralj, A. Zidanscaronek, G. Lahajnar, S. Zcaronumer and R. Blinc, *Physical Review E* **2000**, *62*, 718.

[2] Y. S. Lin, I. Kumakiri, B. N. Nair and H. Alsyouri, *Separation & Purification Reviews* **2002**, *31*, 229-379.

[3] J. i. Hayashi, Y. Watada and K. Muroyama, *Materials Letters* **2001**, *50*, 87-91.

[4] W. Stober, A. Fink and E. Bohn, *Journal of Colloid and Interface Science* **1968**, *26*, 62-69.

[5] A.Van Blaaderen and A. Vrij, *Journal of Colloid and Interface Science* **1993**, *156*, 1-18.

[6] S. C. Chung, S. S. Im, S. I. Shin and S. G. Oh, *Journal of Ceramic Processing Research* **2002**, *3*, 235-240.

[7] A. G. Howard and N. H. Khdary, *Analyst* **2005**, *130*, 1432-1438.

[8] J. S. Beck, J. C. Vartuli, W. J. Roth, M. E. Leonowicz, C. T. Kresge, K. D. Schmitt, C. T. W. Chu, D. H. Olson and E. W. Sheppard, *Journal of the American Chemical Society* **2002**, *114*, 10834-10843.

[9] M. Etienne, B. Lebeau and A. Walcarius, *New Journal of Chemistry* **2002**.

[10] C. T. Kresge, M. E. Leonowicz, W. J. Roth, J. C. Vartuli and J. S. Beck, *Nature* **1992**, *359*, 710-712.

[11] A. Berggren, A. Palmqvist and K. Holmberg, *Soft Matter* **2005**, *1*, 219-226.

[12] A. Dabrowski, *Advances in Colloid and Interface Science* **2001**, *93*, 135-224.

[13] M. E. Davis, *Nature* **2002**, *417*, 813-821.

[14] A. Stein, *Advanced Materials* **2003**, *15*, 763-775.

[15] Z. Yuan, W. Zhou and L. Peng, *Chemistry Letters* **2000**, 1150-1151.

[16] M. Nakamura and K. Ishimura, *Langmuir* **2008**, *24*, 5099-5108.

[17] C. R. Miller, R. Vogel, P. P. T. Surawski, K. S. Jack, S. R. Corrie and M. Trau in *Functionalized Organosilica Microspheres via a Novel Emulsion-Based Route, Vol. 21* **2005**, pp. 9733-9740.

[18] K. Yano and Y. Fukushima, *J. Mater. Chem.*, **2003**, *13*, 2577-2581.

[19] R. Mueller, H. K. Kammler, S. E. Pratsinis, A. Vital, G. Beaucage and P. Burtscher, *Powder Technology* **2004**, *140*, 40-48.

[20] T.-H. Liou, *Materials Science and Engineering A* **2004**, *364*, 313-323.

[21] P. K. Jal, M. Sudarshan, A. Saha, S. Patel and B. K. Mishra, *Colloids and Surfaces A: Physicochemical and Engineering Aspects* **2004**, *240*, 173-178.

[22] C. J. van Oss and R. F. Giese, *Journal of Dispersion Science and Technology* **2003**, *24*, 363-376.

[23] K. C. Vrancken, K. Possemiers, P. Van Der Voort and E. F. Vansant, *Colloids and Surfaces A: Physicochemical and Engineering Aspects* **1995**, *98*, 235-241.

[24] L. N. Lewis, T. A. Early, M. Larsen, E. A. Williams and J. C. Grande, *Chemistry of Materials* **1995**, *7*, 1369-1375.

[25] S. Brandriss and S. Margel, *Langmuir* **1993**, *9*, 1232-1240.

[26] A. Stein, B. J. Melde and R. C. Schroden, *Advanced Materials* **2000**, *12*, 1403-1419.

[27] D. Liu, J.-H. Lei, L.-P. Guo, X.-D. Du and K. Zeng, *Microporous and Mesoporous Materials* **2009**, *117*, 67-74.

[28] S. V. Mattigod, X. Feng, G. E. Fryxell, J. Liu and M. Gong, *Separation Science and Technology* **1999**, *34*, 2329 - 2345.

[29] M. Volkan, O. Y. Ataman and A. G. Howard, *Analyst* **1987**, *112*, 1409-1412.

[30] A. G. Howard, M. Volkan and O. Y. Ataman, *Analyst* **1987**, *112*, 159-162.

[31] P. I. Girginova, A. L. Daniel-da-Silva, C. B. Lopes, P. Figueira, M. Otero, V. S. Amaral, E. Pereira and T. Trindade, *Journal of Colloid and Interface Science 345*, 234-240.

[32] X. J. Leng, K. Starchev and J. Buffle, *Langmuir* **2002**, *18*, 7602-7608.

[33] L. M. Rossi, L. Shi, F. H. Quina and Z. Rosenzweig, *Langmuir* **2005**, *21*, 4277-4280.

[34] M. Nakamura, M. Shono and K. Ishimura, *Anal. Chem.* **2007**, *79*, 6507-6514.

[35] G. Göktürk, M. Delzendeh and M. Volkan, *Spectrochimica Acta Part B: Atomic Spectroscopy* **2000**, *55*, 1063-1071.

[36] E. F. S. Vieira, A. R. Cestari, J. de A. Simoni and C. Airoldi, *Thermochimica Acta* **1999**, *328*, 247-252.

[37] E. Vieira, J. Simoni and C. Airoldi, *Journal of Materials Chemistry* **1997**, *7*, 2249-2252.

[38] X. Feng, G. E. Fryxell, L. Q. Wang, A. Y. Kim, J. Liu and K. M. Kemner, *Science* **1997**, *276*, 923-926.

[39] L. Mercier and T. J. Pinnavaia, *Environmental Science & Technology* **1998**, *32*, 2749-2754.

[40] J. Brown, R. Richer and L. Mercier, *Microporous and Mesoporous Materials* **2000**, *37*, 41-48.

[41] R. I. Nooney, M. Kalyanaraman, G. Kennedy and E. J. Maginn, *Langmuir* **2000**, *17*, 528-533.

[42] X. Liang, Y. Xu, G. Sun, L. Wang, Y. Sun and X. Qin, *Colloids and Surfaces A: Physicochemical and Engineering Aspects* **2009**, *349*, 61-68.

[43] H. Lee and J. Yi, *Separation Science and Technology* **2001**, *36*, 2433 - 2448.

[44] T. Yokoi, H. Yoshitake, T. Yamada, Y. Kubota and T. Tatsumi, *Journal of Materials Chemistry* **2006**, *16*, 1125-1135.

[45] B. Lee, Y. Kim, H. Lee and J. Yi, *Microporous and Mesoporous Materials* **2001**, *50*, 77-90.

[46] D. E. Leyden, G. Howard Luttrell, A. E. Sloan and N. J. DeAngelis, *Analytica Chimica Acta* **1976**, *84*, 97-108.

[47] A. M. Liu, K. Hidajat, S. Kawi and D. Y. Zhao, *Chemical Communications* **2000**, 1145-1146.

[48] L. Bois, A. Bonhommé, A. Ribes, B. Pais, G. Raffin and F. Tessier, *Colloids and Surfaces A: Physicochemical and Engineering Aspects* **2003**, *221*, 221-230.

[49] H. Yoshitake, T. Yokoi and T. Tatsumi, *Chemistry of Materials* **2003**, *15*, 1713-1721.

[50] G. P. Knowles, J. V. Graham, S. W. Delaney and A. L. Chaffee, *Fuel Processing Technology* **2005**, *86*, 1435-1448.

[51] X. Wang, J. C. C. Chan, Y.-H. Tseng and S. Cheng, *Microporous and Mesoporous Materials* **2006**, *95*, 57-65.

[52] S. Sayen and A. Walcarius, *Journal of Electroanalytical Chemistry* **2005**, *581*, 70-78.

[53] J. G. P. Espínola, J. M. P. de Freitas, S. F. de Oliveira and C. Airoldi, *Colloids and Surfaces A: Physicochemical and Engineering Aspects* **1994**, *87*, 33-38.

[54] K. A. Venkatesan, T. G. Srinivasan and P. R. Vasudeva Rao, *Colloids and Surfaces A: Physicochemical and Engineering Aspects* **2001**, *180*, 277-284.

[55] Y. Yamada and K. Yano, *Microporous and Mesoporous Materials* **2006**, *93*, 190-198.

[56] S. R. Al-Abed, G. Jegadeesan, J. Purandare and D. Allen, *Chemosphere* **2007**, *66*, 775-782.

[57] D. Shaw, *Engineering Geology* **2006**, *85*, 158-164.

[58] M. Jang, J. S. Hwang and S. Il Choi, *Chemosphere* **2007**, *66*, 8-17.

[59] K. Loska and D. Wiechula, *Microchimica Acta* **2006**, *154*, 235-240.

[60] C. Y. Zhou, K.Wong, L. L. Koh and Y. C. Wee, *Mikrochim. ACTA* **1997**, *127*, 77-83.

[61] J. Yan, M. C. Estevez, J. E. Smith, K. Wang, X. He, L. Wang and W. Tan, *Nano Today* **2007**, *2*, 44-50.

[62] F. Gouanve, T. Schuster, E. Allard, R. Meallet-Renault and C. Larpent, *Advanced Functional Materials* **2007**, *17*, 2746-2756.

[63] R. Vogel, P. P. T. Surawski, B. N. Littleton, C. R. Miller, G. A. Lawrie, B. J. Battersby and M. Trau, *Journal of Colloid and Interface Science* **2007**, *310*, 144-150.

[64] S. Laferty and I. Piirma, *In Polymer Latexes; American Chemical Society*, Washington, DC **1992, p 255-271**, p.

[65] X.-k. Ma, N.-H. Lee, H.-J. Oh, J.-W. Kim, C.-K. Rhee, K.-S. Park and S.-J. Kim, *Colloids and Surfaces A: Physicochemical and Engineering Aspects 358*, 172-176.

[66] A. G. Howard and N. H. Khdary, *Analyst* **2004**, *129*, 860-863.

[67] T. López Arbeloa, M. J. Tapia Estévez, F. López Arbeloa, I. Urretxa Aguirresacona and I. López Arbeloa, *Journal of Luminescence 48-49*, 400-404.

[68] V. Martinez Martinez, F. Lopez Arbeloa, J. Banuelos Prieto, T. Arbeloa Lopez and I. Lopez Arbeloa, *The Journal of Physical Chemistry B* **2004**, *108*, 20030-20037.

[69] A. A. da Silva, J. Flor and M. R. Davolos, *Surface Science* **2007**, *601*, 1118-1122.

[70] H. S. Kim, C. O. Bae, J. Y. Kwon, S. K. Kim, M. Choi and J. Yoon, *Bull. Korean Chem. Soc.* **2001**, *22*, 929-931.

Chapter 3

Preliminary evaluation of the behaviour of colloidal particles during filtration

3.1 Introduction

3.1.1 Size fractionation by filtration

It is widely recognised that the colloidal particles that are presented in natural water affect the transport of organic and inorganic pollutants [1-6] (Chapter 1). In order to obtain an insight into the role of these colloids in aquatic systems, a good fractionation method is required to separate environmental samples into well defined particulate, colloidal and dissolved fractions. Several approaches have been taken to size fractionation including centrifugation, ultrafiltration and membrane filtration (Section 1.5.1). Filtration is frequently employed in an analytical and environmental chemistry because of its field-portability, simplicity, and low cost operation [7-10]. An understanding of the behaviour of particles during filtration is therefore essential if the transport and fate of colloid bound pollutants is to be understood.

The simplest description of the action of a filter is that particles having sizes larger than the pore size of the filter are stopped at the surface of the filter. Large sized of particles are prevented from entering and/or passing through the pores. During filtration some of the pores become partially blocked by particles, resulting in a reduction of the effective pore size and retention of extremely small particles. When natural waters are being filtered particles collide with the membrane surface in a number of ways. Some of them collide with the membrane surface some distance from the pores whilst others hit the pore entrances. If particles are larger than the pore size, they may remain within the pores and block the entrances. Conversely, particles

are smaller the pore size, they will penetrate into the pores and some will collide with the pore walls resulting in the retention by chemical or electrostatic attachment to the walls (Figure 1). The rest of the particles will continue to move through the pore channels and eventually pass through the membrane. However, clogging or adsorption of particles onto filters and other filtering equipment gives rise to a reduced particle concentration in the filtrate. This may lead to a false interpretation. A 'cake' or bed 'thick layer' of trapped particles being built up on the surface of the filter surface during use causes clogging, which then results in a decreased filtration rate and increased operating time [11],[10],[12].

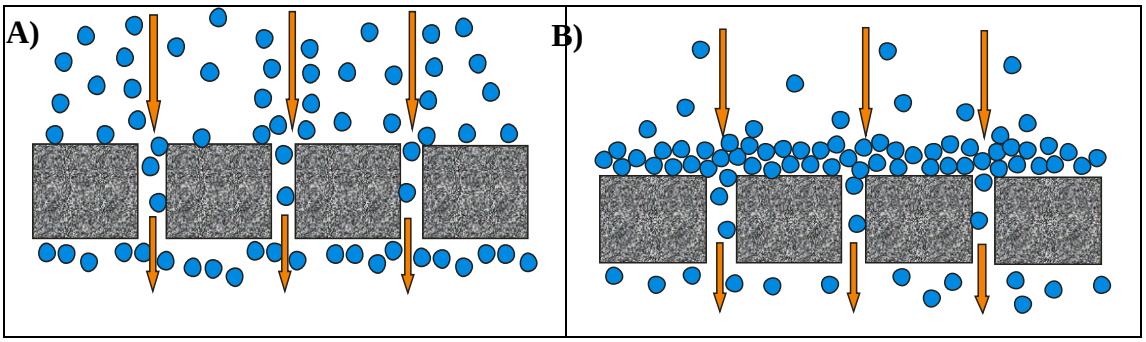

Figure 1 Action of the particles being filtered through the pore filter (A) some of the particles pass through whilst some are trapped within the pores and (B) the layer of trapped particles being built up on the filter surface.

A number of researchers have demonstrated that using filtration to prepare water samples for the purpose of trace element determination can cause significant errors in various ways. These include contamination, adsorption of solutes and colloids, and membrane clogging [12-15]. For example, Haygarth et al.[16] used filter and ultrafiltration methods to separate different colloidal size ranges in river water. Those authors found that the colloids aggregated at the filter surfaces. Buffle and Leppard [15] suggested that colloids also interacted directly with the filter resulting in the particles being retained. Hong et al.[17] studied the colloidal fouling which acts as a physical barrier for the suspended particles or colloids in the feed stream. All particles larger than the pores were retained on the feed side of the filter, and hence accumulated on the surface of the filter and increased the resistance to water flow across the filter.

3.1.2 Types of filters

Two types of filters are usually used in conventional filtration. The first is a tortuous path (TP) or **'depth'** filter (100-150 µm thick)[18] which is made from materials such as cellulose acetate and cellulose nitrate (e.g. Millipore and Sartorius filters). The second is a sieve-type filter (S) or **'plain'** (10-15 µm thick)[18] filter which is usually made from polycarbonate (e.g. Nuclepore filter). The S filters can retain some particles that have smaller particle sizes than the filter pore size and do not clog easily compared with the TP filters. Figure 2 shows typical micrographs of filter surfaces for the TP type (Figure 2A and 2B) and the S type (Figure 2C).

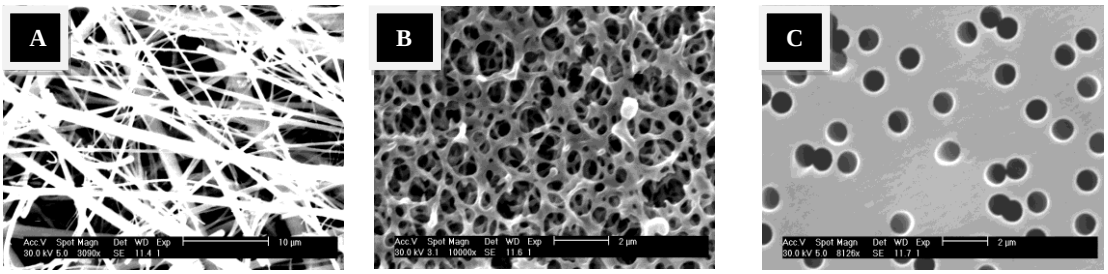

Figure 2 Electron micrographs of clean filters: A = glass microfiber (1.6µm Whatman GF/C) and B = cellulose membrane filter (0.45µm, HA Millipore) and C = polycarbonate Track-Etch membrane filter (1.0µm Nuclepore).

Depth filters are widely used for biological samples [19, 20]. It can be clearly seen from Figure 2A that the GF/C filter pore sizes vary over a wide range. This filter has no well defined pore size as it consists of a rather thick layer of borosilicate glass fibres with diameters less than 1 µm. The pore size distribution of such filters may not be suitable for particle size separation but nominal pore sizes are given by the manufacturers [21]. These depth filters combine fast rates with high loading capacity and the retention of very fine particles, extending into the sub-micron range. These depth filters can be used at temperatures up to 500 ^{o}C and are ideal for use in applications involving air filtration and for gravimetric analysis of volatile materials where ignition is involved. Howard and Statham [22] suggested that depth filtration relies on the interaction of the particle in the samples with the filter matrix, either by physical trapping or surface contact. Nevertheless, this type of filter suffers from problems due to adsorption of species directly on to the large available filter surfaces

as the sample passes through. It could be influenced the quantity and size distribution of the particles, as clogging of the pores may reduce the effective pore size during filtration.

The plain filters composed of polycarbonate film e.g. Nuclepore filters are recommended for all analysis in which sample is to be viewed on the surface of the membrane (Figure 2C). It has a very uniform pore size and is transparent. They have a thickness of approximately 15 μm and a porosity between 5 and 20%. The pores are circular at the filter surface. The visible pore diameter is said to be the effective pore size. Sheldon[23] found that Nuclepore membranes had a retention size close to their nominal pore size, which does not change up to the point of overloading.

Membrane filtration has commonly been used as a first step in the preparation of natural water samples in order to separate particulate matter from the sample for analysis. Although different filters with various pore sizes are commercially available, filtration is usually performed using 0.45 μm membrane filters. Generally, the fraction which passes through the membrane filter is termed "dissolved" whereas the fraction which is retained on membrane filters is termed the "particulate" fraction. According to the conventional colloid size definition, colloidal particles can either pass through or be retained on the 0.45 μm filters. Moreover, while passing with a liquid phase through the pores, the colloidal particles may either adhere to the pore surface or flow without capture or be retained at pore constrictions. Before choosing an analytical filter, its physical and chemical properties must be carefully examined. Information regarding to the behaviour of colloidal matter during filtration step involved in the analysis of colloidal metals in natural waters, is therefore the subject of interest.

This chapter reports a study of the behaviour of colloidal particles during double filtration and compares the performance of the *first* filter (8.0 μm or 1.6 μm or 1.0 μm or 0.45 μm filters) and the *second* filter (0.1 μm filter) for the filtration of laboratory prepared and natural sols. These operational cut-offs of different filters were

evaluated using engineered homogenous particle dispersions. Engineered particles (Chapter 2) were used to represent the colloidal matter in natural waters. This method allows a better understanding of the true behaviour of colloidal sized particles during filtration. Traditional membrane filtration (cellulose nitrate, polycarbonate and glass fibre) was used to fractionate particulate matter to allow the impact of colloidal particles on the filter surface measurements to be evaluated. Different pore sizes and filter types, glass microfibre, cellulose nitrate and polycarbonate (Nuclepore) filters, were employed.

In this thesis, the practical terms used are in the following;

Double filtration:

- The material stopped by the *first* filter ($d \geq 0.45$ µm) is called the "large particulates" includes large organic or inorganic particles, crystal and most of the suspended sediment.
- The solution passing through the *first* filter is named "the 1st filter filtrate" includes aqueous solution or suspension containing ions through to colloidal sized particles ($d < 1.0$ µm) e.g. viruses or very small sediment particles.
- The material collected on the *second* filter is regarded as a "colloidal particles" which is, in theory, particles with diameter 0.1 µm $<d < 1.0$ µm.
- The solution passing through the *second* filter is called a "dissolved" phase and in theory some colloidal particles (0.001 µm $<d < 0.1$ µm) are included within this 'operational' fraction.

Triple filtration:

- The material stopped by the *first* filter ($d \geq 1$ µm) is called the "large particulates".
- The solution passing through the *first* filter is named "the 1st filter filtrate".

- The material collected on the *second* filter (0.45 μm filter) is regarded as the "large colloidal particles".
- The solution passing through the *second* filter is named "the 2nd filter filtrate"
- The material collected on the *third* filter (0.1 μm filter), the final filter used is regarded as the "fine colloidal particles".
- The solution passing through the *third* filter is called a "dissolved" phase and in theory some colloidal particles (0.001 μm <d < 0.1 μm) are included within this 'operational' fraction.

1.6 μm cut-off filters were chosen as the *first* filter in this study, as the closest available match to the IUPAC recommended value of 1 μm that sets the size boundary between particles and colloids. The total colloidal phase is distributed between the "large colloidal" and the "fine colloidal" phases.

3.2 The behaviour of natural colloidal particles during filtration

An investigation of the importance of natural colloids during a conventional filtration of samples from Southampton Water was the main subject of this study.

3.2.1 Materials and methods

3.2.1.1 Materials

The filters used in this study were a 1.0 μm (Nuclepore) membrane and a 0.45 μm HA (Millipore) cellulose acetate membrane. These filters were dried in an oven at 200 ^{o}C for 4 hours prior to use.

1 litre of polyethylene bottles (HDPE) were employed to collect the water samples. All containers were soaked in 5% v/v hydrochloric acid for 24 hours and rinsed with deionised water prior to use. Deionised water was purified using an Elga Option 4 system. An engineered colloidal thiol functionalised silica with approximate particle diameters of 250 nm was used as a tracker of inorganic colloids in natural waters (synthesis described in Section 2.2.2.3).

3.2.1.2 Sampling of the natural water

Surface high salinity samples were collected from Southampton Water at the quay of the National Oceanography Centre of the University of Southampton (NOCs) during the high tide in the morning of 20th June 2008. The polyethylene bottles and caps were rinsed at least three times with seawater before samples were taken from the top 50 cm of the water column.

3.2.1.3 Filtration method

Vacuum filtration was employed using a membrane filter holder assembly. The 47 mm Millipore filter unit contained a fritted glass support bed (Figure 3). The filter funnel support bed and receiver flask are fitted with interchangeable ground joint and one aluminium clamp was provided to hold the filter funnel and support bed properly. Possible contamination from glassware was minimised by rinsing with deionised water.

Figure 3 Vacuum filtration apparatus used in this study.

The water samples were double-filtered first through a 1.0 µm polycarbonate membrane (Nuclepore) and then a 0.45 µm HA cellulose acetate (Millipore) filter as soon as they arrived in the laboratory.

250 nm diameter thiol modified silica was mixed (*ca.* 250 µg) into the water samples (1 litre). The particle-spiked water sample was then shaken gently. 50 mL of the suspended water sample was sequentially filtered through a 1µm filter followed by a 0.45 µm filter. The used filter was then dried at 60^{o}C in an oven for 3 hours and kept overnight in a desiccator.

3.2.1.4 Characteristics of material collected on the filter surfaces

The surfaces of the used filters were examined using a scanning electron microscope (SEM). A random small piece of the dried filter was put on a SEM stub, gold coated and then examined by SEM. The SEM used was a Philips Co., XL-30 ESEM normally operating at an acceleration voltage of 20-30 kV with the standard detection mode, secondary electron imaging or SEI.

3.2.2 Results and discussion

Figure 4a and 4b show typical images of the natural particles that were collected on the 1.0 µm Nuclepore and 0.45 µm Millipore filters. These particles were in general typical of diatoms naturally found in estuarine water as illustrated in Figure 5. Inorganic matter is also expected to be present but is less readily identifiable.

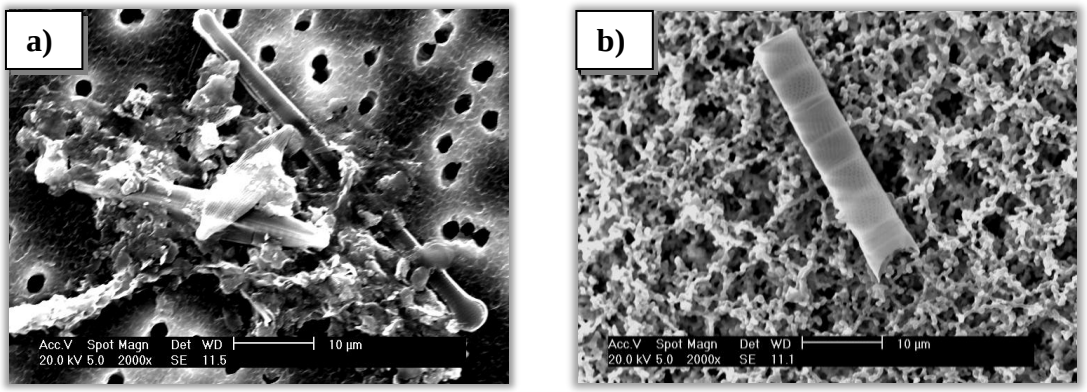

Figure 4 Natural matter collected on (a) the 1 µm Nuclepore and (b) 0.45 µm Millipore filters (2,000 x magnifications). The sample was the estuarine water from the quay at the National Oceanography Centre of the University of Southampton (NOCs).

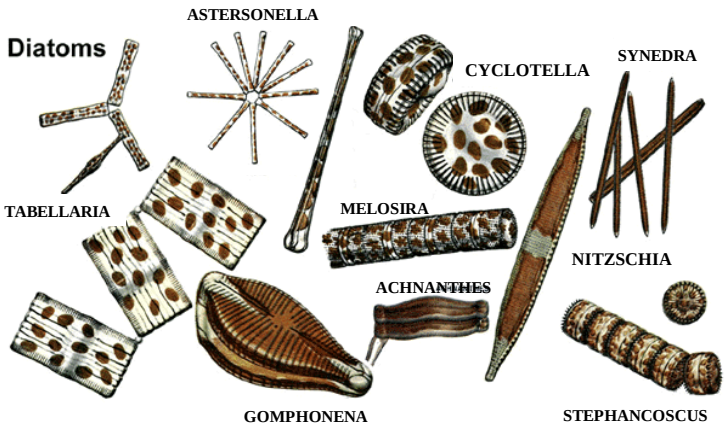

Figure 5 Diatoms in natural waters[24].

In general, surface waters contain NOM, micro-organisms and inorganic colloids. Inorganic colloids in surface waters may be the oxy/hydroxides of Mn, Fe, Al and Si, as well as carbonates and clays, with a size range from a few nanometres to micrometres [25]. The existing evidence (Figure 4) suggests an abundance of natural matter in this water system. There are concerns that natural particulate matter can

adsorb sub-micrometer scale particles, via several mechanisms such as electrostatic interaction or specific chemical affinity.

Figure 6(a) shows the material removed from the water sample to which had been added silica particles. Some clogging of the filter pores was evident. The attachment of natural particulate particles with engineered particles was also found. It can be seen that natural materials adsorbed on the filter surface (Figure 6a) and formed a cake layer, leading to a blocked pore filter. Aggregation occurred not only among the added silica but also between the silica and the matter (Figure 6b) naturally present in the seawater. A combination of blocking and bridging (Figure 6c) also occurred during filtration. It has been suggested[26] that the association between natural particulate matter and particles in the colloidal size range in water, once they mix and become aggregates, may play a role in the fractionation method e.g. membrane filtration.

According to the effect of salinity on the aggregated colloids, this also results in the sedimentation of colloidal particles in natural water [27, 28]. The high salinity of this studied water samples (*ca.* 30 parts per thousand) is assumed to lead to an increased association and retention of colloidal particles that would normally pass through the filter. Interactions between the colloidal particles and particulate matter or natural organic matter in estuarine water system are commonly repeated in previous studies [29-31].

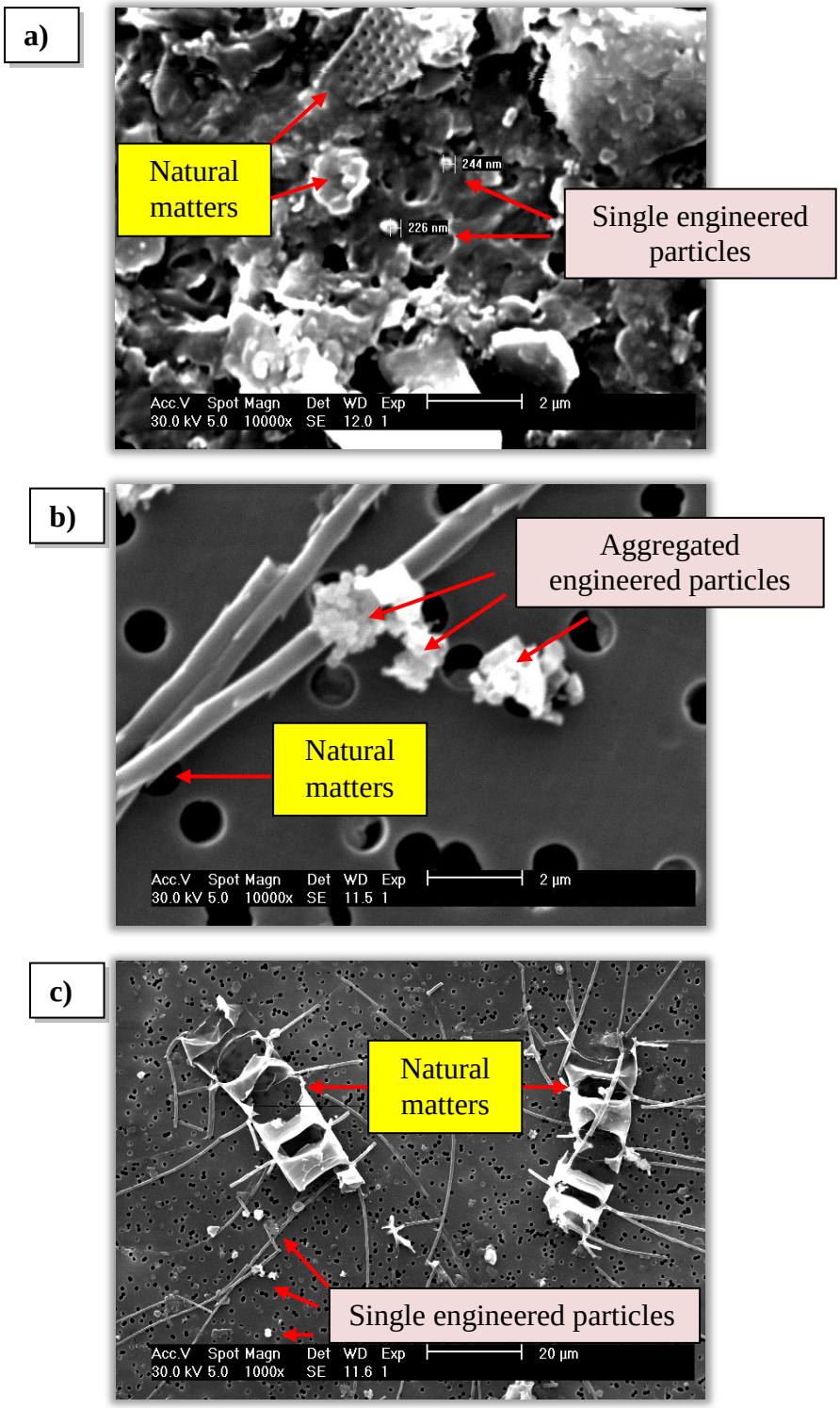

Figure 6 (a) Electron micrograph of engineered particles and natural particulate matter collected on the 1µm Nuclepore filter. (b) Images of discrete aggregates formed with high magnification (x10,000). (c) The overview of surface filter collected by materials with 1,000x magnification.

Associations between our engineered particles and the natural materials were observed in Figure 6b. The sizes of these clusters become too big to pass through the filter pores. These clusters possibly could be explained by the high abundance and high specific surface areas of these colloidal particles (nm in range) in the suspension, resulting in the association of particles with materials in natural water. Colloidal particles in the natural environment commonly exhibit a negative surface charge due to the adsorption of NOM on the surface and this can stabilise the colloids[32]. However, particles larger than the nominal pore size may sometimes pass through the filter due to the presence of some large pores resulting from pores overlapping; there are some double and multiple pores visible in the track etched filter shown in Figure 7.

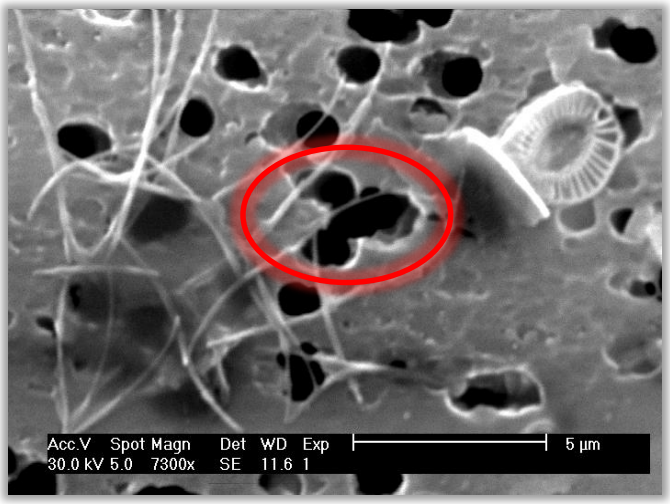

Figure 7 SEM micrograph of materials collected from surface seawater on a1µm (Nuclepore) filter. The red circle shows an example of overlapping pores.

3.2.3 Conclusions

This study has found that engineered colloidal particles added to natural seawater can highly become associated with natural particulate matter changing the particle sizes collected by filtration. Particles that would otherwise pass through the filter were retained.

3.3 Studies of labelled synthetic particles during filtration

To obtain a better understanding of behaviour of natural colloids and their influence on filtration, a simple system was needed for study. In this thesis, synthetic silica was studied whilst these particles were visually recognisable from their uniform spherical shapes quantitative evaluations required the attachment of a chemical label to the particles.

3.3.1 Using arsenic labelled particles

This experiment was designed to study the behaviour of the small, synthetic colloidal particles when filtered using large pore filters. The sizes of particles were designed to be smaller than the filter's pores. This was to investigate whether large pore filters that should, in theory, pass through the filter could trap significant quantities of small particles.

A suspension of *ca.* 250 nm engineered arsenic-loaded colloidal silica particles (Section 2.2.2.5.1) was sequentially passed through the *first* filter either a 1.6 μm GF/C filter or a 8.0μm Nuclepore filter and then the *second* filter, a 0.1 μm cut-off membrane filter. The concentrations of arsenic on the *first* and the *second* filters were measured and used to track the behaviour of the particles during filtrations.

3.3.1.1 Materials and methods

3.3.1.1.1 Materials

Two types of filters were employed: a 1.6 μm GF/C glass fibre, depth filters (TP), 8.0 μm and 0.1 μm track-etched Nuclepore membrane plain filters (S).

Hydrochloric acid (~37% HCl, laboratory grade) was obtained from Fluka (Gillingham, UK.). Nitric acid (HNO_3, laboratory grade) was obtained from Aldrich (Poole, UK). Water was purified by deionization using an Elga Option 4 system. Arsenic was released from the silica particles using 4 ml of a 3.5:10.5 (v/v) mixture of concentrated HNO_3 and concentrated HCl (aqua regia). The acid samples were then analysed by either hydride generation (HG-AAS) or cryogenic trap hydride generation (CT-HG-AAS) atomic absorption spectrometry using the parameters described in Appendices A and B.

3.3.1.1.2 Filtration method

Double filtration was employed, the apparatus and method used was carried out as described in detail in Section 3.2.1.3 using a 1.6 µm (or 8.0 µm) filter for the *first* filter and a 0.1 µm filter, the *second* filter.

Ca. 10 mg of the arsenic-loaded thiol modified silica was suspended in 250 mL of deionised water for 3 hours using ultrasonication in order to disperse aggregated particles. These colloidal arsenic-loaded silicas were double-filtered through the 1.6µm GF/C filter (or 8.0 µm Nuclepore filter), followed by the 0.1 µm filter using vacuum filtration. After being filtered, each of the used filters was digested in aqua regia. The resulting solution was diluted with deionised water and its arsenic content measured using HG-AAS. The filtrate fractions were centrifuged to isolate the silica particles which were then digested and analysed for their arsenic content by CT-HG-AAS after digestion.

3.3.1.1.3 Characteristics of the silica particles and filter surfaces

The particle size distributions (PSD) of the silica particles prior to and after filtration were determined by a dynamic light scattering (DLS). The PSD of these suspended

colloidal particles was measured with covering the range of 40-1,000 nm. The surfaces of the filters before and after use were examined by SEM (Section 3.2.1.4).

3.3.1.2 Results and discussion

The particle size distributions (PSD) of the synthetic silica particles prior to and after filtration are shown in Figure 8a and 8b, respectively. The characteristics and particle size of the silica particles examined using SEM are shown in Figure 8c. It can be seen that the particle size distribution of the particles before (Figure 8a) and after filtration (Figure 8b) appeared to be very similar. However, some very small particles (55 – 65 nm) are also present in the filtrate after filtration (Figure 8b). It is possible that during the high speed centrifugation an aggregate of small particles became separated. The mean particle sizes of the synthetic silica particles were found to be *ca.* 230-320 nm. These corresponded to the average size of particle measured by SEM (Figure 8c).

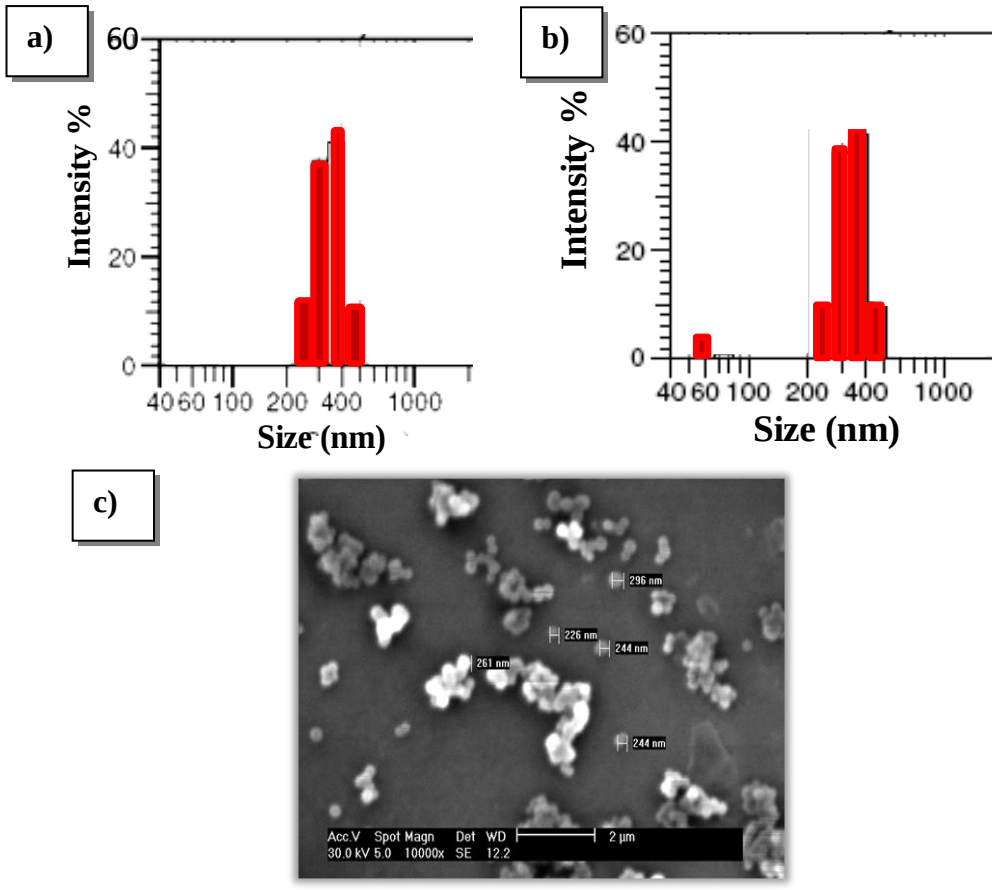

Figure 8 Particle size distributions of synthetic silica particles (a) before and (b) after filtration using a 1.6 µm GF/C filter. (c) SEM images of the particles before filtration.

The analysis of arsenic collected from used filters showed that 45% (108.73 µg) and 21% (51.45 µg) of total arsenic in the silica suspension (241.80 µg) was found on or within the GF/C and the 0.1 µm filters, respectively. These results suggested that silica particles had been retained inside the filters and this had caused the filter pores to be clogged. The filters were also examined by SEM (Figure 9). It was apparent from the micrographs that there were large colloidal aggregates associated with the fibre structures of the GF/C filters. These particles were trapped inside the filter possibly due to the association of the particles with the filter fibres (electrostatic attraction) [33]. This result explained why the arsenic contents of the filtrates were lower than expected.

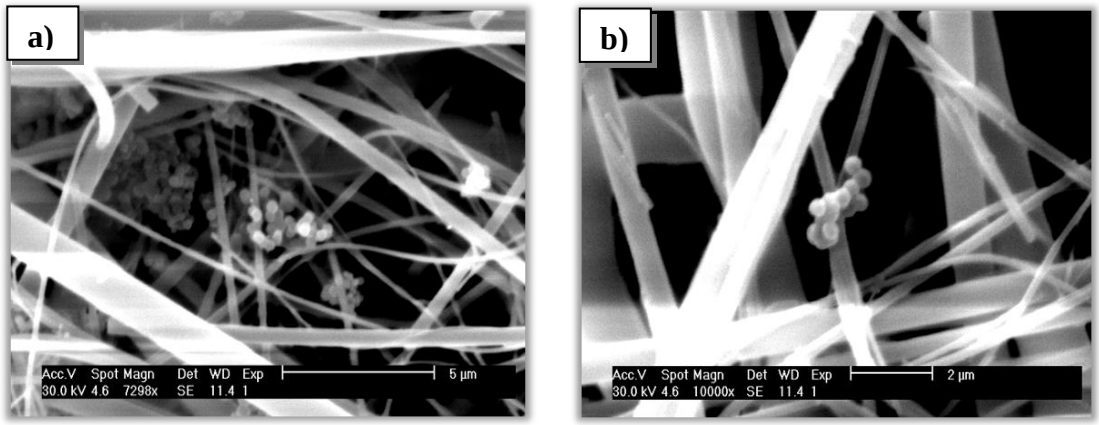

Figure 9 SEM image of the 1.6 µm GF/C filter surface after filtration of the particle suspension (a) 7,298x magnification and (b) 10,000x magnification.

Filtration of the suspension of synthetic silica particles using Nuclepore filter was also investigated. This filter was representative of polycarbonate and polyester plain filter membranes having non-fibrous structures. In theory, the particles having a small diameter, e.g. 250 nm, should easily pass through a filter with 8 µm pore diameter. Interestingly, the result (Figure 10) shows that the Nuclepore filter was completely covered by a layer of silica particles.

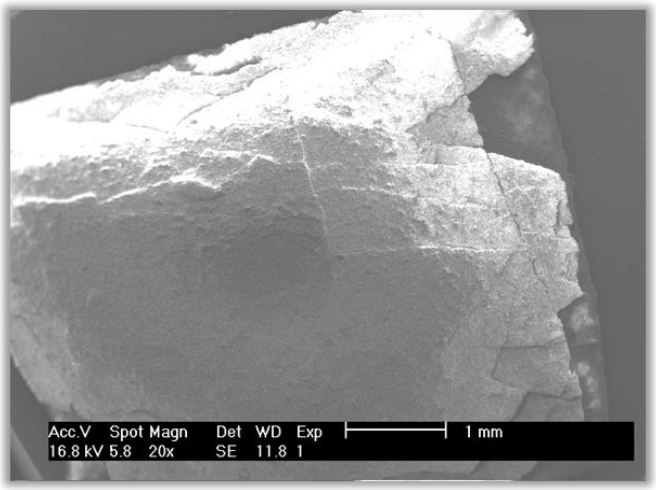

Figure 10 SEM micrograph illustrates a cake layer covered on a 8μm Nuclepore surface.

Closer examination on the filter surface after removing the layer was performed. Figure 11 illustrates that the 8μm pores of the Nuclepore had been clogged by silica particles. From analysing the arsenic contents of the Nuclepore filters after use, 163.91 μg of arsenic was found with the filters, corresponding to 65 % of the total arsenic filtered (253.50 μg arsenic). Only 5% (12.68 μg arsenic) was retained on the 0.1μm filter used to isolate particles that had previously passed through the larger pore size filters.

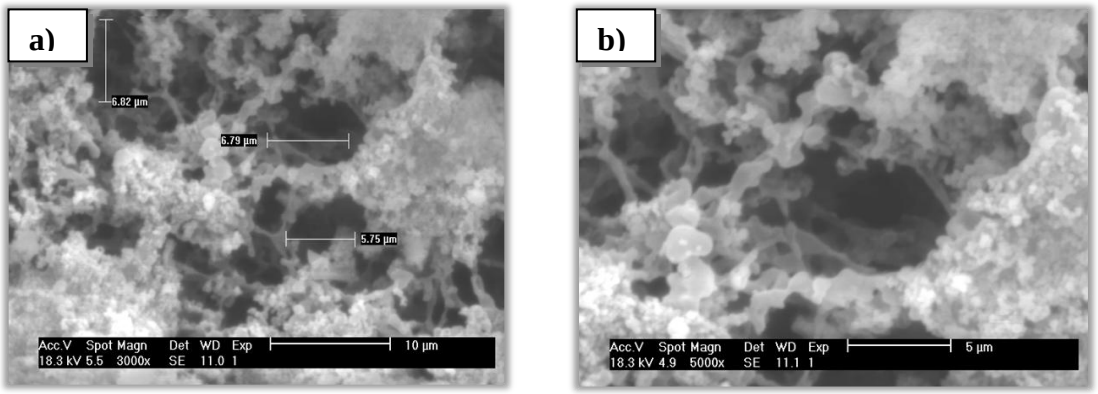

Figure 11 SEM micrographs showing the pores of the 8 μm Nuclepore filter surrounded by silica particles.

The high concentration of arsenic collected by the Nuclepore filter was probably due to particle aggregation and the high concentration of particles used for the filtration. The results indicated rapid clogging of the membrane through the accumulation of colloidal and particulate matter on the filter surface, which leads to increased retention of particles that would normally pass through the filter.

According to our results, all possible hypotheses of the blocked pore filter can be assumed for some reasons. Firstly, some chemical reaction, e.g. electrostatic repulsion of particles, affects their movement during filtration, influencing on clogging at the pores of filters. Bowen[34] suggested that an electrochemical interaction possibly caused a cake layer formation resulting in the increasing accumulation of the particles on the membrane surface. In addition, high concentration of particles in the suspension resulted in increased blocked pore filter. Several particles attempt to pass simultaneously into a pore of filter, but fail to do so and form a cake over the pore entrance. This finding agreed with the work by Wakeman[35] who suggested that clogging occurs particularly when the particles are at a higher concentration in the feed. Moreover, some literature [36] also suggested that increasing feed concentration increases particle aggregation, and consequently in pore blocking, resulting in permeability reduction.

3.3.1.3 Conclusion

This experiment demonstrated that small, synthetic colloidal particles were still being filtered from their sol using filters having pore diameters significantly larger than the particle size. Filter clogging of the *first* filter is accompanied by a decrease in the effective pore size of the *second* filter, in this study reducing the concentration of solid material as 'the colloidal particles' to less than 30% of its original concentration. These results have revealed that clogging and aggregation of particles have significantly influenced filtration efficiencies with particles that are smaller than the filter's pore being retained on or inside the filters. The retention of the particles

depended also the internal structure of the type of filter used. The effective pore size is also influenced by the amount of particles on the filters.

3.3.2 Using fluorescent labelled particles

The influence of the volume of water sample on the filtration efficiency was investigated using the fluorescent labelled silicas. In addition, the effect of particle size on the filtration was also studied. The Rhodamine labelled silica (SiSH-Rh) (Section 2.2.2.5.2) was used for these experiments.

3.3.2.1 Materials and methods

As in the previous experiment, a double filtration was performed. The filters used were the 1.6 µm glass microfiber filter (Whatman GF/C) and a 0.1 µm Nuclepore track-etched membrane.

Sodium hydroxide (NaOH) and reagent grade methanol (MeOH) were purchased from Fisher Scientific (Leicestershire, UK). The Rhodamine B was released from the silica particles using 5 mL of 1M methanolic NaOH (Section 2.2.3.5.2). Fluorescence was measured using 543 nm excitation and 564 nm emission with a Perkin Elmer LS-5B spectrometer. Water was purified by deionisation using an Elga Option 4 system.

3.3.2.1.1 The effect of water volume on filtration efficiency

A particle suspension was prepared by adding *ca.* 1.25 mg of 250 nm of SiSH-Rh to 500 ml of deionised water. After mixing, the suspension was continuously sonicated until filtered. This suspension was transferred into five containers, so that each contained 100 ml (c*a.* 250µg SiSH-Rh) of the suspension. These suspensions were sequentially passed through the 1.6 µm GF/C filter and then the 0.1 µm Nuclepore filter. Before filtering the next 100 ml of suspension, the 0.1 µm Nuclepore filter was

replaced by a fresh membrane. Meanwhile the remainder of the suspension was kept continuously sonicating for the period of the filtration processing. All the used-filters, the first 1.6 μm GF/C filter and five 0.1 μm Nuclepore filters, were collected. The particles in the used filters were quantified by releasing the Rhodamine label from the silica using 1M methanolic sodium hydroxide digestion. The released rhodamine was determined by relating the fluorescence of the resulting solution to the rhodamine content of the silica (Section 2.2.3.5). The fluorescent solution was determined for 3 replications by fluorescence spectrometry. The proportion of the particles trapped by the filters could be determined.

In a further experiment the volumes of the suspension that were filtered was varied. Five batches of suspension (*ca.* 250 μg SiSH-Rh suspension in each batch) were filtered. These suspensions ranged in volume from 100 to 500 ml. After sequential filtration, there were two filters (1.6 and 0.1μm filters), from each batch, that were analysed to assess the quantity of particles collected by each filter.

3.3.2.1.2 The effect of silica particle sized on filtration efficiency

To study the effect of particle size on the filtration, SiSH-Rh particles with diameters of 100, 250 and 600 nm (Section 2.2.1.3.2) were used. *Ca*. 250 μg of the SiSH-Rh was suspended in 500 ml of deionised water and continuously sonicated. Three batches of suspension with particle of different sizes were prepared. These suspensions were double-filtered through a 1.6 μm GF/C filter, followed by a 0.1 μm Nuclepore filter. After filtration, the filters were collected and their Rhodamine contents measured.

3.3.2.2 Results and discussion

3.3.2.2.1 The effect of water volume on filtration efficiency

The major objectives of this study were to investigate how the volume of suspension and the size of particle in that suspension controlled the filtration efficiency.

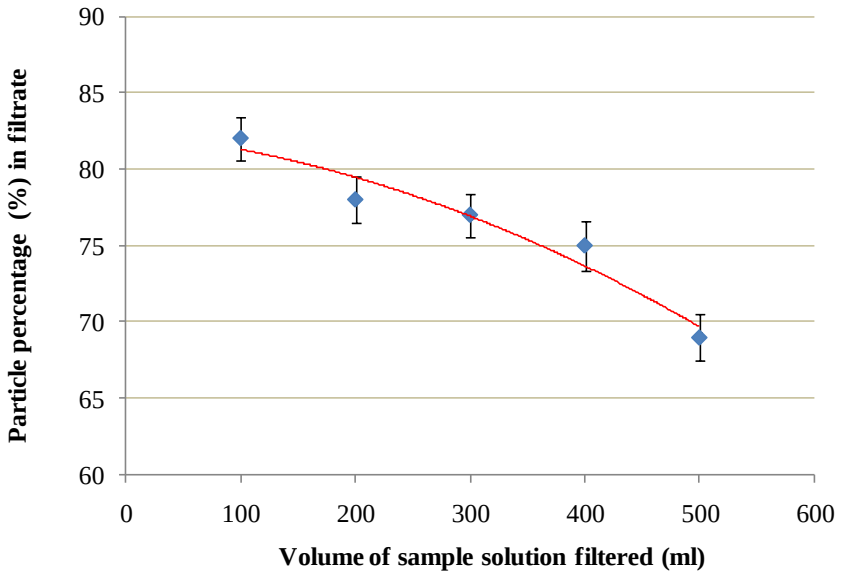

Figure 12 Percentage of the 250 nm Rh-labelled particles (SiSH-Rh) collected by a 0.1µm filter following Whatman GF/C filtration of 100 ml sample aliquots with 3 replications of each sample.

Increasing the volume of suspension passed through the *first* filter (GF/C) resulted in lower particles being collected on the *second* filter (Figure 12). When a 1.6 µm GF/C filter was used to filter 500 ml of the suspension just 10% of its particle content was collected from the 1st filter filtrate. The error in the measurement of Rhodamine content on filters samples is estimated to be ±2%. Results reveal that up to 85% of the particles collected on the *second* filter while only 10% were found to be collected on the *first* filter. It is assumed that the rest of the suspended particles (about 5% of the total particles) were in the final filtrate. In order to prove this assumption, the final filtrates were examined using DLS. The result is shown in Figure 13.

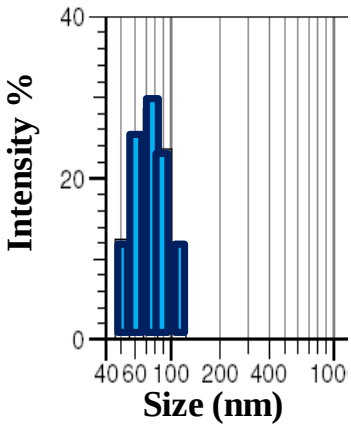

Figure 13 Size distribution of the filtrate which passed through the 0.1 μm filter

Figure 13 illustrates the size distribution of particles remaining in the filtrate after it had passed through the 0.1μm cut-off filter. The average particle size was found to be 76.4 ± 20.0 nm. Our particles used in the suspension were in the size of 250 nm diameter of particle. Theoretically, only particles having sizes smaller than 100 nm can pass through the 0.1 μm filter. It was possible that the particles found in the filtrates were originally the aggregates of small particles and that these fragments had separated apart during sonication.

A further investigation was carried out to measure the amount of particles that would be retained on the *first* filter. It can be seen from Figure 14 that the percentage of SiSH-Rh particles found on the *first* (red bars) filter increased as the volume of water sample used increased. The percentage of SiSH-Rh particles found on the *second* (green bars) filter decreased as the volume of water sample used increased.

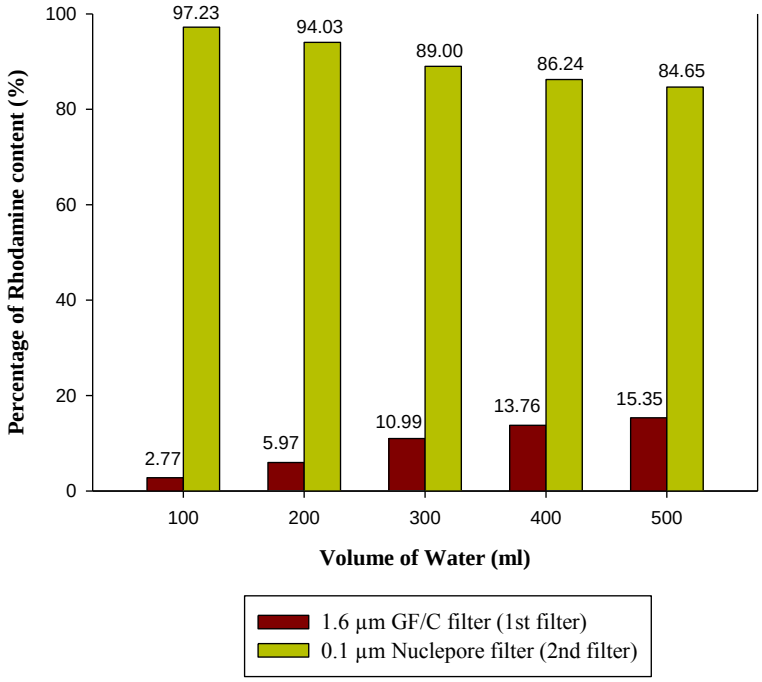

Figure 14 Rhodamine labelled silica collected on filters by double filtration.

It can be concluded from the experiments that when the sample volume was increased, more labelled particles were collected on the *first* filter (1.6 µm filter), resulting in fewer labelled particles being collected on the *second* filter (0.1 µm filter). This effect was due to an increase in particle trapping on/within the *first* filter, clogging the filter during filtration. Results here strongly suggest dilution effects on a particle retention by the *first* filter. It can be ascribed that a higher concentration (less dilution, e.g. a 100 ml of suspension) could enhance the particles to come together and became aggregates, resulting to increased particle retention of the pore *first* filter. This also can be explained by interactions between particles that are greatest when the particles are small and hence smaller particles become more readily aggregated than larger particles [35]. It is assumed that the rest of the suspended particles (approximately 20 %) were in the final filtrate. This result was in agreement with the study by Horowitz, et al. [13] whose work demonstrated that the volume of sample filtered significantly affected the filtrate concentration of Fe and Al in river water samples. Whilst this variation reflected the actual concentrations of these engineered colloidal particles in the water, it may also be attributable to the differential retention of various colloidal fractions as the filtration progressed [37, 38].

3.3.2.2.2 The effect of silica particle sized on filtration efficiency

The effect of particle size on the performance of filters is shown in Figure 15. Increasing the particle size (from 100 to 600 nm) leads to an increase in the amount of particles collected on the primary filter (1.6 µm filter).

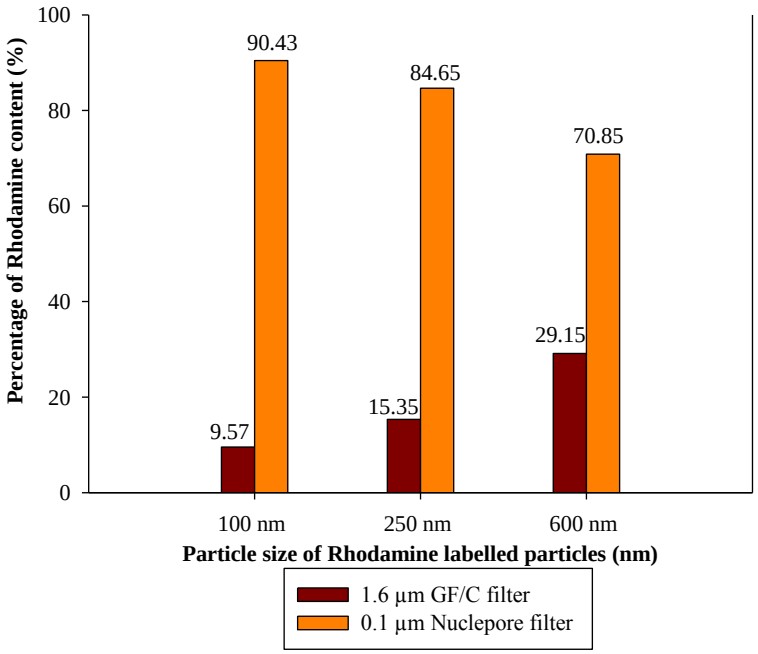

Figure 15 Effect of particle size on filtration characteristics.

All the particle sizes being studied were generally smaller than nominal pore sizes of filter and hence they should pass through the filter. Significant amount of the large particles (29.15% of the 600 nm particles) was found on the primary filter but fewer of the smaller size particles (9.57% of the 100 nm particles) were collected. On the contrary for the second filters, fewer large particles (70.85% of the 600 nm particles) were collected than of the small size particles (90.43% of the 100 nm particles).

From a previous experiment it was suspected that some particles had aggregated and clogged the filter during filtration and that depended very much on the particle concentration and hence the volume of water sample. In this study, the volume of water sample was fixed (500 ml) whilst the particle sizes of particles suspended in the waters were varied. Interactions between particles and the surfaces of the filters possibly exerted more influence to the filtration performance. When particles are principally larger than the sizes of the pores of the filter, they deposit on the plain polymer surface of a Nuclepore. When particles are commonly smaller than the pores sizes of a filter, deposition occurs within the internal structure of the depth filter (Whatman GF/C).

3.3.2.3 Conclusion

In this study, the effects of the volume of water sample and the size of particles being filtered on the filtration was investigated using fluorescent labelled silicas. Both aspects were found to affect the filtration. These effects are believed to be caused by the interactions between particles and the liquid media and the interactions between particles and the surfaces of the filters.

3.4 Filtration of the colloidal suspensions

This section attempts to investigate the behaviour of the colloidal particles on the filter during their filtration. Various materials and pores size of filter were assessed by SEM imaging of the filter to show characteristic particle associations and morphologies at the filter surface.

3.4.1 Materials and methods

3.4.1.1 Materials

Two filters, a 1.0 µm polycarbonate (Nuclepore) membrane and 0.45 µm type HA (Millipore) membrane were used in this study. Silica particles having a variety of different modified surfaces (non-modified, thiol-modified and DTC-modified) were chosen to represent an inorganic colloid in natural water (syntheses described in Sections 2.2.1 and 2.2.2). 1 litre of polyethylene bottle was employed. Deionised water was purified by an Elga Option 4 system. All containers were cleaned in 5% v/v hydrochloric acid for 24 hours and rinsed with deionised water prior to use.

3.4.1.2 Filtration studies

Colloidal suspensions were prepared by dispersing *ca*. 250 nm modified and non-modified silicas (*ca.* 250 µg) in 500 ml of deionised water. The particle sol was then shaken gently and 50 ml of the suspension was sequentially passed through a 1µm (Nuclepore) filter then a 0.45 µm HA (Millipore) filter.

The used filters were dried in a desiccator overnight over silica gel awaiting further analysis. All used filters were characterised as described in Section 3.2.1.4.

3.4.2 Results and discussion

Figure 16 and Figure 17 show a 1.0 μm (Nuclepore) and a 0.45 μm (Millipore) filter surfaces after they had been used to filter three types of colloidal suspension. Despite the different surface functionalities, the clustering of particles was found to be similar in all cases. The deposition of large aggregates rather than single particles on the *first* filter surface was always apparent (Figure 16). Most of these clusters can be assumed to be; aggregation occurred in the suspension prior to the filtration due to the high surface area of the colloidal size particles and, hence, the high potential adsorptive capacity for each other. They probably occurred due to physical and electrostatic interactions between colloidal particle and filter surface property leading to some particles can be induced to aggregate then collected at the filter surface.

As a result of clogging on the *first* filter surface, only a small amount of individual particles was collected on the 0.45μm filter surfaces (Figure 17). From these results the colloidal particle is therefore influenced by aggregation or disaggregation processes during filtration.

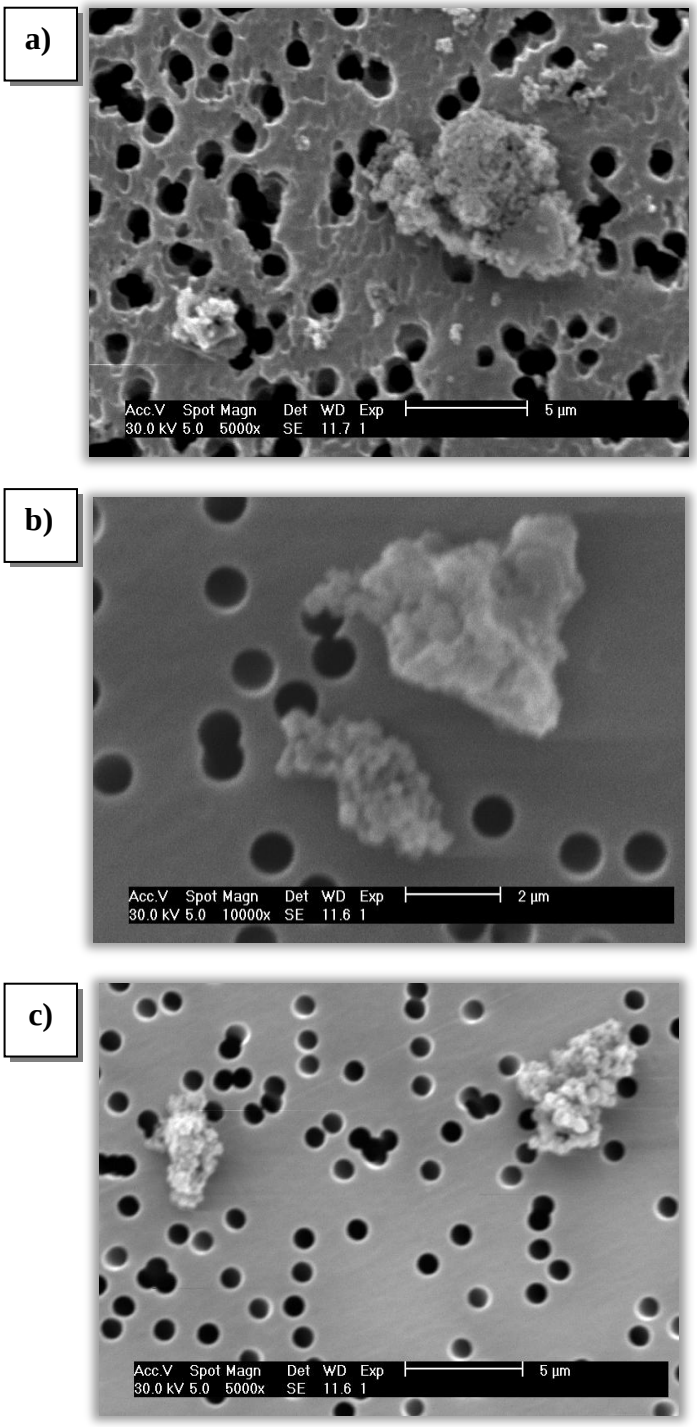

Figure 16 SEM micrographs of different modified engineered-particles added in deionised water samples; (a) DTC-silicas (b) thiol-silicas and (c) non-modified silicas (1.0 µm Nuclepore filter).

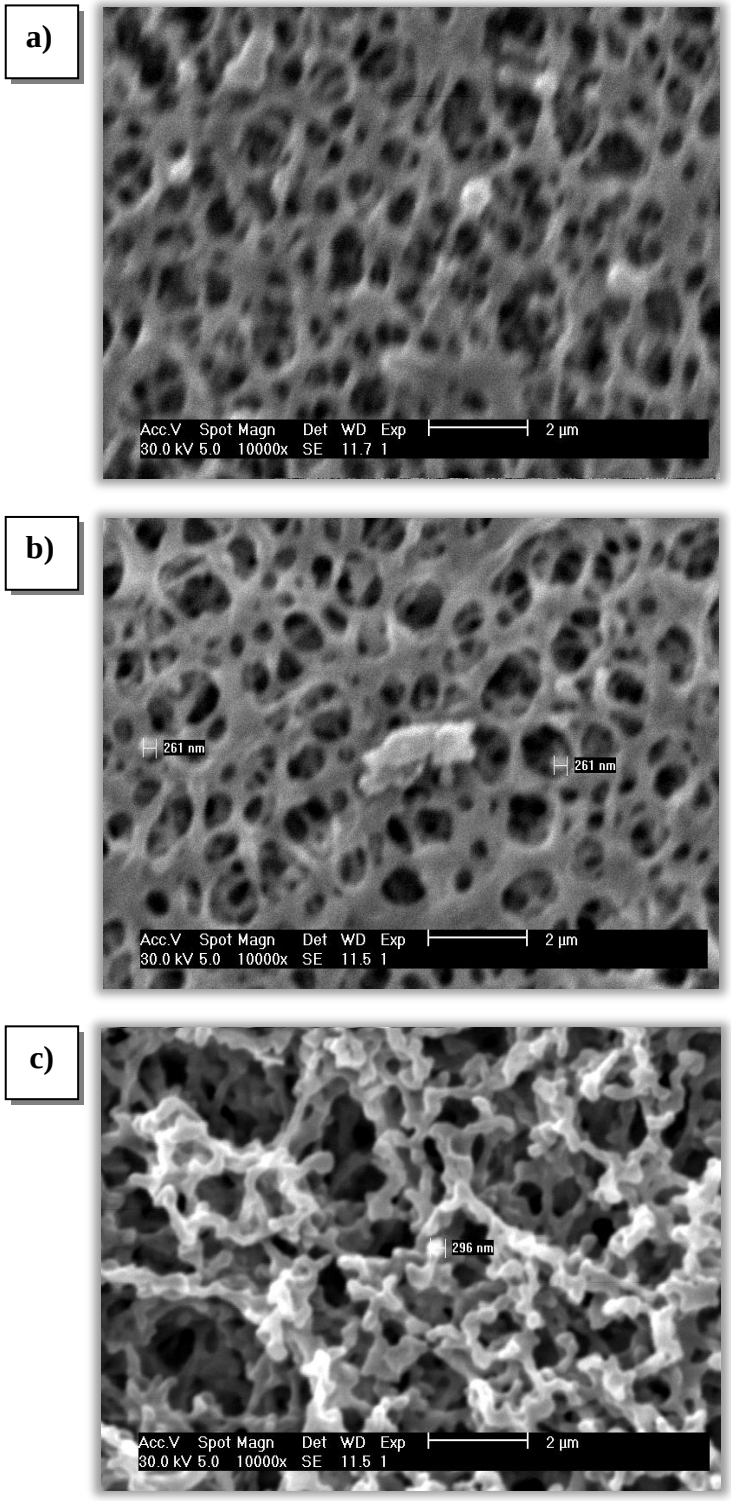

Figure 17 SEM micrographs of 0.45 µm Millipore filters used to filter 250 nm modified engineered-particles added in deionised water samples; (a) DTC-silicas (b) thiol-silicas and (c) non-modified silicas (0.45 µm Millipore filter). Suspension previously filtered using a 1 µm Nuclepore filter.

Typical clogging effects on filters due to particle aggregations are shown in Figure 18. According to the morphologies of Nuclepore filter surface after filtration, all possibilities of associated particles with surface filter can be considered. Aggregated particles or single particle are partially collected the pore (Figure 18a), leading to a reducing the effective pore size. It can also completely fill the pore (Figure 18b). Moreover, when aggregates are associated with some natural particulates (Figure 18c) and become a larger material and consequently, blocking the pore of filter. This affects an ability of pore size on filtration. An aggregated particle remaining between the pores is also apparent (Figure 18d). This cluster can influence the particle that should easily pass through the pore by delay its flowing and also being capture at surface filter. The size of aggregates shows a considerable amount of a single particle remaining trapped on the filter (Figure 18d and 18e) that in turn affects filter performance.

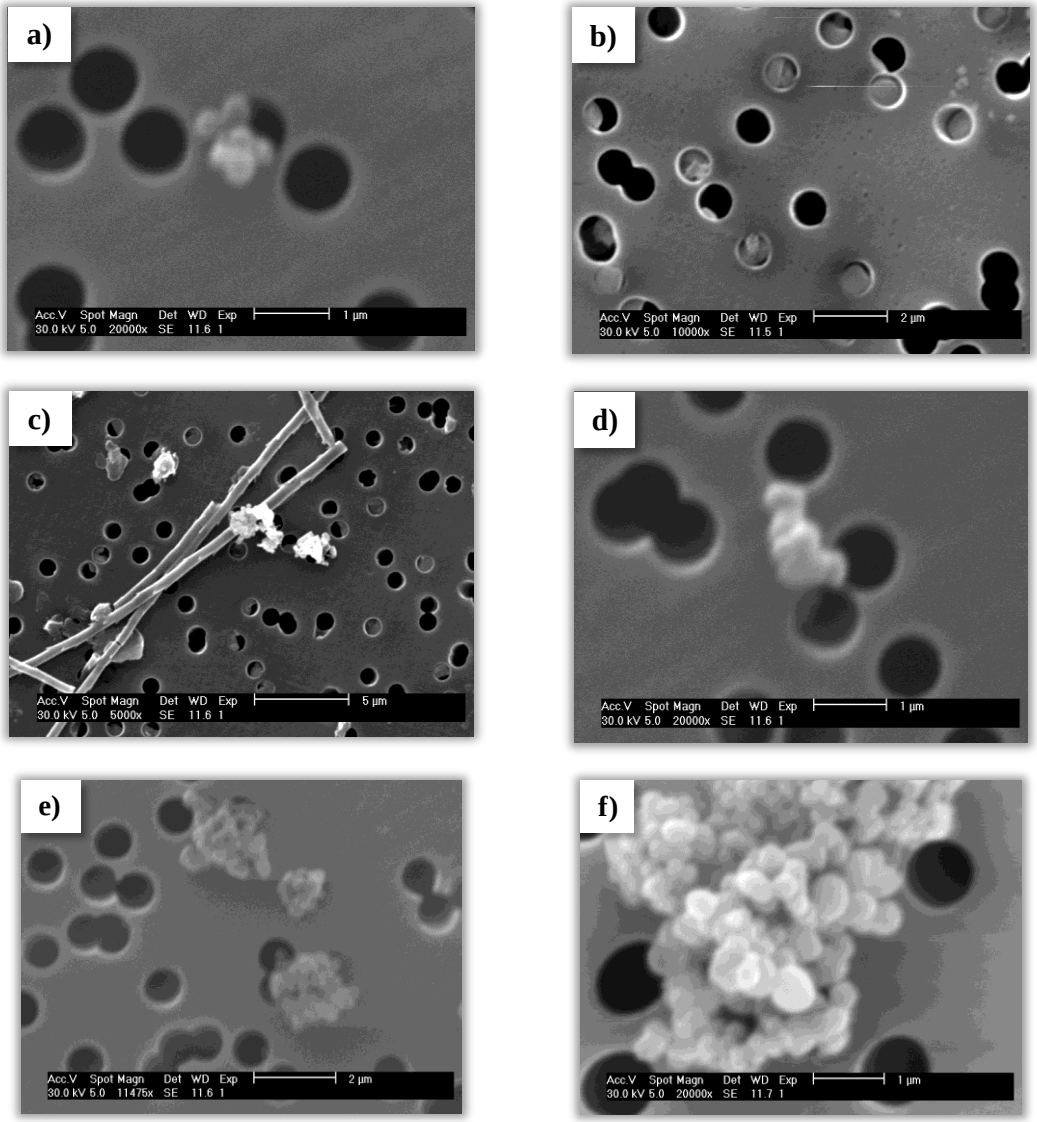

Figure 18 images showing of sub-micron particles on a 1µm polycarbonate, Nuclepore filter; (a) collecting around side of the pore resulting to the pore closure (b) trapping then blocking the filter pore (c) attaching to natural organic matter (d) sticking on the surface nearby the pore (e) aggregates and then totally (f) blocks the pore of filter.

Within this Chapter, the role of particle size on filter collection efficiency was examined. A model of the clogging and building up a cake layer is shown schematically in Figure 19 and Figure 20. Particles which were smaller than the nominal pore size of the filter can be deposited either within the internal structure or at the surface of the pore. Both of the latter can lead to pore closure (Figure 19). Additionally, aggregates of small particles which normally occur can cause pore blockage in the filters by attempting to enter a filter pore (Figure 20).

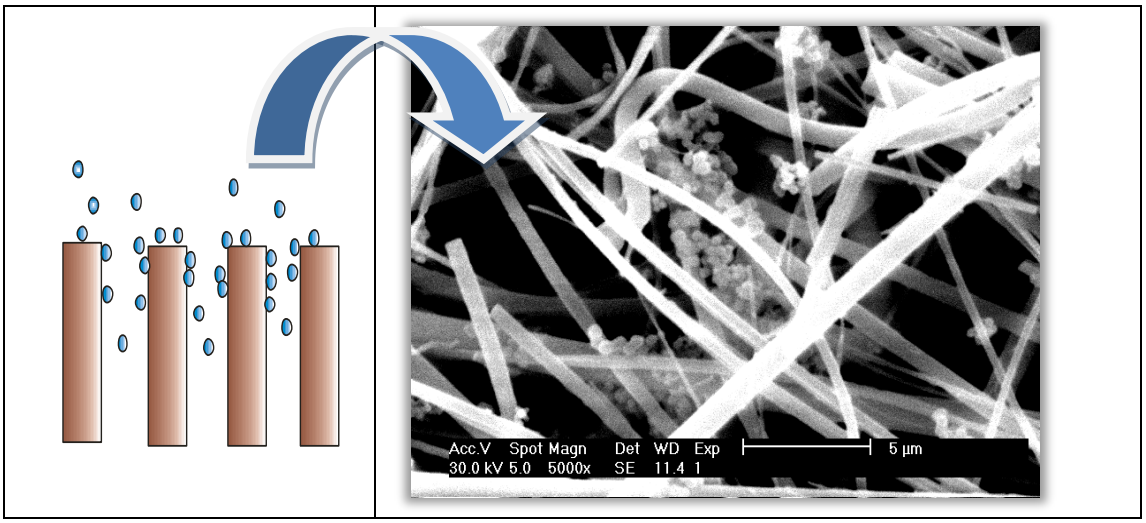

Figure 19 shows modelling of aggregated particles formed and stick inside surface filter (1.6µm Whatman GF/C filter).

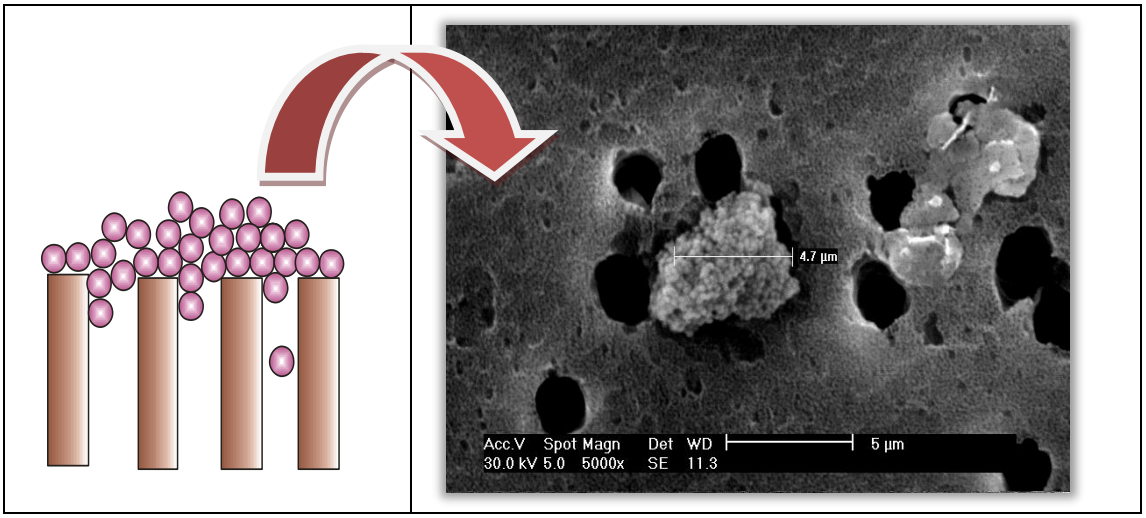

Figure 20 shows modelling of aggregated particles formed and stick on surface filter (2.0µm Nuclepore filter).

3.4.3 Conclusion

In this study, small particles, especially in the colloidal size range, have been formed to be significantly aggregated either by electrostatic attraction or chemical affinity, resulting in larger objects that could either sediment or become trapped within the filters. The morphology of particle aggregations was that of large clusters, mostly with sizes larger than 2,000 nm. This phenomenon provides an additional increasing resistance to filtration efficiency, due to colloidal particles being retained on the filter. This can result in misleading results if filtration is employed to estimate the size distribution of particles in suspension.

3.5 Summary

In this chapter, the associations of natural materials in Southampton coastal water with synthetic particles during filtration were investigated. These associations capture on the filter surface could be the result of physical and electrostatic interactions between molecules of natural material, engineered particles and filter surface properties. Physical adsorption is caused by attractive force between two particles while for chemical adsorption the electrons between particle and filter surface structure are shared, which produce a relatively high strength bond.

The behaviour of synthetic colloidal particles was also assessed. It was revealed that clogging and aggregation of particles influenced the filtration efficiency. During the filtration, particles in the colloidal size range deposited on the filter surface or in the pores, depending on the size and shape of the colloids. Relatively small particles, compared to the filter's pore, were retained on or inside the filters while those with a larger size than the pores will deposit as a cake layer on the filter surfaces and cause pore blockages. Aggregation and clogging altered the effective size cut-off of the filters.

The retention of particles depended not only on the pore size diameter but also the internal structure of the type of filter used. The volume of water sample and the size of particles being filtered were also keys to the filtration performance. It was found that both the volume of water sample in which the particles were suspended and the size of particle themselves affect the filtration. Different types of filter were assessed by investigating the filtration of colloidal particle suspensions. The typical track-etched filter, type S (Nuclepore), was found to be affected by many small particles attempting to enter a filter pore at the same time, resulting in the high retention of particles on filter surface. Whereas the GF/C depth filter (type TP), the particle can pass through this filter with the higher amount, in comparison with, track-etched filter, even though of a bigger pore size. These results can therefore suggest that the stated pore size of a filter may be not a good indicator of its effectiveness for separating size fractions of particles.

3.6 References

[1] J. M. Greenamoyer and S. B. Moran, *Marine Chemistry* **1997**, *57*, 217-226.

[2] R. Kretzschmar and H. Sticher, *Environmental Science & Technology* **1997**, *31*, 3497-3504.

[3] K. T. Valsaraj and I. Sojitra, *Colloids and Surfaces a-Physicochemical and Engineering Aspects* **1997**, *121*, 125-133.

[4] R. Kretzschmar, M. Borkovec, D. Grolimund and M. Elimelech in *Mobile subsurface colloids and their role in contaminant transport*, *Vol. 66* **1999**, pp. 121-193.

[5] J. M. Ross and R. M. Sherrell, *Limnology and Oceanography* **1999**, *44*, 1019-1034.

[6] D. Vignati and J. Dominik, *Aquatic Sciences* **2003**, *65*, 129-142.

[7] Y. Ran, J. M. Fu, G. Y. Sheng, R. Beckett and B. T. Hart, *Chemosphere* **2000**, *41*, 33-43.

[8] L. Sigg, H. B. Xue, D. Kistler and R. Sshonenberger, *Aquatic Geochemistry* **2000**, *6*, 413-434.

[9] C. Gueguen and J. Dominik, *Applied Geochemistry* **2003**, *18*, 457-470.

[10] L. G. Danielsson, *Water Research* **1982**, *16*, 179-182.

[11] D. P. H. Laxen and I. M. Chandler, *Analytical Chemistry* **1982**, *54*, 1350-1355.

[12] R. Saindon and T. M. Whitworth, *Aquatic Geochemistry* **2006**, *12*, 365-374.

[13] A. J. Horowitz, K. A. Elrick and M. R. Colberg, *Water Research* **1992**, *26*, 753-763.

[14] J. Buffle and G. G. Leppard in *Characterization of Aquatic Colloids and Macromolecules. 1. Structure and Behavior of Colloidal Material*, *Vol. 29* **1995**, pp. 2169-2175.

[15] J. Buffle and G. G. Leppard in *Characterization of Aquatic Colloids and Macromolecules. 2. Key Role of Physical Structures on Analytical Results*, *Vol. 29* **1995**, pp. 2176-2184.

[16] P. M. Haygarth, M. S. Warwick and W. A. House, *Water Research* **1997**, *31*, 439-448.

[17] S. Hong, P. Krishna, C. Hobbs, D. Kim and J. Cho, *Desalination* **2005**, *173*, 257-268.

[18] C. Orr., *Filtration, Principles and Practices Part II*, Marcel Dekker, Inc., New York, **1979**, p.

[19] W. Hickel, *Marine Ecology-Progress Series* **1984**, *16*, 185-191.

[20] R. Zonta, R. Cecchi, F. Costa, F. Simionato and G. Ghermandi, *Science of the Total Environment* **1994**, *143*, 163-172.

[21] D. Vignati, J. Loizeau, P. Rossé and J. Dominik, *Water Research* **2006**, *40*, 917-924.

[22] A. G. Howard and P. J. Statham, *Inorganic Trace Analysis: Philosophy and Practice*, Wiley, **1997**, p.

[23] R. W. Sheldon, *Limnol. Oceanogr.* **1972**, *14*, 441-444.

[24] C. M. Palmer in *Algae in water supplies., Vol. 657* Public Health Service Publication, Government Printing Office, Washington, D.C., **1959**.

[25] F. M. M. Morel; and J. G. Hering, *Principles and Applications of Aquatic Chemistry*, Wiley-Interscience, New York, **1993**, p.

[26] C.-H. Kim, M. Hosomi, A. Murakami and M. Okada, *Water Science and Technology* **1996**, *34* 157-164.

[27] E. R. Parker in *The role of colloidal material in the fate and cycling of trace matals in estuarine and coastal waters., Vol. Ph.D.* University of Southampton, **1999**, p. 426.

[28] A. Gunnars, S. Blomqvist, P. Johansson and C. Andersson, *Geochimica Et Cosmochimica Acta* **2002**, *66*, 745-758.

[29] D. I. Kaplan, P. M. Bertsch and D. C. Adriano, *Ground Water* **1995**, *33*, 708-717.

[30] T. Kanti Sen and K. C. Khilar, *Advances in Colloid and Interface Science* **2006**, *119*, 71-96.

[31] A. W. Zularisam, A. F. Ismail and R. Salim, *Desalination* **2006**, *194*, 211-231.

[32] M. Filella and J. Buffle, *Colloids and Surfaces A: Physicochemical and Engineering Aspects* **1993**, *73*, 255-273.

[33] O. Gustafsson and P. M. Gschwend, *Limnology and Oceanography* **1997**, *42*, 519-528.

[34] W. R. Bowen, N. Hilal, M. Jain, R. W. Lovitt, A. O. Sharif and C. J. Wright, *Chemical Engineering Science* **1999**, *54*, 369-375.

[35] R. Wakeman, *Separation and Purification Technology* **2007**, *58*, 234-241.

[36] L. Seminario, R. Rozas, R. Bórquez and P. G. Toledo, *Journal of Membrane Science* **2002**, *209*, 121-142.

[37] M. A. Morrison and G. Benoit, *Environmental Science & Technology* **2001**, *35*, 3774-3779.

[38] S. Batchelli, F. L. L. Muller, M. Baalousha and J. R. Lead, *Marine Chemistry* **2009**, *113*, 227-237.

Chapter 4

Colloidal arsenic in an estuary system

4.1 Arsenic in the colloidal fraction of an aquatic environment

4.1.1 Toxicity of arsenic in the environment

Most studies of estuarine systems have usually employed particulate-dissolved fractionation based on 0.45 μm filtration and thus, do not take into account the colloidal fraction. Because of their large specific surface area, which exposes a high number of reactive functional groups, colloidal particles can adsorb considerable amounts of metals [1-3]. They are therefore thought to play a very important role in controlling the speciation and the cycling of many elements in natural waters.

Exposure to arsenic contaminated water has been associated with a significant number of health problems. In the mining industry, some mine and tailing water from mineral processing plants, particularly from non-ferrous metal mines, contain arsenic. There have been instances of arsenic poisoning in various parts of the world due to the processing of arsenical ores, or related to the residues of such operations. Besides, arsenate is widely used in agriculture. The discharge of wastewater containing arsenic into an aquatic systems poses a potential threat to the environment, affecting human health, animals, and plant life. Arsenic contamination of the environment is especially a problem when drinking water is affected (e.g. Bangladesh, India) [4]. The most

severe contamination of groundwater was quite recently discovered in the Ganges Delta, where millions of people are at risk[5].

Arsenic is a human carcinogen and potentially toxic trace constituent of all natural waters. It has an interesting environmental chemistry, involving many different inorganic and organic forms. The biological effects of arsenic depend mainly on the chemical form in which the element is ingested, the route of entry, the dose and the duration of exposure. In groundwaters inorganic arsenic is mostly in the form of trivalent arsenite (As (III)) or as pentavalent arsenate (As(V)). Contaminated drinking water is the greatest threat to human health caused by arsenic. The WHO and Vietnamese guidelines for maximum arsenic levels in drinking water are less than 10 ppb (µg l^{-1}) and 50 ppb (µg l^{-1}) [4, 6]. It is impossible to know if the drinking water contains arsenic without doing measurement, since arsenic is tasteless, colourless and without smell.

4.1.2 Chemistry of arsenic compounds

Although arsenic may exist in the environment and in biological systems in different chemical forms, the most important forms of inorganic arsenic are the anions arsenite and arsenate (Figure 1).

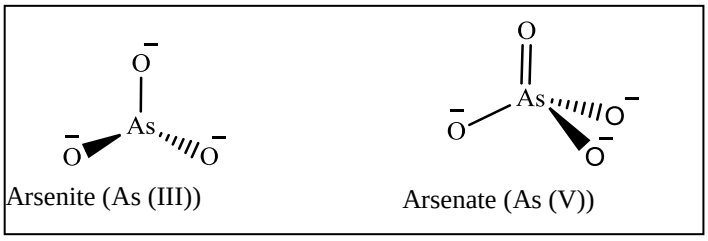

Figure 1 Common species of arsenic.

Because of theirs toxicities, inorganic compounds containing arsenic such as arsenic acid, arsenic(III) oxide, and arsenic(V) oxide, have been specified as hazardous waste by the Environmental Pollution Agency (EPA). Therefore, it is necessary to treat wastewater containing arsenic. The pentavalent forms, H_3AsO_4 (aq), $H_2AsO_4^-$ (aq),

$HAsO_4^{2-}$ (aq) and AsO_4^{3-} (aq) are typically predominant in oxidizing environments whereas the trivalent H_3AsO_3 (aq), $H_2AsO_3^-$ (aq), $HAsO_3^{2-}$ (aq) and AsO_3^{3-} (aq) are mostly found in reducing environments[7]. In water at 25°C, aqueous solutions of inorganic arsenite contain $As(OH)_3$ at pH 8 (pKa_1 = 9.32) [8],[9], whereas various species of arsenic (V) acid occur depending on pH (the first, second and third H_3AsO_4 p*Ka* values are 2.24, 6.94 and 12.19, respectively) [10]. However, due to slow redox transformations, both arsenite and arsenate are found in the environment.

Since arsenic is generally present in groundwaters as anions, it is easily adsorbed by colloids and minerals with positive charges such as Fe and Mn oxide minerals (goethite and gibbsite, ferrihydrite) and clay minerals.[11],[12] According to Berg and colleagues[6], the arsenic in sediments may be associated with iron oxyhydroxides and be released to the groundwater by reductive dissolution of such deposits. Oxidation of sulfide phases could also release arsenic to the groundwater. The pH is also the main factor influencing the activity of arsenic, high pH favouring arsenic enrichment in groundwater[13]. Moreover, since arsenic can be transported to other areas through the mobile colloids and can create secondary arsenic-contamination sites, arsenic-contaminated colloids must be treated in a safe way.

In general, the arsenic levels in water resources are recorded in the parts per billion (ppb, 10^{-9}) to parts per million (ppm, 10^{-6}) ranges. With such a wide concentration range of arsenic, a great number of techniques have been applied to its determination[14],[15],[16],[17],[18],[19]. One technique commonly used is hydride generation (HG) that has found wide application in the determination of trace levels of arsenic in combination with atomic absorption spectroscopy (AAS) [20],[21],[22, 23],[24]. The direct determination of very low levels of arsenic in parts per trillion (ppt, 10^{-12}) range is possible and the technique provides reliable results.

4.1.3 Association and transportation of colloidal arsenic

The majority of the arsenic released into the water comes from human, biological activities and natural sources. In water bodies arsenic can migrate as dissolved species, associated with suspended particles or as part of the bulk sediment load.

Several recent studies have reported the role of colloids in the long-distance transport of arsenic in waters [25],[26],[27-29],[30]. In addition, arsenic was found to be associated with metals and dissolved organic matter in the colloidal size range. Puls and Powell [31] performed experiments on the transport of As(III) in the presence of colloidal ferric oxide particles and showed that the transport of colloid-associated arsenate is 21 times faster than that of the dissolved arsenate. Cullen and Reimer [32] suggested in their review that arsenite is most often in a neutral form ($As(OH)_3$) and is more mobile than other arsenic forms. Arsenic species transformation occurred in the soil, resulting in the co-occurrence in the percolate water of four arsenic species, arsenite (As(III)), arsenate (As(V)) and the organic forms monomethylarsonic acid (MMA) and dimethylarsinic acid (DMA)[33]. A laboratory study on arsenic mobility in the soils collected from some golf courses demonstrated that the arsenic that was present in these soils was relatively mobile, suggesting potential for arsenic leaching. Arsenic binding to the soil is reported to be dependent on the pH and redox potential of the environment [34],[35],[36]. Arsenic mobility tends to increase with decreasing pH. On the other hand, an increase in pH can result in desorption of arsenic due to the lower stability of otherwise stable metal oxide arsenic complexes[35, 36].

The association of arsenic with colloidal organic matter is of interest because the dispersible colloidal particles may also be mobile in surface environments and thus transport significant amounts of contaminant to groundwater[37]. A number of studies have been carried out on arsenic speciation and cycling in the waters of Devon and Cornwall estuary systems [38-40]. Whereas in most estuary systems the major source of arsenic is the sea, the estuaries of rivers such as the Tamar provide an ideal

opportunity to study a system in which a large proportion of the arsenic is derived from the freshwater input. The distribution of colloidal As in the Tamar River (UK) is reported because the Tamar valley has historically been the site of the highest concentration of arsenic mining and refining activity in the World with a major main being sited at Morwellen. Drainage from these areas can be considered to be the source of contamination in the waters of the Tamar River.

The main objective of the study reported in this chapter was to improve our knowledge on the interaction of the colloidal arsenic with this river system. The specific objectives were:

- To determine the occurrence and distribution of arsenic colloids during freshwater and estuarine water mixing.
- To determine the filtration behaviour of engineered-colloids spiked into natural water.
- To determine the extent to which the colloidal particles of this estuary are responsible for the transport of arsenic through the estuary.

4.2 Studies of the colloidal arsenic in the Tamar Estuary

Samples of water were obtained from the estuary of the river Tamar. Arsenic is known to occur in this area due to the drainage of arsenic from the historical mines, making the distribution of arsenic in this water system a matter of interest. This section describes work carried out in the Tamar estuary during the summer of 2006. It includes further information on the processes governing the arsenic distribution in the Tamar estuary and reports on the presence and distribution of colloidal arsenic in the system.

4.2.1 Materials

Vacuum filtrations were performed using two-piece Millipore systems (47 mm filters) consisting of a glass reservoir and a fritted-glass base fitted to a 1 litre flask. The filters used in this study were of different material and with various pore sizes. The filters were: a 1.6 µm glass microfiber (Whatman GF/C) and a 0.1 µm polycarbonate track-etched membrane (Nuclepore). Water was purified by deionisation using an Elga Option 4 system. The pH meter was calibrated using buffer solutions at pH 4 and 7. Hydride generation atomic absorption spectroscopy (HG-AAS) or cryogenic trap HG-AAS (for trace levels of arsenic analysis) were employed to measure arsenic. Atomization in an electrically heated silica tube and detection at λ=193.7 nm with a Perkin-Elmer 3100 Atomic Absorption Spectrophotometer were used (using the parameters described in Appendices A and B).

4.2.2 Sampling sites

The sampling locations were selected with the aim of covering the whole of the freshwater–seawater mixing zone. The study, covering a distance of approximately 50 km, included the seaward end of the Tamar estuary and one site on the Dart River. The sampling locations are identified in Figure 2.

Water samples were obtained from 7 sites along the River from south to north in September 2006. Sampling sites were distributed from the estuary (sites 1 Cargreen to site 4 Calstock) to the upper region of the Tamar estuary (sites 5 Horsebridge to site 6 Greystone bridge) and site 7, Two Bridges, on the Dart River. Sampling was undertaken at high tide to avoid the active resuspension of sediments and performed at $\sim$0.5 m below the water surface by a grab method. The samples were collected in 1,000 ml polyethylene bottles which had been cleaned with 5% HNO_3 and rinsed at least three times with water from the sampling site before sample collection. After arrival in the laboratory, the water samples were transferred to a cool room where the temperature was kept constant at *ca.* 4 ^{o}C. Salinity values were measured by Mohr titration measurements of chlorinity in the laboratory.

2A

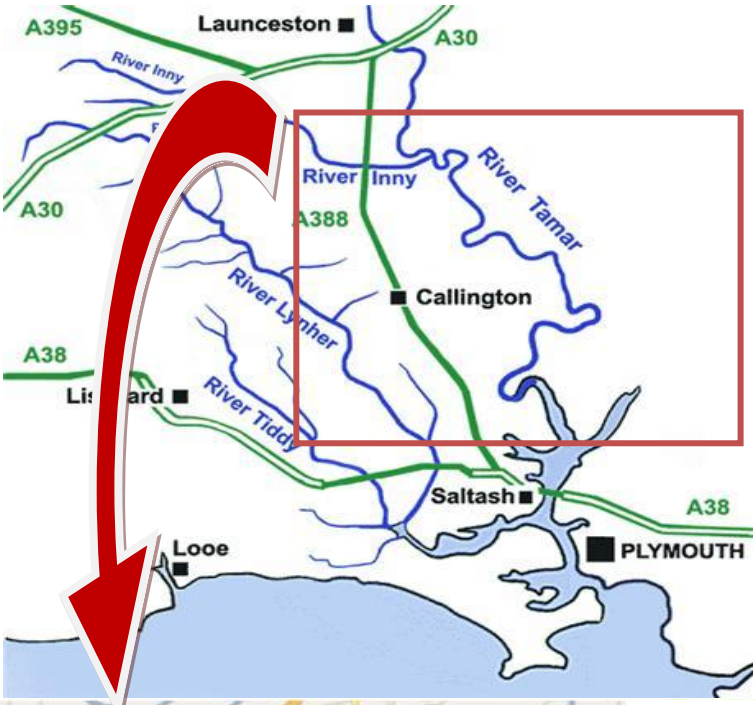

2B

Figure 2A overview of Tamar River at Plymouth, United Kingdom, source: http://maps.google.co.uk/10/05/2010. **2B** shows a magnification of the study area, labels mark the sampling sites.

4.2.3 Filtration experiments

The water samples were processed by double filtration sequentially through a 1.6 μm GF/C (Whatman) filter and then a 0.1 μm polycarbonate (Nuclepore) filter. These filters had been weighed prior to use. Each filter was rinsed with *ca.* 100 ml of deionised water before being used.

After filtration, the filters were oven dried overnight at 150 ^{o}C; they were then transferred to a desiccator to cool, and kept there until further analysis. The large particulates and the colloidal particles remaining on the 1.6 μm and 0.1 μm filters were evaluated by the measurement of the different weight values of the filters before and after filtration. The filters were then analysed for the total 'inorganic arsenic' that had been captured using HG-AAS methods. The filtrate was directly analysed for dissolved arsenic by cryogenic-trap HG-AAS procedures.

The detection limits of the methods for arsenic using the CT-HG-AAS and HG-AAS methods were 0.50 ng l^{-1} and 0.02 μg l^{-l}, respectively.

4.2.4 Results and discussion

The masses of sediment collected on each of the filters and the contents of arsenic (per litre of water), from seven sampling sites in the Tamar and Dart rivers, are reported in Table 1. The mass of arsenic (As) present per litre of water, present in particulate form, is shown in Figure 3.

Table 1 The mass of large particulates, concentrations of arsenic in solid particles and of arsenic present in the water as particulates from the Tamar and Dart rivers water samples.

Site	Salinity (ppt)	Large particulates loading (mg l^{-1})	As in the particles* d > 1.6 μm (μg g^{-1}) (SD ± 0.05)	As present in the water as particles* d > 1.6 μm (μg l^{-1}) (SD ± 0.03)	As present in the water as colloidal particles* 0.1 < d < 1.6 μm (μg l^{-1}) (SD ± 0.002)
Cargreen	35.1	27.4	12.3	0.34	<DL (0.01)
Holton	15.8	44.6	11.5	0.52	<DL (0.01)
Cotehele	9.40	83.3	11.8	0.99	<DL (0.01)
Calstock	3.20	130.5	9.60	1.26	<DL (0.01)
Horsebridge	0.10	1.80	70.5	0.13	0.02
Greystone bridge	0.05	3.20	39.6	0.13	0.02
Two Bridges	0.02	5.70	58.9	0.34	0.14

*Detection limit (DL) of the arsenic measurement = 0.02 μg l^{-1}, n =3.

Table 1 shows the large particulates loading and the concentration of arsenic (As) in the particles from the Tamar and Dart water samples. The concentrations of arsenic (As) present in the water as particulates and colloidal particles per litre of water are also illustrated in the same Table. The waters from Cargreen to Calstock were estuarine water (the salinity of *ca.*3-35 ppt), whereas those from Horsebridge to Two Bridges were true freshwater (the salinity of *ca.*0.02-0.10 ppt).

The mass of large particulates collected by the 1.6 μm filter (the *first* filter) from estuarine water (Table 1) was higher than that obtained from the riverine water. The maximum particulate concentration occurred at Calstock (130.5 mg l^{-1}). These large particulates on the *first* filter include large biological materials collected during the water sampling. Such particulates are derived from a common pool of mixed solids that circulate the estuary during the tidal cycle. The material collected by the *first* filter is highly dependent on tidal energy and the state of the tide during sampling, resulting in the higher particulate loading in these areas.

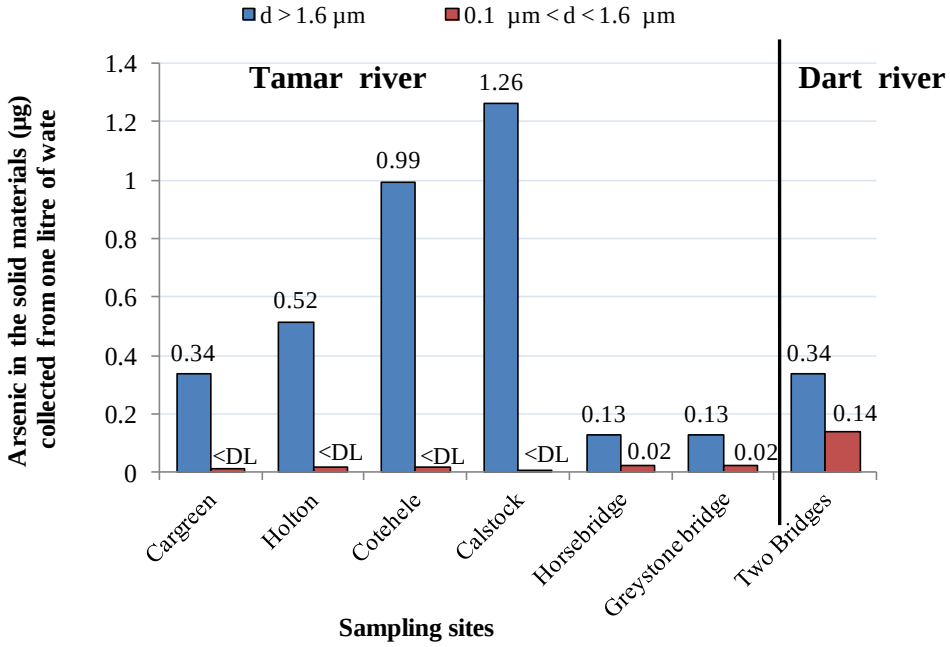

Figure 3 Arsenic concentration due to the large filters and colloidal particles retained by of 1.6 µm (blue bars) and 0.1 µm (red bars). Detection limit (DL) of the arsenic measurement = 0.02 µg l^{-1}, n =3.

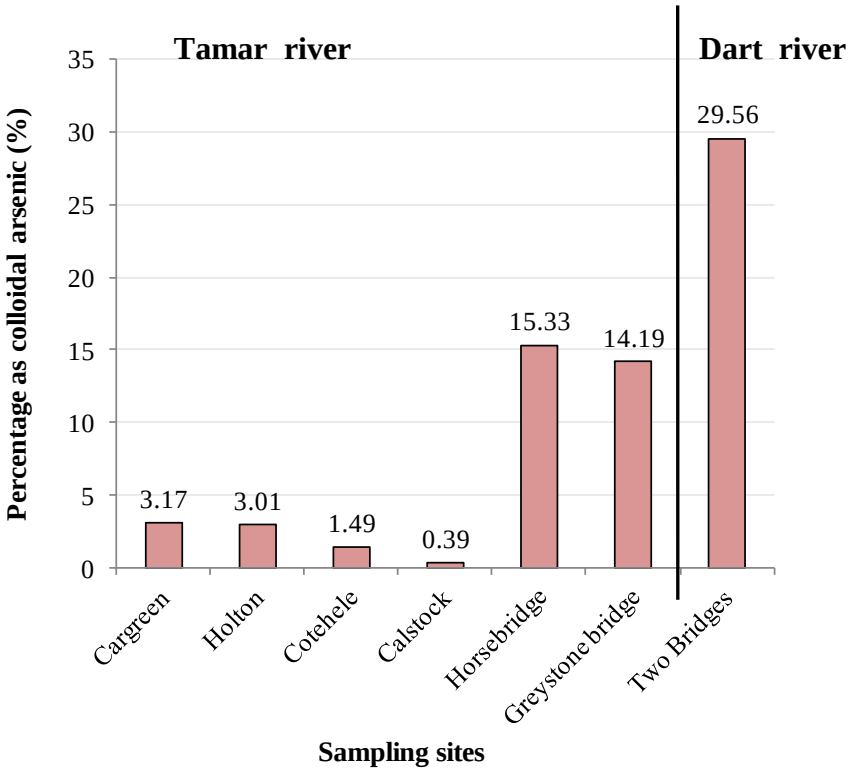

Figure 4 Percentage of the total particulate arsenic present in colloidal particles.

The concentration of As in the solid particles retained by the *first* filter from the estuarine sites (Cargreen to Calstock) were approximately 10-12 μg As g^{-1} (Table 1). Interestingly, the As concentrations in the solid particles in the riverine water (Horsebridge to Two bridges) were significantly higher (~59-70 μg As g^{-1}) (Table 1). In the Tamar estuary, the particulate arsenic loading (d> 1.6 μm) of the water increased upstream as the salinity decreased and the sampling site get closer to the main area of mining activity at Morwellen. Above Morwellen the arsenic levels dropped significantly. The As concentrations present in particulates from the riverine waters (Tamar River: Horsebridge and Greystone bridge and Dart River: Two Bridges) retained by the 0.1 μm filter (the colloidal particles) showed the presence of As (0.02 to 0.14 μg l^{-1}). The As concentrations in arising from colloidal particles at the estuarine sites (Cargreen to Calstock) were undetectable. I confirms the major role of colloid-bound metals play in the contamination of a river [41, 42]. The studied river system has proven to be contaminated by the drainage of As from disused mines. This As occurs in the tin and copper lodes primarily as arsenopyrite (FeAsS) with minor amounts of loellingite ($FeAs_2$). When this As contaminated material is released into a natural water, it results in high levels of As contamination. This can results from both natural erosion of arsenic ores and mining activity over history.

Figure 4 shows the percentage of the As present as colloidal particles (retained by the 0.1 μm filter and referred to as 'colloidal As'). It can be seen that a higher percentage of the As in the solid material is present as colloidal particles at the freshwater sampling sites (Tamar River: Horsebridge and Greystone bridge and Dart River: Two Bridges) than in the estuarine waters (Cargreen to Calstock); up to 30% of the total solid phase As concentration being present as colloidal particles This still however the significantly less As in the colloidal particles than there is in the large particulates (collected by the 1.6 μm filter). This can be due to a number of different factors. Firstly, the particles arise from different sources and do not therefore have to have the same particles sizes at different sites. Secondly, salinity and pH differences at

different sites may result in differences in aggregation of particles with each other or with other mineral and organic phases. Finally, the colloidal As may be collected with the larger particles during clogging by the *first* filter. This may result in less suspended As being retained on the *second* filter. A similar effect has been discussed in Section 3.3.1 for the filtration of synthetic colloidal particles spiked in water.

High amounts of As retained on the *first* filter can result from the aggregation of particles. The suggestion is that increasing the salinity of water can dramatically decrease colloid concentrations by aggregation and precipitation processes[43, 44]. A comparison between the colloidal As distribution and salinity values appears to reveal the effect of increasing salinity on the aggregation of the colloids (Figure 5). The high salinity levels in the estuarine region (Cargreen to Calstock) are therefore expected to increase the aggregation of colloids into larger particles in the environment that then settle out. Besides the high salinity level that could be the reason of an particle aggregation, the turbidity maximum zone (TMZ) and the tide wedge effect should be parameters to be considered as a cause of aggregation. The movement of tide wedge can have a significant effect on sediment distribution by eroding shores, stripping substrates, and suspending sediment for current dispersal. The upper reaches of estuaries are characterised by high levels of suspended particles which also contains a high level of particulates. These areas, known as estuarine turbidity maxima (ETM), created by estuarine physics, are located near the salt fronts. Within the region aggregation of particles is induced by the tidal energy causing the removal of colloidal particles moving downstream.

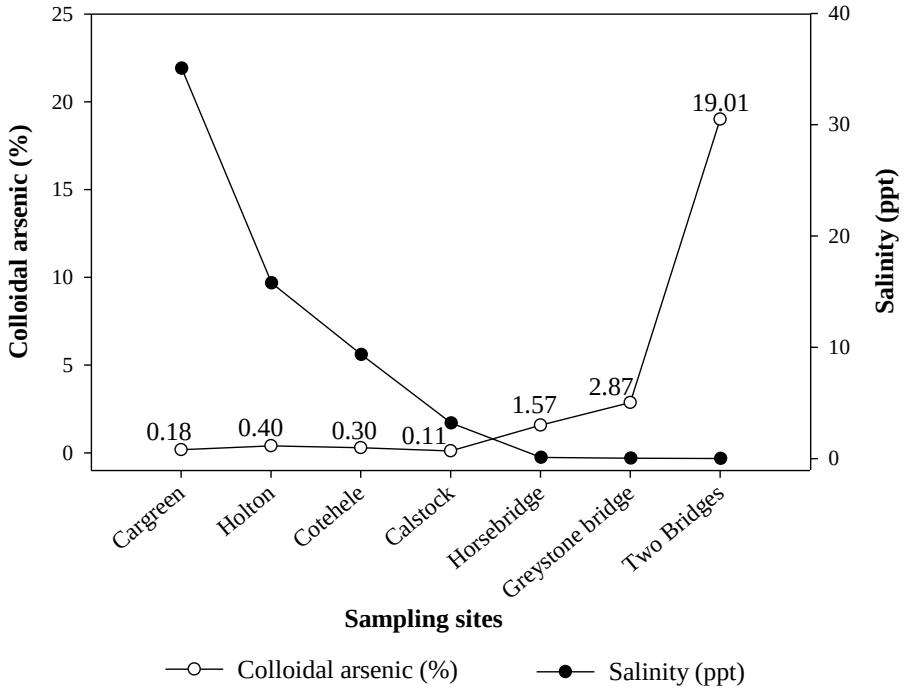

Figure 5 Comparison of arsenic in the colloidal phase (%) and salinity (ppt) from different sampling sites.

The As concentration in both the colloidal and the dissolved phases were further investigated. Figure 6 compares the colloidal As with the dissolved As (in the 0.1 µm filtrate). Significantly higher levels of dissolved As were present in the estuarine waters (3.9-5.8 µg l^{-1}) than in the river but there was more colloidal phase As (up to 0.14 µg l^{-1}) in the freshwater areas (Tamar River: Horsebridge and Greystone bridge and Dart River: Two Bridges).

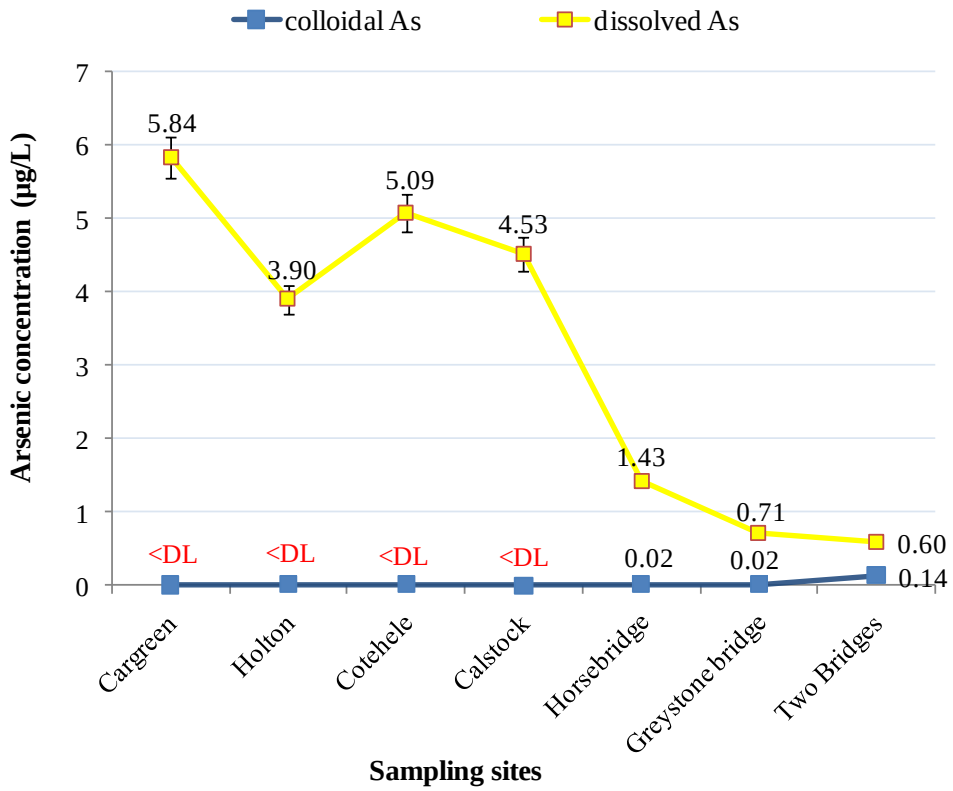

Figure 6 Arsenic concentration of the colloidal (0.1 < d< 1.6, blue) and the dissolved (d < 0.1, yellow) fractions.

The high concentration of As in these filtrates (d<0.1 µm) implies that the majority of the As is in the dissolved form (e.g. As(III) or As(V)). This is impacted to be the result of contamination of the river by drainage waters originating from mines located in the area especially those centred around Morwellen. More colloidal As could be present in smaller particles that pass through the 0.1 µm filter.

To group the As distribution results from the river study, Figure 7 illustrates the proportion of the arsenic that was designated "particulate", "colloidal" and "dissolved" as determined by 1.6 µm and 0.1 µm filtration. The proportion of the As that was in the dissolved fraction (red bar) was consistently highest (*ca.* 55-95%) at all the sampling sites. The colloidal As phase is of particular importance in the freshwater region, increasing to a maximum of 15% (blue bar) total As at the Two Bridges site, even though the concentration of the dissolved arsenic was gradually decreasing from the estuarine water to the freshwater.

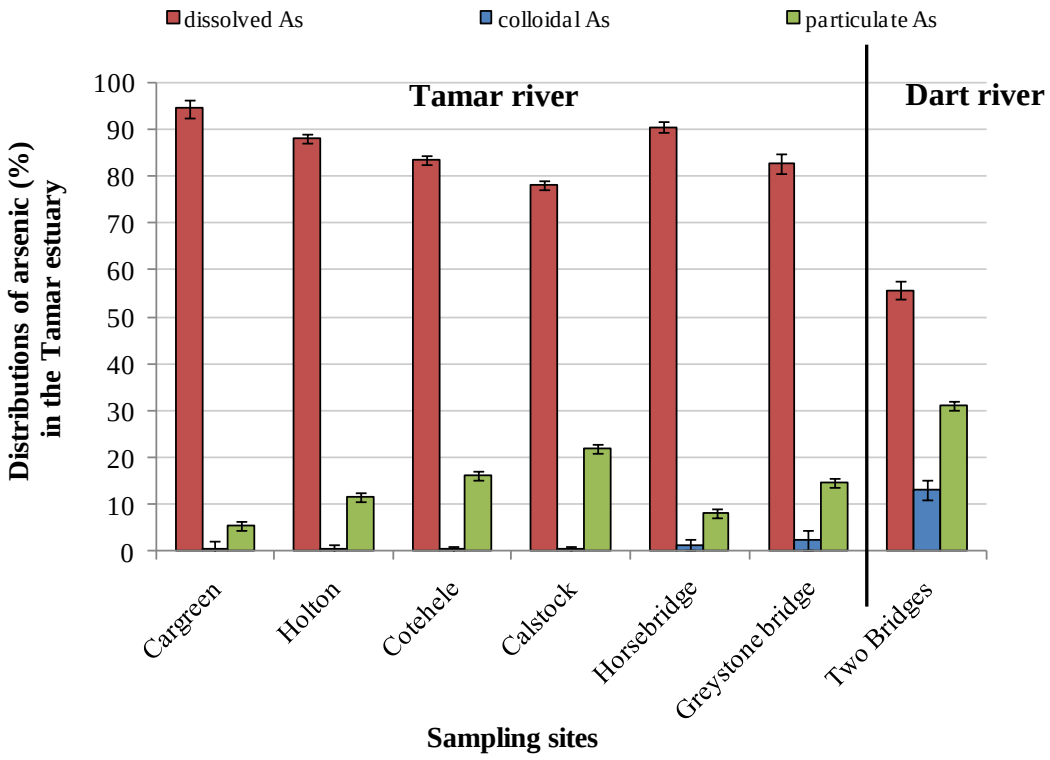

Figure 7 Distribution of arsenic from water samples of the Tamar estuary and Dart river. Three fractions of waters were determined by 1.6 µm and 0.1 µm filters.

4.2.5 Conclusion

This study has reported the distribution of arsenic in the Tamar estuary. The majority of the arsenic was found to be in the dissolved phase. The most probably explanation is that the main sources are from arsenic mining, historical drainage and refining activity. Arsenic-containing minerals such as arsenopyrite (FeAsS) and related ore materials could slowly oxidise to forms that are more soluble in water, leading to contaminated arsenic drainage.

The colloidal size fraction is most relevant at the riverine sampling sites which appear to have a relatively large proportion of the total arsenic as colloidal As (up to 15% of the total As concentration). Significantly larger amounts of the large particle arsenic

were found at the estuarine sites than riverine sites. The results presented here strongly suggest that salinity is one important factor inducing changes in the arsenic concentrations in natural waters. The higher salinity of estuarine waters may stimulate changes in the colloidal arsenic phase, enhancing colloidal aggregation into larger particles in the environment that then settle out, leading to an apparently higher arsenic content in the large size fraction particles. The turbidity maximum zone has to be considered alongside the salinity as a cause of aggregation.

Intrusion of saline water as a tidal wedge and the resulting turbidity maximum zone results in a high level of particulates which are cabable of aggregating with river-borne colloids. A major drop in colloidal arsenic is therefore to be expected in this region due to sudden salinity change and high tidal energy.

4.3 Studies of the colloidal arsenic fraction in River systems on the Devon-Cornwall border

Two river systems on the Devon-Cornwall border were selected for investigation in the summer of 2008. The importance of colloids in their waters was studied by conventional filtration. This section also describes work carried out using engineered-particles to investigate filtration effects.

4.3.1 Materials

The filters used in this study were glass microfibers (GF/C), polycarbonate track-etched membranes and cellulose nitrate (MF) membranes specified in Table 2.

Fluorescent labelled silica particles (Rhodamine silica particles, SiSH-Rh) were used in this study (the synthesis was described in Section 2.2.2.5.2). The Rhodamine label is released from the silica to quantify the silica particles collected by filtration. The released label is measured by fluorescence (Perkin Elmer LS-5B spectrometer with 543 nm excitation and 564 nm emission). The used filters were also characterised by scanning electron microscopy (SEM). The SEM used was a Philips Co., XL-30 ESEM at an acceleration voltage of 30 kV. Other materials used in this study have been described in Section 4.2.1.

Table 2 filter characteristics.

Filter type	Nominal pore size (µm)	Diameter(mm)	Identifier used in this study	Composition
0.1 µm Nuclepore (Whatman)	0.1	47	0.1	Polycarbonate
0.45 µm HA (Millipore)	0.45	47	HA 0.45	Cellulose acetate/nitrate
1.6 µm GF/C (Whatman)	1.6	47	GF/C 1.6	Glass microfibers
2.0 µm Nuclepore (Whatman)	2.0	47	Nu 2.0	Polycarbonate
3.0 µm cellulose (Millipore)	3.0	47	MF 3.0	Cellulose nitrate

4.3.2 Sampling sites

To assess the role colloid-associated As plays in the river systems, the Tamar and Dart Rivers were collected on 9th October 2008. The sampling sites for this study are spread over 50 km. The locations of the 6 sampling sites along the rivers Tamar (sites 1-3) and Dart (sites 4-6) are shown in Figure 8.

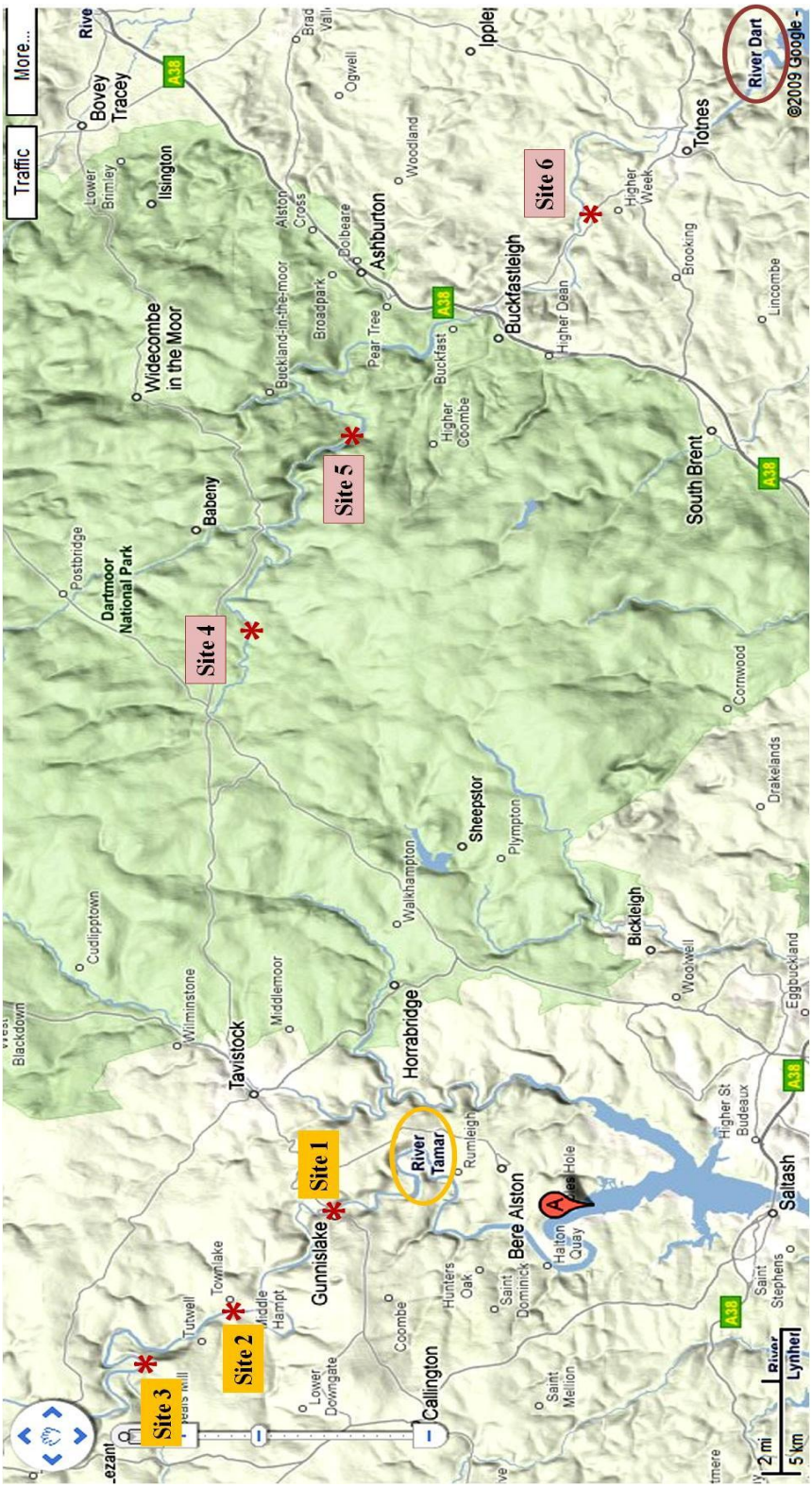

Figure 8 Sampling stations from two Rivers along the Tamar River; Site 1 Gunnislake, Site 2 Horsebridge, Site 3 Bradstone, and West Dart River; Site 4 Two bridges, Site 5 New bridge, Site 6 Starverton. (Source: http://maps.google.co.uk/ on 07/05/09)

The water samples were collected in 2.5 litres polyethylene bottles which had been cleaned with 5% HNO_3. These bottles were rinsed at least three times with water from the sampling stations. On return to the laboratory, the water samples were kept in a cold room (4^oC) prior to laboratory filtration and analysis. Salinity values were derived as described in Section 4.2.2.

4.3.3 Methods

4.3.3.1 The colloidal arsenic fraction of the river waters.

Filtration experiments were performed using various filter types. Two or three step filtration was carried out with the nominal particle size cut-offs of > 1µm, 0.45µm and 0.1µm. These were selected to distinguish between particulates, large colloids, fine colloids, and dissolved arsenic in the water (Figure 9).

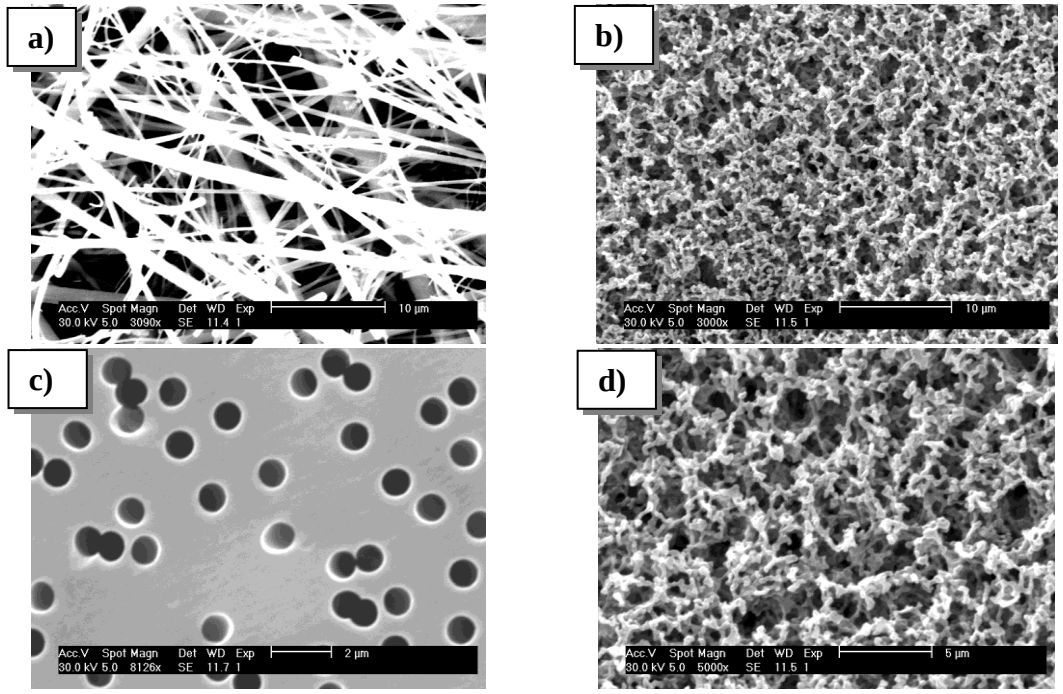

Figure 9 Electron photomicrographs of the cleaned filters that were used in this study; (a) 1.6 µm (GF/C) glass microfiber filter, (b) 3 µm (Millipore) cellulose nitrate filter, (c) 1 µm (Nuclepore) polycarbonate filter and (d) 0.45 µm (HA) cellulose acetate/nitrate filter.

The so-called '*first'* filters used in this study were 0.45 μm HA, 1.6 μm GF/C, 2.0 μm Nuclepore and 3.0 μm cellulose nitrate filters (Figure 10I). Consequently, the particulate fraction consisting of particles with sizes greater than these filter cut-off values were (in theory) collected by the *first* filter. The colloidal and dissolved arsenic passing through the *first* filter was sequentially passed through the '*second'* filter, a 0.1 μm polycarbonate membrane.

Colloids were operationally defined as particles which were larger than 0.1 μm but smaller than 0.45 μm (Figure 10II). The dissolved fraction was defined as the material which passed through the 0.1 μm filter. Duplicate samples were obtained for each water sample.

The mass of the particulates collected on the *first* filter was measured by weighing the filter before and after filtration and was reported per litre of water. The particulate fractions and filters were then digested by aqua-regia and analysed for arsenic concentration by HG-AAS. The filtrate samples were also analysed using the cryogenic-trap HG-AAS (Section 4.2.3).

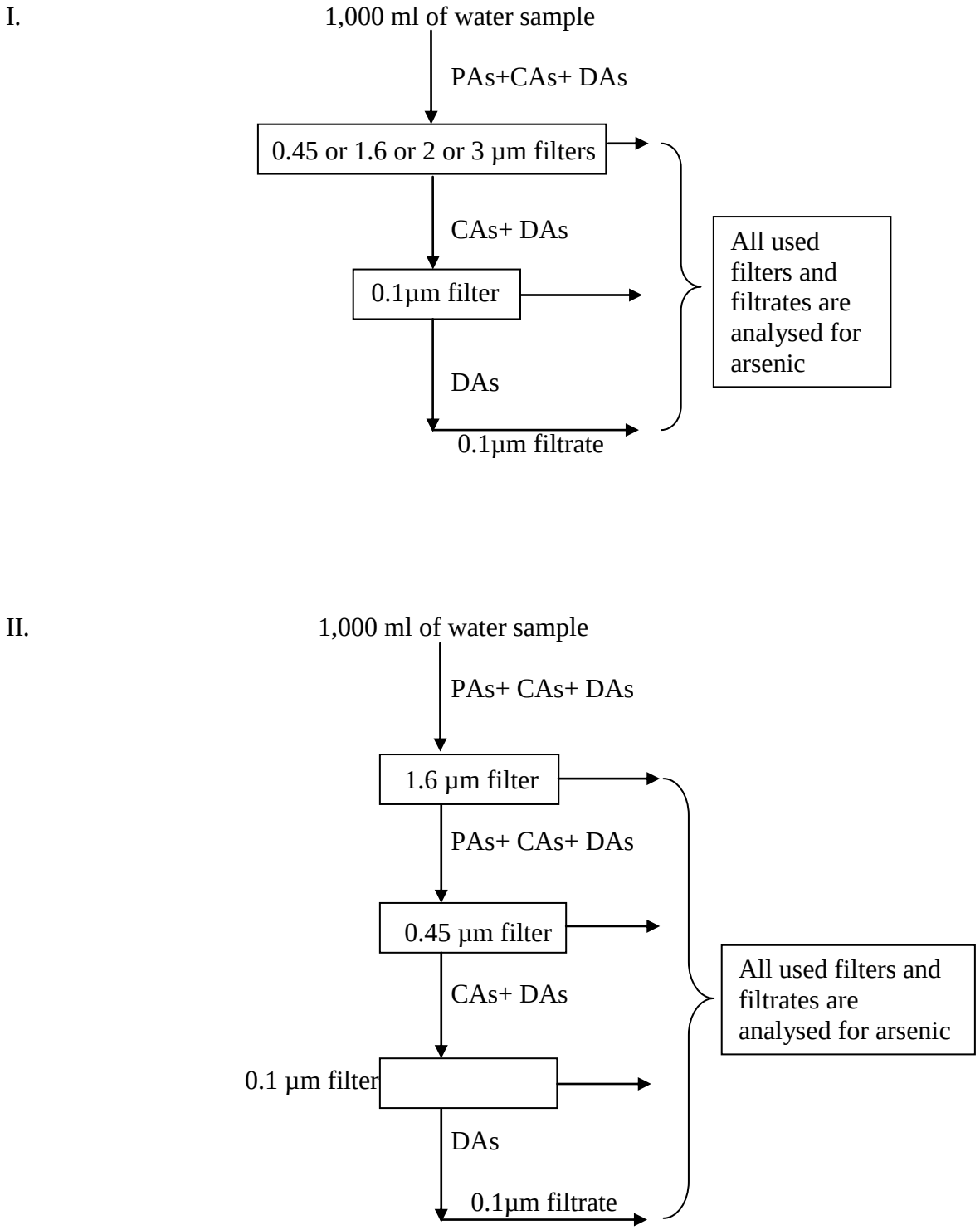

Figure 10 Filtration protocols for the double (I) and triple (II) fractionation schemes used in the study. PAs, CAs, and DAs are particulate, colloidal and dissolved arsenic, respectively.

4.3.3.2 Studies of engineered particles spiked into water samples

This section focuses on a study of the behaviour of engineered particles during the filtration of spiked natural water samples. The engineered-particles used in this investigation were produced as described in Section 2.2.2.

Water samples from the Dart river and Southampton Water were selected so that riverine and estuarine waters could be compared. Riverine water was taken from the Dart river (Starverton, site 6) while the estuarine Southampton Water sample was obtained at the quay of the National Oceanography Centre, University of Southampton (NOCs).

Method

4.3.3.2.1 250 nm sized particle-spiked water samples

In this study, 250 nm fluorescent particles were used. Rhodamine silica particles (SiSH-Rh) were added to 500 ml water from the Dart river to give a concentration of 1 µg ml^{-1}. Three types (the HA 0.45 µm, GF/C 1.6 µm and Nuclepore 2.0 µm) of filter were separately evaluated as the *first* filter in the filtration.

500 ml of the particle-spiked water sample was sequentially passed through the *first* filter and then a 0.1µm Nuclepore, *second* filter (Figure 10I). The experiment was repeated using a particle-spiked Southampton Water sample. Filtration was replicated at least twice for each sample. After filtration, all filters were then dried under vacuum overnight and kept dry until fluorescence measurement.

4.3.3.2.2 Engineered colloidal particle-spiked water samples

500 µg of 100 nm SiSH-Rh was added into 500 ml of water sample taken from the Tamar river (Gunnislake, Site 1). Another batch of the suspended particle was

prepared by using of different sizes of the labelled particles (250 and 600 nm of the fluoresent particles). The suspension was then sequentially passed through the *first* filter (with various pore sizes, HA 0.45 μm Millipore, 1.6 μm GF/C, 2.0 μm Nuclepore and 3.0 μm Millipore) then a 0.1μm Nuclepore filter, the *second* filter. Duplication was carried out for each water sample. After filtration, the filters were dried under vacuum overnight and kept dry until fluorescence measurement. They were also characterised by the SEM to investigate the behaviour of natural materials and engineered colloidal particles collected on the filter.

It should be noted that the Rhodamine contents of the Rhodamine labelled silicas (SiSH-Rh) are described in Table 5, Section 2.3.6.

4.3.4 Results and discussion

4.3.4.1 Colloidal arsenic fraction in the Tamar and Dart Rivers.

The salinities and pH of the water samples were determined (Table 3). The results indicate that the waters from the Tamar river from Gunnislake to Bradstone (Site 1-3), and the Dart River from Two Bridges to Starverton (Site 4-6), were freshwater (<0.05 ppt).

Table 3 salinity and pH of the 6 sampling sites.

Sites	Salinity (ppt)	pH
1 Gunnislake	0.05	7.60
2 Horsebridge	0.05	7.45
3 Bradstone	0.05	7.20
4 Two Bridges	0.02	6.00
5 New Bridge	0.02	6.55
6 Staverton	0.02	6.60

4.3.4.1.1 Double filtration

Samples from the Tamar and Dart rivers, were collected for this study. Dart river was chosen as a comparison with the Tamar river because the Dart has a different catchment area to the Tamar and should be less arsenic polluted. Particulate, colloidal and dissolved arsenic concentrations and other relevant data are listed in Table 4(a-d) for the mass of particulates arsenic retained on the *first* and mass of particulate arsenic per litre of water filtered by double filtration, and in Table 5(a-d) for the As concentration in the colloidal and dissolved fractions. Figure 11 compares the concentration of As in the large particulate (µg g^{-1}) retained on each filter type after filtration of a water sample. The concentrations of the colloidal As of each water sample sites are presented in Figure 12.

The particulate arsenic fraction

Four filter types were used to isolate the particulate fraction. Table 4 (a-d) reports the large particulate loading (mg l^{-1}) from the *first* filter and the concentration of arsenic (As) in the particles (µg As g^{-1}). Interestingly, in some sampling sites, the mass of particulates was found to decrease in the downstream direction, the mass of As increased. For example, the water sample that was taken from the Dart river, higher amounts of particulates mass was found at Two Bridge which is 7.40 mg l^{-1}, containing As concentration of 2.50 µg g^{-1}. Comparing on the mass of particulates at Starverton was 3.8 mg l^{-1} with As 11.0 µg g^{-1} concentration (Table 4a).

Table 4 (a-d) The large particulates loading by the *first* filters and the concentration of arsenic (As) in the particles from the water samples of the Tamar and Dart Rivers.

a) HA 0.45 µm filter:

Site	Particle loading by the 0.45 µm filter (mg l^{-1})	As in the particles (µg As g^{-1})	
		d > 0.45 µm *	0.1 µm < d < 0.45 µm#
1 Gunnislake	9.40	6.30	0.05
2 Horsebridge	0.60	65.0	0.01
3 Bradstone	15.6	1.40	0.00
4 Two Bridges	7.40	2.50	0.01
5 New Bridge	3.80	6.00	0.01
6 Staverton	3.80	11.0	0.04

with the standard deviation, *SD = 24.5 and #SD= 0.02, n=3

b) GF/C 1.6 µm filter:

Site	Particle loading by the 1.6 µm filter (mg l^{-1})	As in the particles (µg As g^{-1})	
		d > 1.6 µm *	0.1 µm < d < 1.6 µm #
1 Gunnislake	1.90	73.0	0.07
2 Horsebridge	1.20	19.0	0.00
3 Bradstone	1.40	0.00	0.01
4 Two Bridges	0.80	22.0	0.02
5 New Bridge	1.00	90.0	0.01
6 Staverton	1.20	36.0	0.04

with the standard deviation, *SD = 34.7 and #SD= 0.03, n=3

c) Nuclepore 2.0 µm filter:

Site	Particle loading by the 2 µm filter (mg l^{-1})	As in the particles (µg As g^{-1})	
		d > 2 µm *	0.1 µm < d < 2.0 µm #
1 Gunnislake	2.70	20.0	0.02
2 Horsebridge	0.00	0.00	0.00
3 Bradstone	2.80	6.00	0.02
4 Two Bridges	1.00	12.5	0.02
5 New Bridge	1.20	14.0	0.00
6 Staverton	1.00	37.5	0.05

with the standard deviation, *SD = 13.3 and #SD= 0.02, n=3

d) Millipore 3.0 µm filter:

Site	Particle loading by the 3 µm filter (mg l^{-1})	As in the particles (µg As g^{-1})	
		d > 3 µm *	0.1 µm < d < 3.0 µm #
1 Gunnislake	2.30	61.0	0.02
2 Horsebridge	1.00	25.0	0.01
3 Bradstone	1.60	16.5	0.02
4 Two Bridges	0.60	33.0	0.01
5 New Bridge	1.20	22.0	0.00
6 Staverton	0.80	45.0	0.04

with the standard deviation, *SD = 16.7 and #SD= 0.01, n=3

The concentration of As in the large particles appear to have higher than in the colloidal particles. The large particulate As concentration in the water (d > 0.45 µm), as determined using different filter types, is shown in Figure 11. Comparing the four filter types it can be observed that the GF/C 1.6 µm filter had the highest retention of particulate As from the Gunnislake and New Bridge samples (90.26 and 64.78 µg l^{-1}, respectively). The large quantity of particulate As retained on the GF/C 1.6µm filter can be explained by looking at the structure of the filter, which is a depth filter (Figure 8). This filter type (TP) has higher collection efficiency of particles[45] when compared with the Nuclepore filter [46]. However, a comparison of the four different filter materials, with varying pore sizes, shows that there was no correlation between pore size and particle retention. This could be suggested that environmental particles, which are physically and chemically heterogeneous, with varying composition and sizes, would have distinctly different degrees of affinity with the different filter types[47].

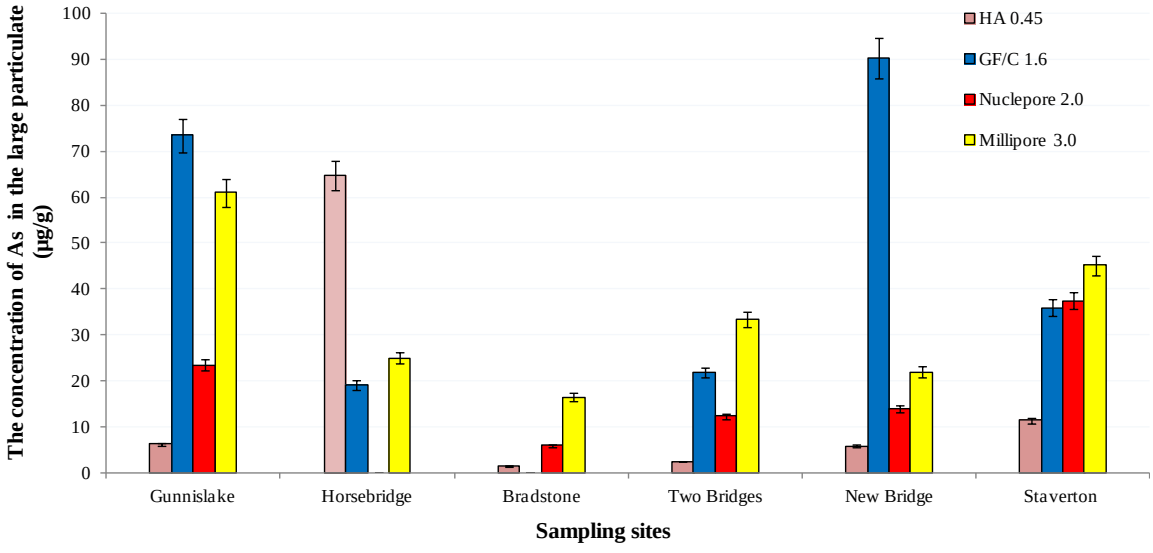

Figure 11 Comparison of the concentration of As in the particles (µg As g^{-1}) of the riverine water samples from different filter types.

The colloidal arsenic fraction

Table 5 (a-d) reports the total As in the colloids separated by different filter types. The majority of the As was in the dissolved phase (<0.1 µm) for all filter types. Additionally, the dissolved As concentration in the downstream sampling sites (Site 1 and Site 6) was higher than in the upstream areas (Sites 2-5). Significantly, the higher amounts of As were found in the dissolved phase for all the sample sites (Table 5). These findings further support the suggestion that As contamination of the area can be related to high concentration of As in the dissolved fraction (Section 4.2.4).

Table 5 (a-d) The concentration of arsenic in colloidal and dissolved fractions present in the Tamar and Dart Rivers. Only the *second* filter (0.1µm filter) and the dissolved fraction are shown.

a) HA 0.45-0.1 µm filters:

Site	As concentration (colloidal particle and dissolved phase) (ng l^{-1})	
	As in the colloidal particle* 0.1 µm < d < 0.45 µm	As in the dissolved phase# d < 0.1 µm
1 Gunnislake	49.0	1168
2 Horsebridge	6.70	413
3 Bradstone	0.00	392
4 Two Bridges	4.70	351
5 New Bridge	11.0	290
6 Staverton	39.0	1147

with the standard deviation, *SD = 20.3 and #SD= 413, n=3

b) GF/C 1.6-0.1 µm filters:

Site	As concentration (colloidal particle and filtrate) (ng l^{-1})	
	As in the colloidal particle* 0.1 µm < d < 1.6 µm	As in the dissolved phase# d < 0.1 µm
1 Gunnislake	69.0	1188
2 Horsebridge	0.00	596
3 Bradstone	13.0	290
4 Two Bridges	21.0	249
5 New Bridge	8.60	351
6 Staverton	36.0	1167

with the standard deviation, *SD = 25.0 and #SD= 433, n=3

Table 6 (a-d) continued;

c) Nuclepore 2.0-0.1 µm filters:

Site	As concentration (colloidal particle and filtrate) (ng l^{-1})	
	As in the colloidal particle* 0.1 µm < d < 2.0 µm	As in the dissolved phase# d < 0.1 µm
1 Gunnislake	20.0	1270
2 Horsebridge	0.00	515
3 Bradstone	29.0	290
4 Two Bridges	22.0	270
5 New Bridge	0.00	392
6 Staverton	47.0	1066

with the standard deviation, *SD = 17.4 and #SD= 428, n=3

d) Millipore 3.0-0.1 µm filters:

Site	As concentration (colloidal particle and filtrate) (ng l^{-1})	
	As in the colloidal particle* 0.1 µm < d < 3.0 µm	As in the dissolved phase# d < 0.1 µm
1 Gunnislake	17.0	902
2 Horsebridge	10.5	596
3 Bradstone	15.5	290
4 Two Bridges	12.0	351
5 New Bridge	0.00	372
6 Staverton	41.0	1168

with the standard deviation, *SD = 13.8 and #SD= 353, n=3

The consequence of the choice of the *first* filter on the material collected by the *second* filter (a 0.1 µm filter) is of interest (Figure 12). Both Table 5 and As colloids plots (Figure 12) suggest that the large majority of the As contaminantion is in the dissolved phase. The results show a difference of As colloids in the natural waters, with considerable higher amounts of As (up to ~ 70 ng l^{-1} As concentration) in the sampling sites which are seaward of the sampling sites (Site 1 and Site 6). These high As level were found in these areas due to they are closed to the arsenic mine activity (Marwellen and Wheal Emma & Brookwood).

Our results indicated that the retention of the particles depended not only on the pore size diameter but also the structure of the type of filter used. As previously mentioned (Section 3.1), the GF/C and Millipore are large pore size (TP) depth type of filters. Better filtration efficiency results in an increased retention of the particles on the *first* filters. These results are important as they confirm the different characteristic between

depth and plain filter types resulting in different filtration efficiency. However, there are also other factors that could influence for the suspended particles collected by the *first* filter. For example, the particulates load can be controlled by water dynamics at the sampling site, governed by tidal energy, local geology and previous rainfall. These may affect the performance of the *first* filter and its impact on the solid material retained by the *second* filter.

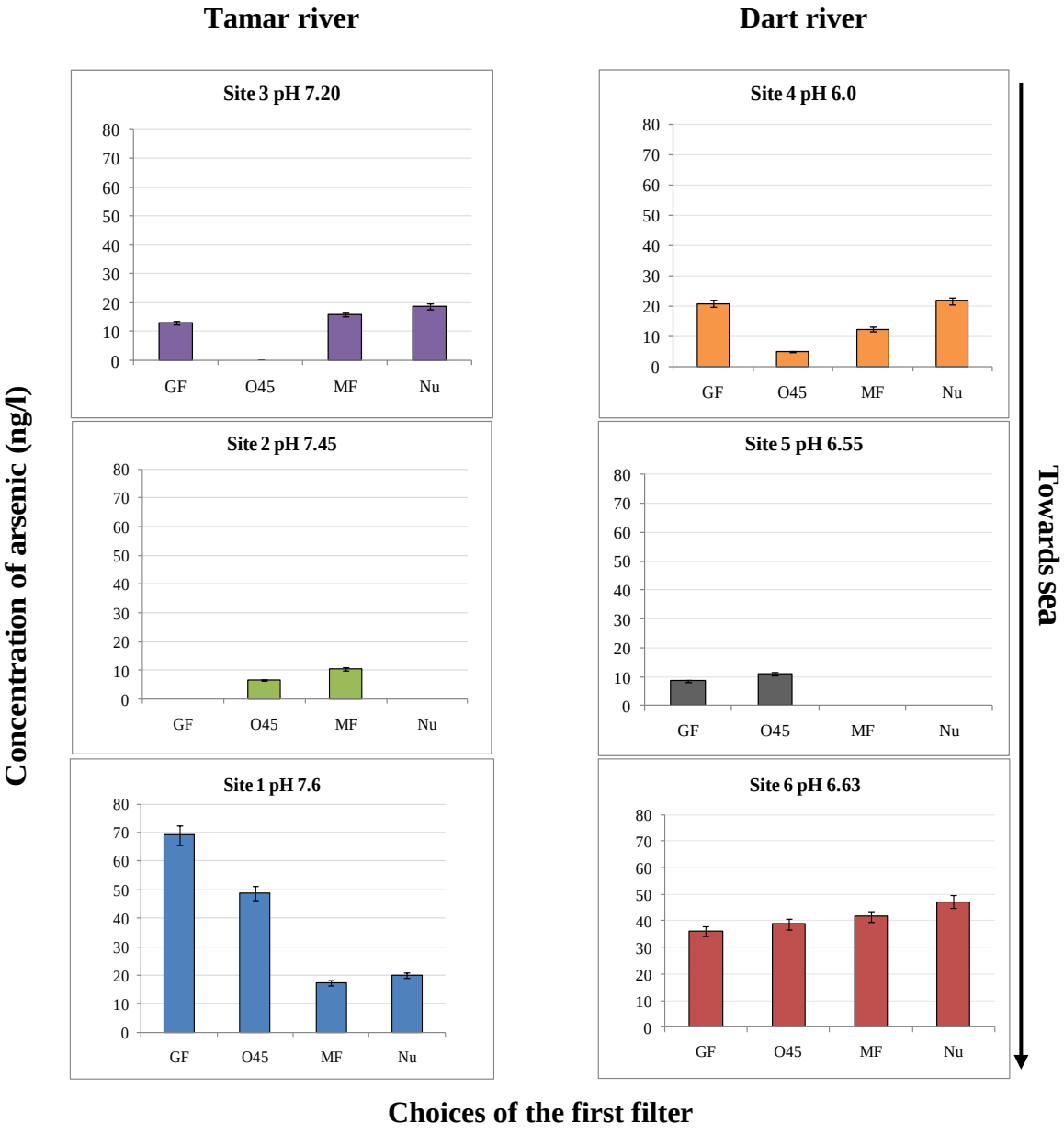

Figure 12 Comparison the impact of the four types of the first filter, on colloidal As retention on a 0.1 µm filter in a double filtration scheme. The colloidal arsenic is reported as the arsenic concentration (ng/l) at each sampling site. The variation of pH is included.

4.3.4.1.2 Triple filtration

This section reports the distribution of As indicated using a three filter fractionation scheme. Table 6 shows the mass of large particulate As and the mass of particulate As per litre of water. A comparison of the mass of particulate arsenic and colloidal arsenic phases per litre of water are presented in Figure 13.

Table 7 The mass of particulates collected by the GF/C 1.6 µm and HA 0.45 µm filters and the concentration of arsenic (As) in the particles from the water sample of the Tamar and Dart rivers.

Site	Particle loading by 1.6 µm filter (mg l^{-1})	Particle loading by 0.45 µm filter (mg l^{-1})	As in the particles (µg g^{-1})		
			d > 1.6 µm *	1.6> d > 0.45 µm #	0.45 > d >0.1 µm ^{x}
1Gunnislake	1.90	1.40	73.0	29.4	0.02
2Horsebridge	1.20	2.00	20.0	18.7	0.01
3Bradstone	1.40	0.40	0.00	0.00	0.01
4Two bridges	0.80	2.00	22.0	7.03	0.02
5New bridge	1.00	13.8	90.0	1.50	0.00
6Staverton	1.20	4.60	36.0	21.4	0.01

with the standard deviation, *SD = 34.7, #SD= 11.9 and ^{x} SD= 0.01, n=3

The *first* filter (the GF/C 1.6µm, blue bars) retained more As sediment than the *second* (the HA 0.45µm, pink bars) and the *third* filters (the Nuclepore 0.1µm, green bars). As expected, most particulates were removed by the 1.6 µm *first* filter (GF/C). The smaller pore size 0.45µm filter still collected significant quantities of particulate As leaving little to be collected on the final 0.1 µm filter. Figure 13 illustrates the concentrations of As in the suspended particle retained in varying quantities with different pore size diameter filters. According to the higher amount of particulate As was retained by GF/C can be related to its potential of depth filter. Significant amounts of particulate As were found from seaward of the Tamar and toward to the sea of the Dart rivers, respectively (site 1and 6) with in agreement with the result of double filtration.

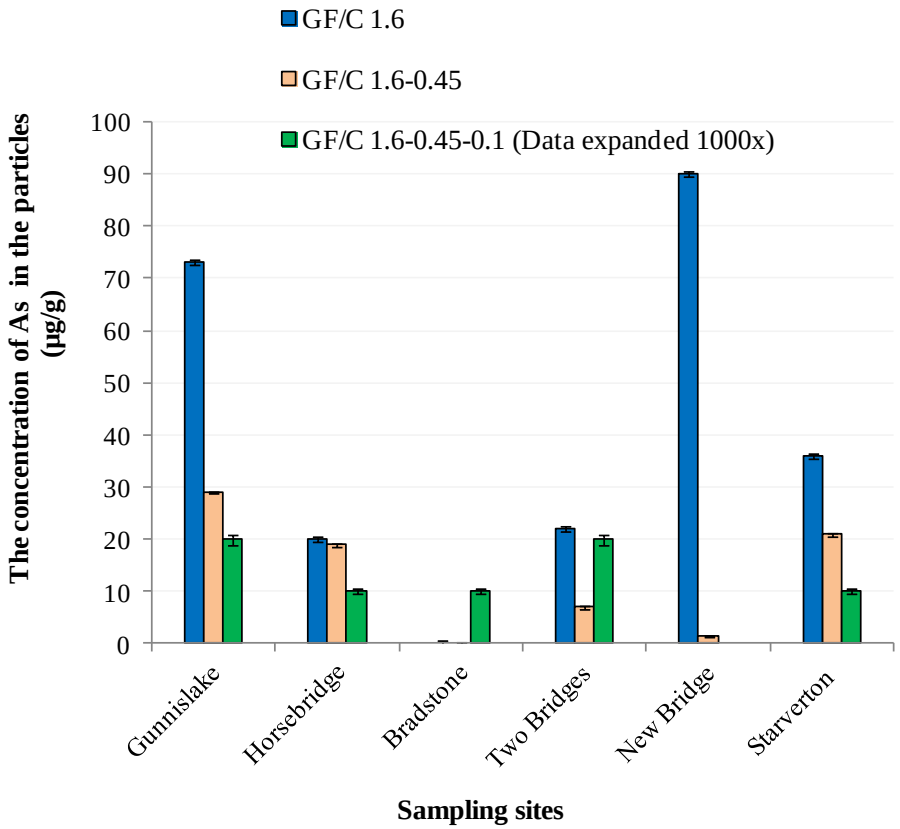

Figure 13 Comparison of the concentrations of arsenic in the particles obtained by triple filtration fractionation (GF/C 1.6 µm, HA 0.45 µm and Nuclepore 0.1 µm filters) of the riverine water samples.

Table 8 The concentration of arsenic in colloids fractionated by triple filtration.

Site	As concentration (colloidal particle and dissolved phase) (ng l^{-1})	
	As in the colloidal particle 0.1 < d < 1.6 µm *	As in the dissolved phase d < 0.1 µm #
1 Gunnislake	49.4	1660
2 Horsebridge	29.7	494
3 Bradstone	11.0	249
4 Two Bridges	22.8	249
5 New Bridge	1.51	351
6 Staverton	31.1	1170

with the standard deviation, *SD = 16.8 and #SD= 584, n=3

In the case of the colloidal fraction, the concentration of As in the colloidal and dissolved phases from each sampling site are shown in Table 7. Figure 14 shows the percentages present as the colloidal and dissolved fractions as determined by the triple filter fractionation. It is clear that the dissolved As concentration were significantly

higher than those the colloidal As, with no major differences between all the water sampling sites. The dissolved As were remarkably constant (90-100% As in the dissolved phase) in both rivers. For these results, the explanation is the same as has been discussed as Section 4.2.4.

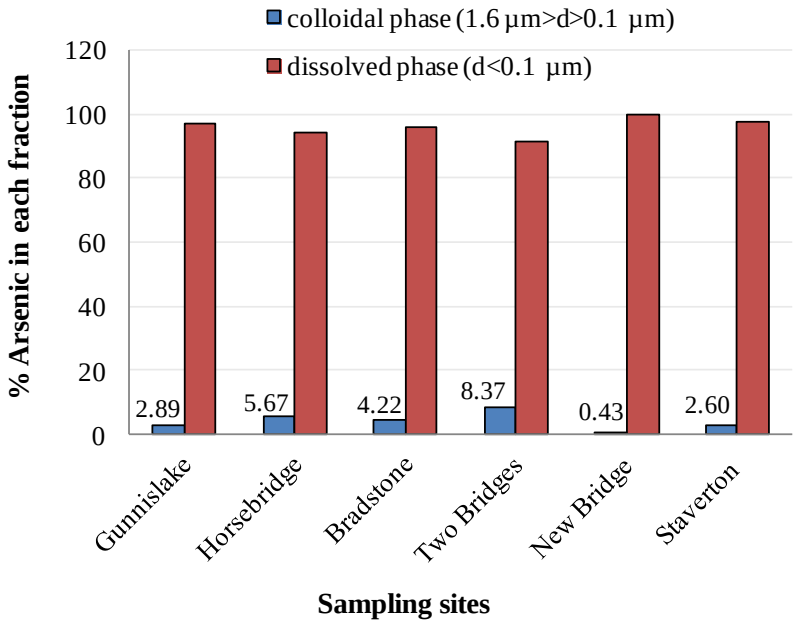

Figure 14 Percentage of sample arsenic present as colloidal (blue bar) and dissolved (red bar) arsenic, measured using GF/C 1.6 µm, HA 0.45 µm and Nuclepore 0.1 µm filters. Samples from Tamar and Dart rivers.

4.3.4.2 Water samples spiked with engineered particles

4.3.4.2.1 250 nm sized particle-spiked water samples

In this study, two natural water samples (Southampton Water and the Dart River) were spiked with fluorescent silica and were investigated using three different first filters (glass fibre, polycarbonate and cellulose nitrate). Figure 15 shows the amount of Rhodamine released from filters used to filter the Rhodamine particle-spiked water samples from Southampton Water (Figure 15a) and the Dart River (Figure 15b). The HA 0.45 µm filter (blue bar) showed the most efficient retention of the Rhodamine labelled particles (0.97 % and 97.34 % of Southampton Water and Dart River, respectively) when compared to the GF/C 1.6 µm (red bar) and Nuclepore 2.0 µm (green bar) filters.

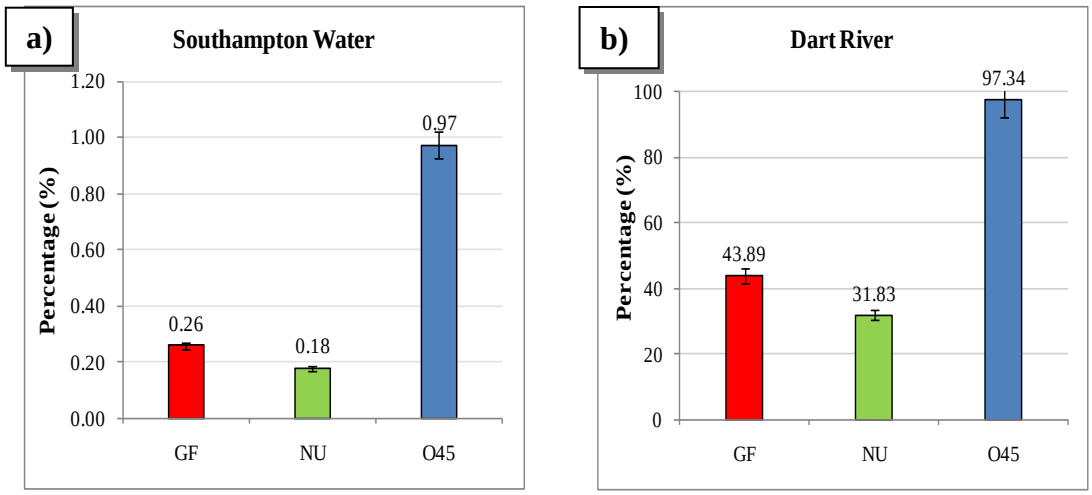

Figure 15 Percentage, %, of the 250 nm Rhodamine-labelled particles (SiSH-Rh) removed by the GF/C 1.6 µm, Nuclepore 2.0 µm and HA 0.45µm filters; n = 3. a) from Southampton Water salinity 30 ppt and b) from the Dart River salinity 0.05 ppt sample waters.

Comparing the results from the three different filter materials (glass fibre, polycarbonate and cellulose nitrate) with varying pore sizes (0.45, 1.6 and 2.0 µm pore size filters), there is a correlation between pore size and retention of our 250 nm diameter size engineered particles. As might be expected the larger pore size filters retained fewer of the labelled particles. Both the GF/C filter and the track-etched Nuclepore filter retained the same percentage of the labelled particle (Figure 15). Sheldon[47] suggested that the shape and the amount of particles in a water sample in filtration can influence the effectiveness of a specific pore size filter.

Electron micrographs of the filters after use illustrate some of the materials collected from the particle-spiked Southampton Water (Figure 16) and the Dart River (Figure 17). Many natural materials are apparent in the Dart River water sample (Figure 17b and Figure 17c) but aggregates of the spiked particles can also be seen on the filters from Southampton Water (such as Figure 16b). It is possible that the association of natural particles and our engineered colloidal particles may influence the higher amounts (*ca.*30-90%) of Rhodamine particle collected on the filter used for the Dart River sample, compared with the Southampton Water sample (*ca.* 0-1%). This finding

confirmed influences of salinity on the association of colloidal matter with other natural materials, as found by other researches [48-50].

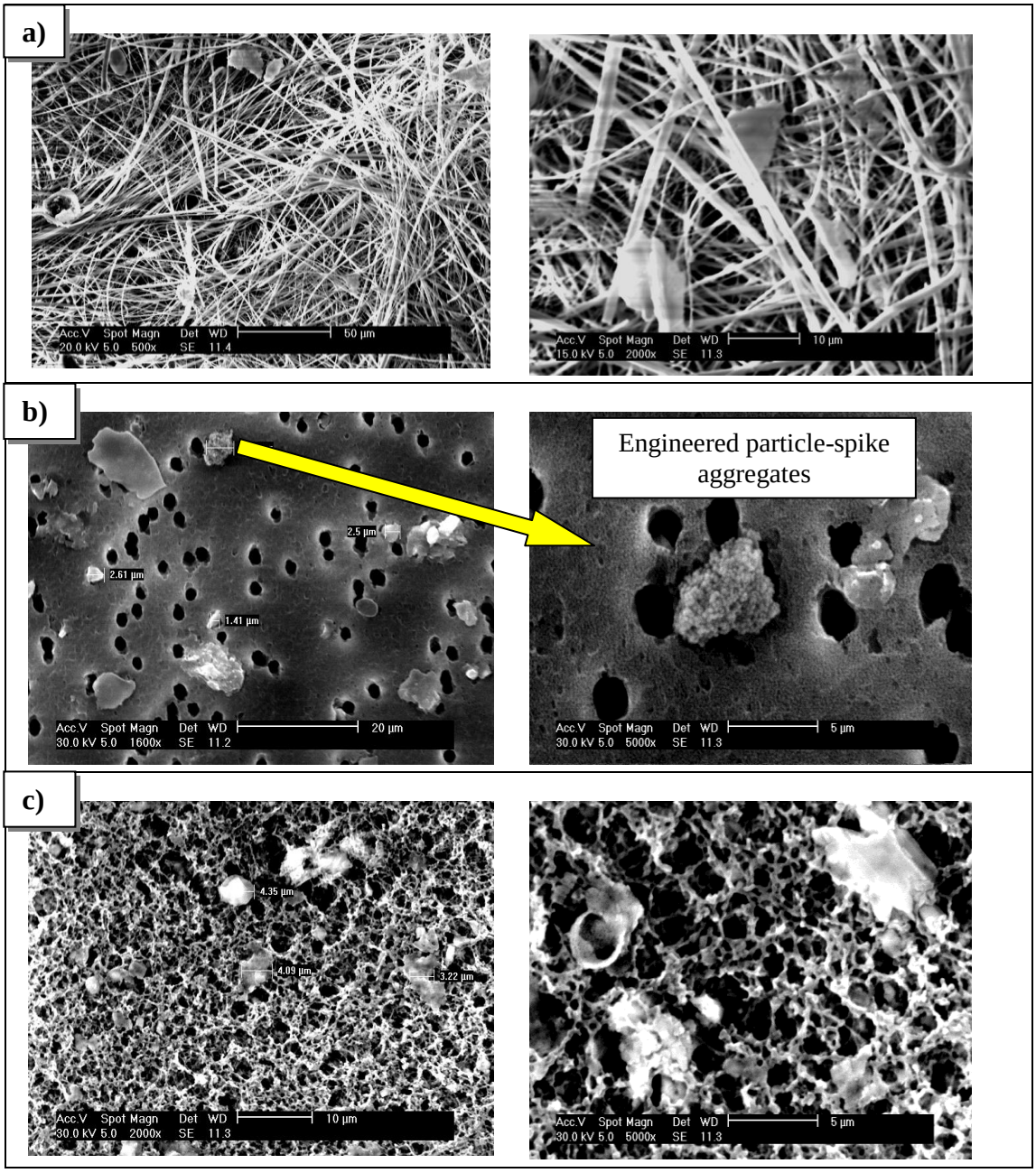

Figure 16 SEM images of materials collected on various types of filter; a) 1.6 µm glass fibre (Whatman), b) 2.0 µm polycarbonate (Nuclepore) and c) 0.45 µm HA (Millipore) filters. Water sample from Southampton Water.

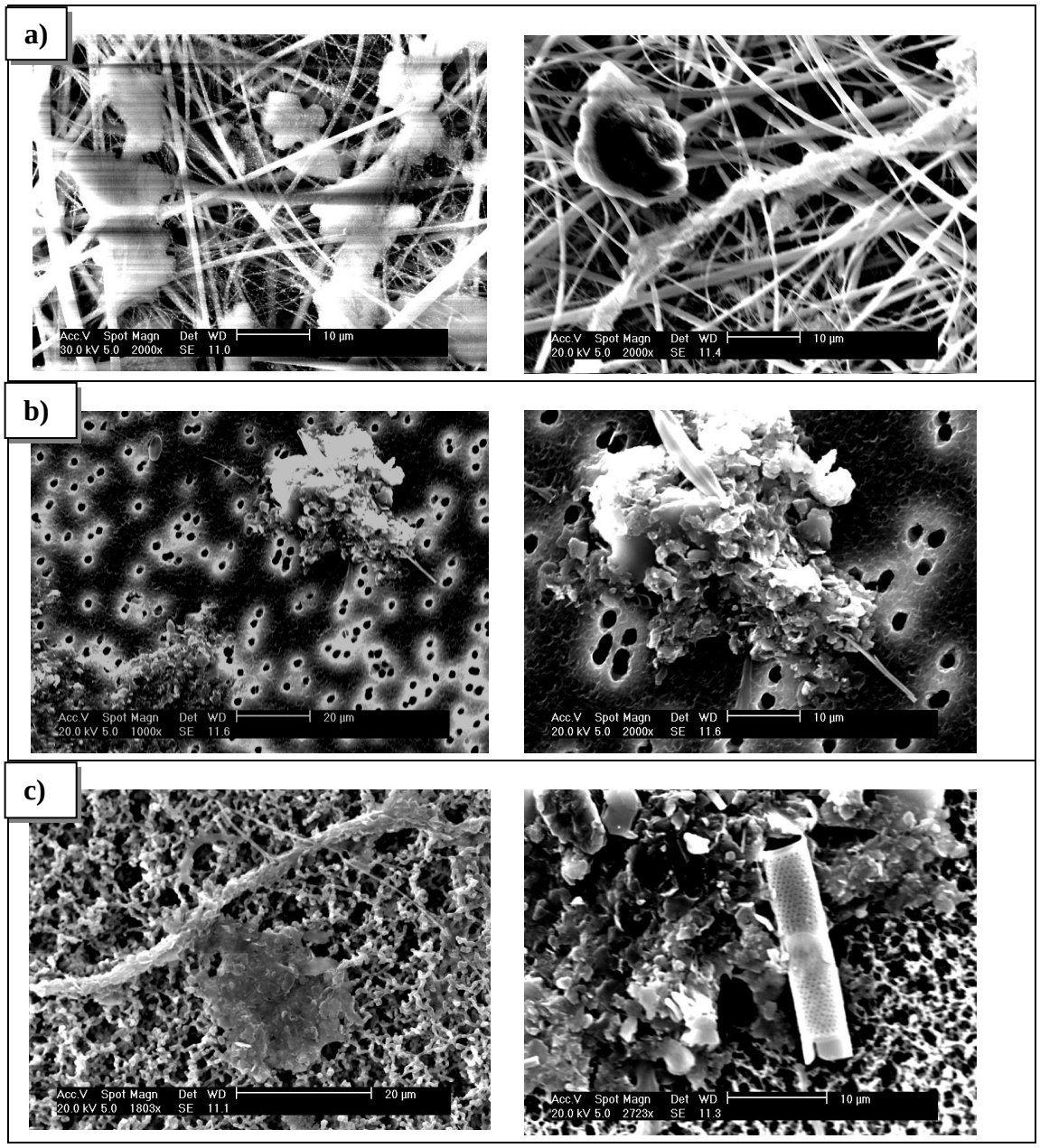

Figure 17 SEM micrographs of materials collected on various types of filter; a) 1.6 µm glass fibre (Whatman), b) 2.0 µm polycarbonate (Nuclepore) and c) 0.45 µm HA (Millipore) filters. Water sample from the Dart River.

Consequently, as a large proportion of the particles was collected by the *first* filter, only a small amount of the particles remained to be retained by the *second*, a 0.1 μm filter (Figure 18). Interestingly, less than 1% of the particles were retained on the *second* filter for both Southampton Water and the Dart River samples. Preliminary experiments (Section 3.3) have suggested the collection of large quantities of solid on the *first* filter may play an active role in controlling the retention by the *second* filter. Aggregation of the particles can lead to 100% of the particles being removed by the *first* filter (in the case of the HA 0.45 μm filter). In addition, colloidal particles can easily be attached to large natural particulates, increasing particle retention on the *first* filter.

For both water samples there was no difference in the quantity of particles collected by a 0.1 μm Nuclepore filter (Figure 18). However, there was also less than 1% of the particles collected by the *first* filter for Southampton Water sample. Results imply that most of the labelled Rhodamine was released into solution by the estuarine water, resulting in the engineered particles collected on the filter failing to be detected by fluorescence measurement. The preliminary experiments carried out to assess the quantification of Rhodamine labelled engineered particles were performed in deionised water. A plausible explanation for this is that the high salinity of the water sample had affected the measurement of the Rhodamine labelled particles and therefore prevented a definitive measurement of the labelled particles.

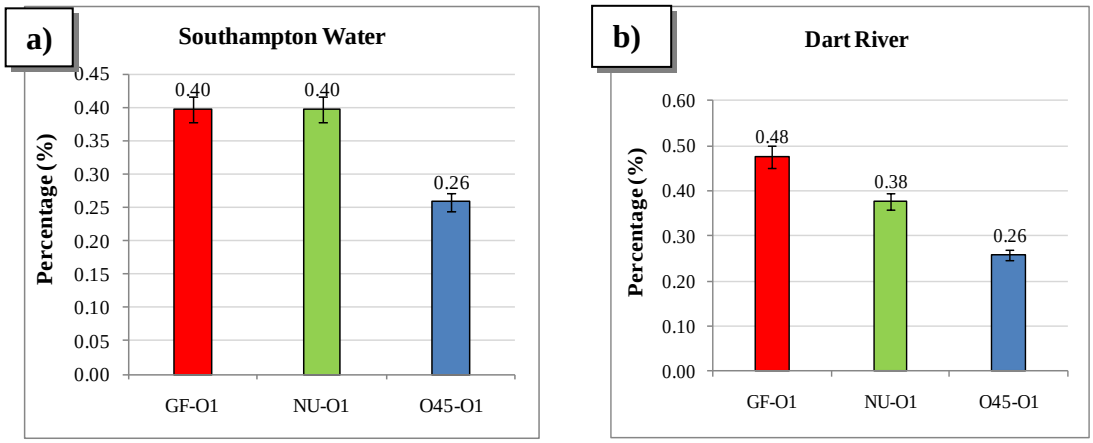

Figure 18 Percentage, % of Rhodamine labelled silica removed by 0.1 µm Nuclepore second filters (n = 3). Water samples from a) Southampton Water and b) the Dart river.

SEM micrographs show that some of our engineered single particles had passed through the *first* filter and had been collected on the *second* filter (Figure 19).

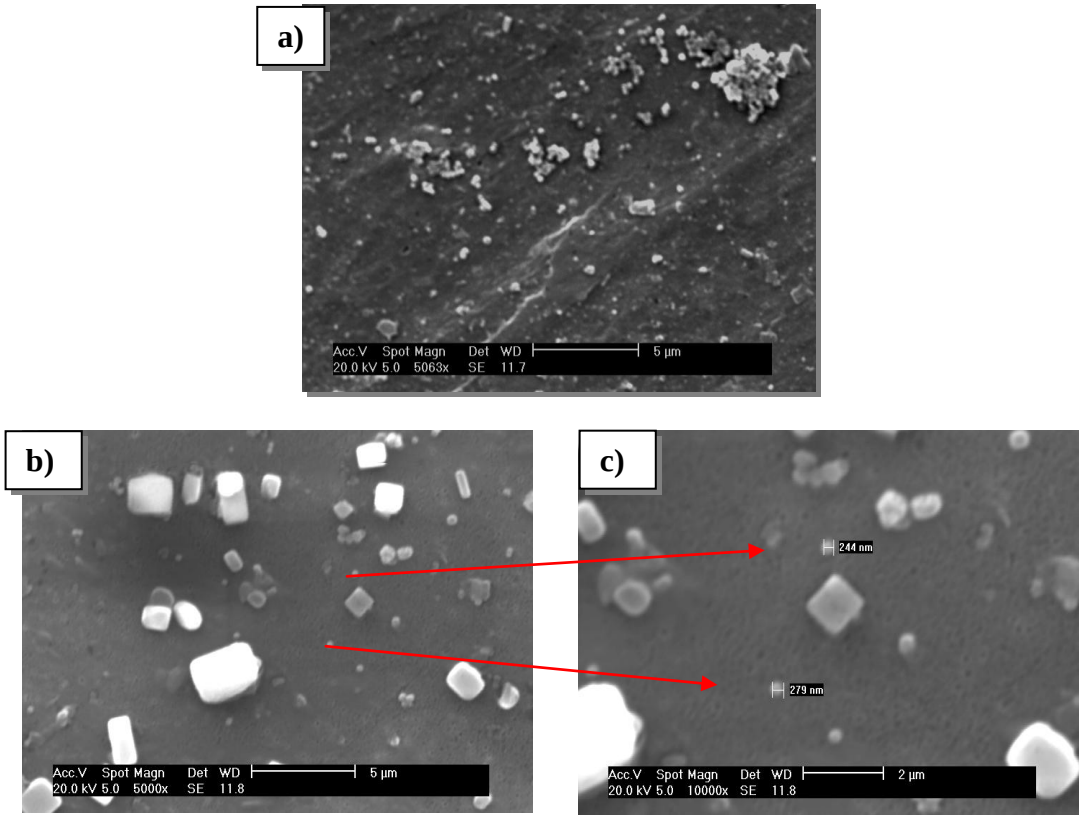

Figure 19 SEM micrographs of the engineered particles and materials retained on a 0.1 µm Nuclepore filter. a) Single and aggregated engineered particles. b) Showing crystalline sodium chloride (NaCl) and some single engineered particles. c) High magnification (x10,000) SEM micrograph of engineered particles.

4.3.4.2.2 Engineered colloidal particle-spiked water samples

The variable data for the particle-spiked Tamar water sample (Gunnislake, Site 1) is illustrated in Figure 20. It compares the amount of Rhodamine released from 100, 250 and 600 nm particles collected on the *first* filter (blue bars, glass fibre GF 1.6 µm, polycarbonate Nu 2.0 µm, cellulose nitrate MF 3.0 µm and HA 0.45 µm filters) and the *second* filter, a 0.1 µm polycarbonate Nuclepore filter (yellow bars).

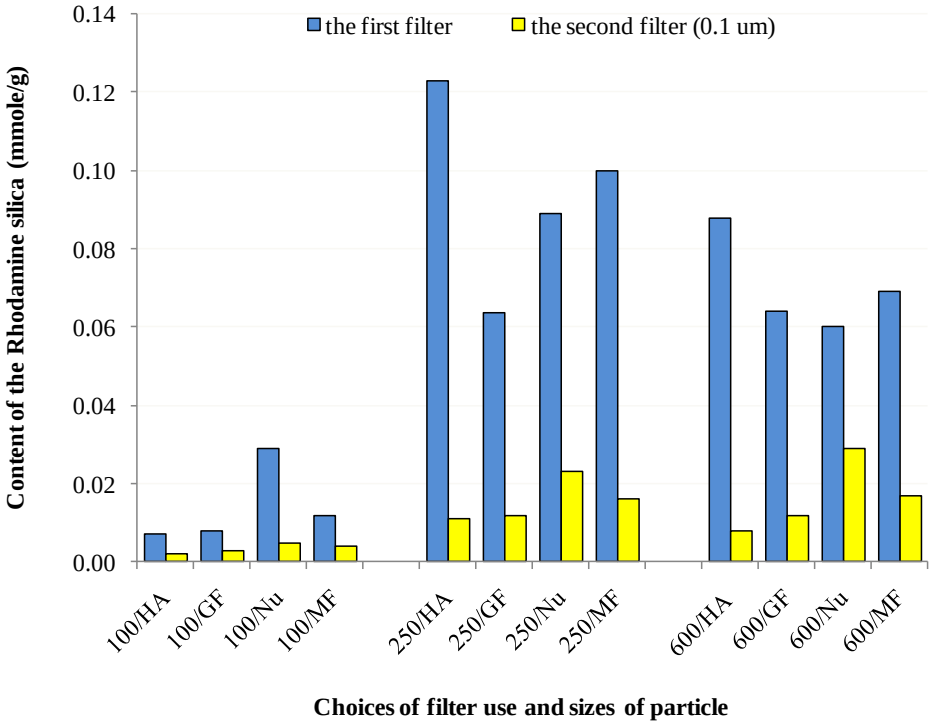

Figure 20 Comparison of the three different material filters and sizes of particle-spiked water samples.

A 250 nm labelled particles show the highest retention on the *first* filter (blue bars); the HA 0.45 µm filter in particular retained 0.123 mmol/g of 250 nm Rhodamine silica. The smaller particles (100 nm) could pass through the *first* filter easier than the larger particles (250 and 600 nm sized particles) whichever the type of filter. Furthermore, the particles may bond with natural material, leading to their effective

particle sizes becoming bigger. This implies that the suspended particles, especially with filter clogging, were relatively assured of being retained by the filter.

Despite the low collection of 100 µm particles by the *first* filter little Rhodamine was found on the 0.1 µm filter (yellow bars). The Rhodamine released from the 0.1 µm Nuclepore filter are ranged from 0.003 to 0.030 mmol/g. The majority of the Rhodamine was retained by a 0.45 µm filter (250 nm particle-spiked water sample). The association of engineered particles with natural materials can be responsible for their difficulty of passing through the filter (Figure 21). This may lead to an increased retention of our colloidal particles that should normally pass through the *first* filter.

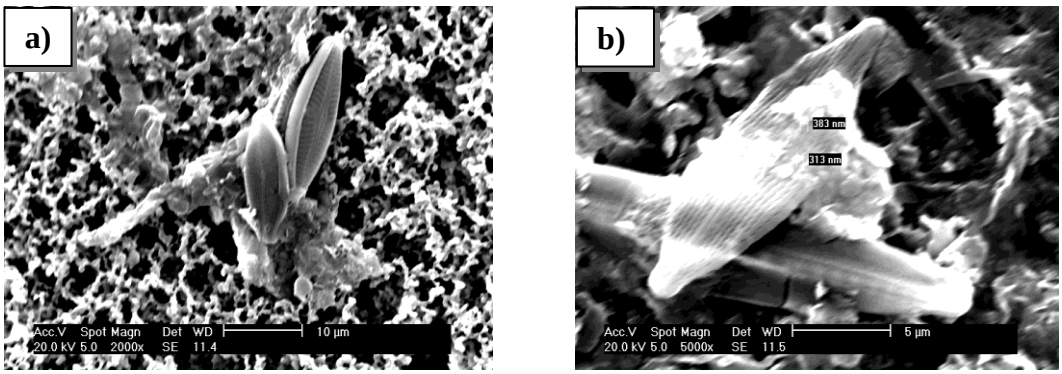

Figure 21 SEM micrograph images of some of the engineered particles and natural materials collected on a) the HA 0.45 µm and b) 2 µm Nuclepore filters.

4.3.5 Conclusion

This section has reported the distribution of arsenic in river systems on the Devon-Cornwall border in southern of England. Different filter types were compared in the study. After a detailed comparison of the four different filter types, results support that the GF/C 1.6 µm filter had a higher filtration efficiency, having a higher retention of arsenic than the others (HA 0.45 µm, Nuclepore 2.0 µm and Millipore 3.0 µm) filters. One major limitation of the Nuclepore filter is that it clogs more easily than the depth filters. Although, a double filtration step can be problematic if aggregation occurs at the membrane surface, results obtained by triple filtration showed a similar trend.

The majority of the arsenic is present in the dissolved phase (*ca.* 90-100% of the total arsenic concentration). The mass of particulates in downstream waters were found to be higher than in upstream areas.

Particle-spiking into natural water samples showed that, in general, there was aggregation, an association of engineered colloidal particles, either with themselves or with natural matter in the water, resulting in the collection of these aggregates on the filter. This leads to an increased retention of colloidal particles which would normally pass through the filter.

4.4 Summary

These experiments have provided particle size distributions in the dissolved, colloidal and particulate size fractions of water using filtration with different types of filters. The analysis of the natural waters containing arsenic was studied.

Arsenic concentrations are highest in the waters and suspended particles of the Tamar and Dart Rivers at the more downstream sampling sites (Gunnislake and Staverton) due to effect of mining activity just above the seaward sites. The measured amounts of particulate arsenic decreased as the pore sizes of the filters became greater. This was simply due to the larger size particles being retained by the filters. The characteristics of the filter are highly important in governing the measured particle loading and filter clogging may influence the concentration of arsenic in the filtrate. Results reported here support the view that the shape of the aggregates, and the amount of particles in the water sample can influence the effectiveness of the filter. The fraction of arsenic in the colloidal form was very low, probably because the majority of arsenic in this river system is dissolved resulting in the loss of arsenic from this fraction. It is concluded that the measured filtrate concentration of arsenic in river water samples can be significantly affected by the choice of filter type, pore diameter and filtration method.

4.5 References

[1] J. R. Lead, J. Hamilton-Taylor, W. Davison and M. Harper, *Geochimica Et Cosmochimica Acta* **1999**, *63*, 1661-1670.

[2] O. Gustafsson and P. M. Gschwend, *Limnology and Oceanography* **1997**, *42*, 519-528.

[3] D. Vignati and J. Dominik, *Aquatic Sciences* **2003**, *65*, 129-142.

[4] in *http://www.who.int/water_sanitation_health/dwq/arsenic/en/*, *Vol. 2009*.

[5] T. Dittmar, *Science of the Total Environment* **2004**, *325*, 193-207.

[6] M. Berg, H. C. Tran, T. C. Nguyen, H. V. Pham, R. Schertenleib and W. Giger, *Environmental Science & Technology* **2001**, *35*, 2621-2626.

[7] M. J. La Force, C. M. Hansel and S. Fendorf, *Environmental Science & Technology* **2000**, *34*, 3937-3943.

[8] G. Pokrovski, R. Gout, J. Schott, A. Zotov and J.-C. Harrichoury, *Geochimica Et Cosmochimica Acta* **1996**, *60*, 737-749.

[9] S. Wood, C. D. Tait and D. Janecky, *Geochemical Transactions* **2002**, *3*, 31.

[10] M. Sadiq, *Water, Air, & Soil Pollution* **1997**, *93*, 117-136.

[11] M. A. Anderson and D. T. Malotky, *Journal of Colloid and Interface Science* **1979**, *72*, 413-427.

[12] G. A. Waychunas, B. A. Rea, C. C. Fuller and J. A. Davis, *Geochimica Et Cosmochimica Acta* **1993**, *57*, 2251-2269.

[13] H. M. Guo, Y. X. Wang, G. M. Shpeizer and S. L. Yan, *Journal of Environmental Science and Health Part a-Toxic/Hazardous Substances & Environmental Engineering* **2003**, *38*, 2565-2580.

[14] M. Krachler, H. Emons, C. Barbante, G. Cozzi, P. Cescon and W. Shotyk, *Analytica Chimica Acta* **2002**, *458*, 387-396.

[15] W. M. Mok and C. M. Wai, *Talanta* **1988**, *35*, 183-186.

[16] N. Campillo, P. Vinas, I. Lopez-Garcia and M. Hernandez-Cordoba, *Analyst* **2000**, *125*, 313-316.

[17] C. L. Babiarz, S. R. Hoffmann, M. M. Shafer, J. P. Hurley, A. W. Andren and D. E. Armstrong, *Environmental Science & Technology* **2000**, *34*, 3428-3434.

[18] R. Feeney and S. P. Kounaves, *Talanta* **2002**, *58*, 23-31.

[19] S. B. Rasul, A. K. M. Munir, Z. A. Hossain, A. H. Khan, M. Alauddin and A. Hussam, *Talanta* **2002**, *58*, 33-43.

[20] S. Nielsen and E. H. Hansen, *Analytica Chimica Acta* **1997**, *343*, 5-17.

[21] N. C. Munksgaard and D. L. Parry, *Marine Chemistry* **2001**, *75*, 165-184.

[22] T. Guo, J. Baasner and D. L. Tsalev, *Analytica Chimica Acta* **1997**, *349*, 313-318.

[23] D. Q. Hung, O. Nekrassova and R. G. Compton, *Talanta* **2004**, *64*, 269-277.

[24] G. Ma, W. B. Xie and R. Feng, *Chinese Journal of Analytical Chemistry* **2006**, *34*, S254-S256.

[25] R. W. Puls, C. J. Paul and D. A. Clark, *Colloids and Surfaces a-Physicochemical and Engineering Aspects* **1993**, *73*, 287-300.

[26] C. J. Tadanier, M. E. Schreiber and J. W. Roller, *Environmental Science & Technology* **2005**, *39*, 3061-3068.

[27] A. J. Slowey, S. B. Johnson, M. Newville and G. E. Brown Jr, *Applied Geochemistry* **2007**, *22*, 1884-1898.

[28] H. M. Anawar, J. Akai, T. Yoshioka, E. Konohira, J. Y. Lee, H. Fukuhara, M. T. K. Alam and A. Garcia-Sanchez, *Environmental Geochemistry and Health* **2006**, *28*, 553-565.

[29] D. Shaw, *Engineering Geology* **2006**, *85*, 158-164.

[30] R. Schaeffer, K. A. Francesconi, N. Kienzl, C. Soeroes, P. Fodor, L. Varadi, R. Raml, W. Goessler and D. Kuehnelt, *Talanta* **2006**, *69*, 856-865.

[31] R. W. Puls and R. M. Powell, *Environmental Science & Technology* **2002**, *26*, 614-621.

[32] W. R. Cullen and K. J. Reimer, *Chemical Reviews* **2002**, *89*, 713-764.

[33] J. E. S. Min Feng, Raymond Snyder, George H. Snyder, Ming Chen, John L. Cisar, and Yong Cai, *J. Agric Food Chem.* **2005**, *53*, 3556-3562.

[34] S. R. Al-Abed, G. Jegadeesan, J. Purandare and D. Allen, *Chemosphere* **2007**, *66*, 775-782.

[35] J.-K. Yang, M. O. Barnett, P. M. Jardine, N. T. Basta and S. W. Casteel, *Environmental Science & Technology* **2002**, *36*, 4562-4569.

[36] P. H. Masscheleyn, R. D. Delaune and W. H. Patrick, *Environmental Science & Technology* **1991**, *25*, 1414-1419.

[37] M. X. Guo and J. Chorover, *Soil Science* **2003**, *168*, 108-118.

[38] S. R. Aston, I. Thornton, J. S. Webb, B. L. Milford and J. B. Purves, *Science of the Total Environment* **1975**, *4*, 347-358.

[39] A. G. Howard, M. H. Arbab-Zavar and S. Apte, *Estuarine, Coastal and Shelf Science* **1984**, *19*, 493-504.

[40] A. G. Howard, S. C. Apte, S. D. W. Comber and R. J. Morris, *Estuarine, Coastal and Shelf Science* **1988**, *27*, 427-443.

[41] K. A. Howell, E. P. Achterberg, A. D. Tappin and P. J. Worsfold, *Environmental Chemistry* **2006**, *3*, 199-207.

[42] H. C. Teien, W. J. F. Standring and B. Salbu, *Science of the Total Environment* **2006**, *364*, 149-164.

[43] A. Gunnars, S. Blomqvist, P. Johansson and C. Andersson, *Geochimica Et Cosmochimica Acta* **2002**, *66*, 745-758.

[44] B. Stolpe and M. Hassellöv, *Geochimica Et Cosmochimica Acta* **2007**, *71*, 3292-3301.

[45] B. Knefelkamp, K. Carstens and K. H. Wiltshire, *Journal of Experimental Marine Biology and Ecology* **2007**, *345*, 61-70.

[46] W. Hickel, *Marine Ecology-Progress Series* **1984**, *16*, 185-191.

[47] R. W. Sheldon, *Limnol. Oceanogr.* **1972**, *14*, 441-444.

[48] T. Kanti Sen and K. C. Khilar, *Advances in Colloid and Interface Science* **2006**, *119*, 71-96.

[49] K. A. Howell, E. P. Achterberg, A. D. Tappin and P. J. Worsford, *Environ.Chem.* **2006**, *3*, 199-207.

[50] A. W. Zularisam, A. F. Ismail and R. Salim, *Desalination* **2006**, *194*, 211-231.

Chapter 5

Conclusions

5.1 Conclusions

The general aim of this study was to explore methods used to investigate the transport of colloidal particles in natural waters. The investigation was centred on the use of filtration as a size fractionation method. Particles were synthesised within the colloidal size range and dispersed in water to provide a model for colloidal particles in natural waters. The investigation involved both the study of artificial colloidal silica particles and the particles contained in natural water samples.

Chapter 1 reviewed the general study of colloidal phases in waters including their physical and chemical effects on the environment. The role of colloids in the transport of pollutants such as pesticides, nutrients, heavy metals and organic compounds [1-3] in natural river systems was described.

Chapter 2 reported the synthesis of colloidal silica particles and their characterisation. The methods for the synthesis and their functionalisations were adopted from the literature [4-7]. Engineered colloidal particles were successfully produced and characterised within the desired size range (100-1,000 nm). Problems with aggregation of particles during sample preparation to determine the size of the particles by SEM method were solved by covalently linking the particles to the stub during the SEM preparation; these particles were then retained their separation on the surface and their size accurately determined by SEM. This technique was then routinely used for all SEM characterisations in this study.

Size fractionation by filtration of the engineered particles was reported in Chapter 3. Natural water samples from Southampton Water were also analysed, both as collected and after spiking with engineered particles. In the latter case aggregation of engineered colloidal particles with the natural particulates contained in the water samples resulted in more material collecting on the filter. Aggregates caused by companion of the double layer due to high ionic strength of the saline water. This result was attributed to the high salinity of the water system as observed previously[8, 9], where high salinity led to an increased association and retention of colloidal particles that would normally pass through the filter. The association can result from physical and electrostatic interactions between NOM molecules, engineered particles and the filter surface. During the filtration, particles in the colloidal size range either deposit on the filter surface or in the pores, depending on the size and shape (aggregates) of the colloids. The retention of the particles depended not only on the pore size diameter but also on the internal structure of the filter used. The clogging and aggregation of colloidal particles affect filtration efficiencies, altering the effective size cut-off of the filters during their use. To sum up, the influence of the associated and aggregated particles on the filter in this study, were grouped into (a) collecting around the side of the pore resulting in pore closure, (b) trapping then blocking the filter pores, (c) attaching to natural particulates, (d) remaining on the surface near the pore, (e) particle aggregates and then (d) blockage of the filter pore.

Arsenic distributions were measured in two rivers in Devon and Cornwall during summer of 2006 and 2008 (Chapter 4). A study of the presence of colloidal particles in these river systems was undertaken to assess the presence of arsenic in the colloidal fraction. Sites on the Tamar estuary, a historically arsenic-contaminated river, were sampled on both occasions, while another arsenic contaminated river, the Dart, was only sampled during the summer of 2008.

Four different types of filter were compared in this study. Results using the double filtration method show that the GF/C 1.6 µm filter had a higher filtration efficiency, based on the higher loading of particulate arsenic collected on this when compared to the other filters (HA 0.45 µm, Nuclepore 2.0 µm and Millipore 3.0 µm). A major limitation of the Nuclepore filters was that they clog more easily than the depth filters. Furthermore the shape (aggregates) and the amount of particles in the samples can influence the effectiveness of the particular pore size employed. The results suggest that aggregating and clogging on the first filter may have retained most of the colloid, and that the accuracy of the determination of particulate, colloidal and dissolved arsenic in river water samples may be seriously affected by filtration effects e.g. the filter types, pore size and filtration processes.

High arsenic concentrations in waters and sediments of the Tamar and Dart Rivers were found at the downstream sampling sites of the two rivers. Larger amounts of arsenic were found in particulates from estuarine than riverine sampling sites (only River Tamar studied in this case). This was possibly due to the aggregation of contaminated colloids with large size organic matter, which resulted in more arsenic being retained on the filters. The fraction of arsenic in the colloidal form was in most cases very low, whilst the major fraction of arsenic was found in the dissolved phase (*ca.* 90-100% of the total arsenic concentration).

The differences in the salinity values between fresh and estuarine waters were found to stimulate changes in the colloidal arsenic phase by enlarging the aggregated colloids, and leading to higher the particulate phase in the environment that then settle out. This result is a further confirms of the effect of salinity on the stability of colloids, and it strongly suggests that salinity is an important factor inducing changes in the arsenic concentrations in natural waters.

5.2 Future work

Our current understanding on the presence of colloidal phase in waters is based upon a number of their physical and chemical of the colloidal particle. Following the investigations described in this thesis, a number of projects could be taken up, involving the modified colloids studied:

- Further testing of fluorescence quenching in saline water;
- It would be interesting to obtain other studies of colloids in natural waters, especially: iron, manganese, lead, zinc and copper;
- effect of loading on the modified colloid;
- Further data collection of the study the effect of changes in environmental strategy. For example, changes in acidity, ionic strength and metal ion complexation in natural waters can all affect stability of a colloidal dispersion and once destabilised (i.e. repulsion barrier has been attenuated).

5.3 References

[1] S. Irace-Guigand and J. J. Aaron, *Analytical and Bioanalytical Chemistry* **2003**, *376*, 431-435.

[2] Y. Ran, J. M. Fu, G. Y. Sheng, R. Beckett and B. T. Hart, *Chemosphere* **2000**, *41*, 33-43.

[3] R. W. Puis and R. M. Powell, *Environmental Science & Technology* **1992**, *26*, 614-621.

[4] W. Stober, A. Fink and E. Bohn, *Journal of Colloid and Interface Science* **1968**, *26*, 62-69.

[5] A. G. Howard and N. H. Khdary, *Analyst* **2005**, *130*, 1432-1438.

[6] C. R. Miller, R. Vogel, P. P. T. Surawski, K. S. Jack, S. R. Corrie and M. Trau in *Functionalized Organosilica Microspheres via a Novel Emulsion-Based Route*, *Vol. 21* **2005**, pp. 9733-9740.

[7] Y. Yamada and K. Yano, *Microporous and Mesoporous Materials* **2006**, *93*, 190-198.

[8] A. Gunnars, S. Blomqvist, P. Johansson and C. Andersson, *Geochimica Et Cosmochimica Acta* **2002**, *66*, 745-758.

[9] B. Stolpe and M. Hassellöv, *Geochimica Et Cosmochimica Acta* **2007**, *71*, 3292-3301.

Appendices

Specialise analytical techniques and other methods employing in the project

Introduction

This chapter aims to review the analytical techniques that were used to quantify arsenic and fluorescence labelled particles. Particularly, man-made colloid particles were characterised for the physical properties using these techniques.

appendix A) Hydride Generation techniques-AAS

i) Method

Atomic absorption spectrometry (AAS) is one of the most important techniques for the analysis and characterization of the element composition of materials and samples. There is considerable information regarding the speciation of arsenic in water. Hydride generation (HG) technique is widely used in arsenic speciation analysis due to their ability high efficiency and simplicity. HG has become the most essential technique in arsenic speciation and quantitation by atomic absorption spectrometry [1-5].

In this technique, a reducing agent such as sodium borohydride ($NaBH_4$) is employed for the conversion of arsenic to volatile form (AsH_3), as illustrated in Scheme 1. The reduction reagents $NaBH_4$ and KBH_4 have proved to be exceptionally reliable reagents for the conversion of the sample to volatile forms[6].

$As(OH)_3 + 3BH_4^- + 3H^+ \longrightarrow AsH_3 + 3BH_3 + 3H_2O$ reaction 1

$BH_3 + 3H_2O \longrightarrow H_3BO_3 + 3H_2$ reaction 2

Scheme 1 Hydride generation reaction

After these additions will all arsenic in the sample be present in the form of arsenic acid (H_3AsO_3). The sample is introduced to the hydride generation system, were hydrochloric acid and tetrahydroborate (BH^{4-}) is added. It is important to prepare the tetrahydroborate daily because it will react with the water and lose its activity otherwise. A red-ox reaction takes place in the hydride generation system and the volatile compound arsine (AsH_3) is produced (reaction 2).

The arsine and the hydrogen gas is carried by the inert gas argon into the electrically heated quartz tube were a radical reaction takes place. Inside the oven reacts oxygen and hydrogen radicals with arsine and produces atomised arsenic. The atomised arsenic is detected by the arsenic hallow cathode lamp and the absorbance is measured.

ii) Instrument optimisation

Materials: Sodium borohydride ($NaBH_4$) was purchased from Avocado Research Chemical Ltd. (Heysham, UK), Hydrochloric acid (HCl) was obtained from Fluka (Gillingham, UK). Deionised water was used throughout the experiment. The arsenic reagents used were as follows: arsenious oxide (As_2O_3) Analar grade was obtained from Hopkin&Williams Ltd, (London). Sodium arsenate ($Na_2AsO_4 \cdot 7H_2O$) was

obtained from BDH (Poole, UK). The stock solutions, 1,000 µg ml^{-1} were prepared monthly and kept refrigerated at 4 ^{o}C. Working standard solutions were prepared daily. Sodium borohydride solution was prepared just prior to use. The glassware was cleaned by soaking in 5% (v/v) HCl overnight and then rinsed well with deionized water.

Arsenic calibration

- Preparation of calibration curves for arsenate

A 1,000 (As)/ml (as arsenate) stock solution was prepared by dissolving 4.163 g of $Na_2AsO_4 \cdot 7H_2O$ in 1 L water. 5 standard solutions 0, 10, 20, 30, 50 and 100 ppb were prepared by serial dilution of the arsenic stock solution.

- Preparation of an arsenite standard solution.

To prepare a 1,000 ppm arsenite standard solution, 132 mg of As_2O_3 was dissolved into a beaker with some water and 1 pellet of NaOH was added. After everything had completely dissolved, HCl solution was added until a pH of 7 was achieved. The solution was then made up to 100 ml (1,000 ppm) with deionised water.

The determinations of arsenic reported in the majority of this part were accomplished using a continuous flow HG-AAS system, employing sodium borohydride as the reducing agent, and hydrochloric acid as the pH regulator. A continuous-flow hydride generation system was constructed based on an atomic absorption spectrometer (model 3100, Perkin Elmer) (Figure 1). The sodium borohydride was made up daily in 2% (w/v) in water. A peristaltic pump controlled the flow of sample (2.5 ml min^{-1}), acid (2.5 ml min^{-1}), and borohydride (2.5 ml min^{-1}) in the system.

The sample and 4M hydrochloric acid (HCl) are merged first and followed by the addition of 2% (w/v) sodium borohydride ($NaBH_4$). Air and nitrogen are then introduced into the liquid stream while the mixture flows through the reaction coil.

The resulting solution was passed through a reaction coil to allow time for arsine generation to occur and for the arsine to be stripped from the liquid. Nitrogen is used to provide an inert atmosphere where needed and to speed transport of the arsine through the system while air is required in the atomization stage.

Arsine generated in the HG system is then atomized in a furnace tube (700 – 1,000 °C) aligned in the light path of the spectrometer[7].

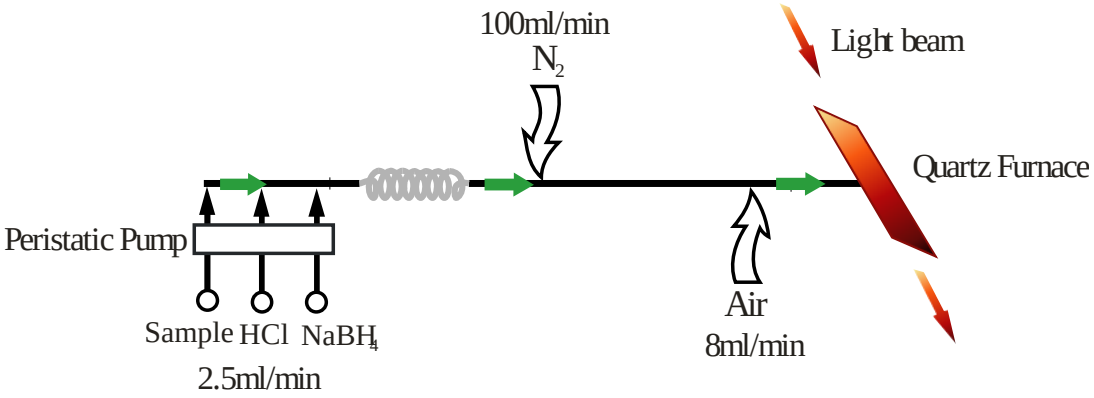

Figure 1 Schematic diagram of a flow HG-AAS system

Experiments were run to assess the performance of the hydride generation atomic absorption instrumentation (HG-AAS) for the determination of low level arsenic. The instrumental parameters employed are given in Table 1.

Table 1 Instrumental parameters for HG-AAS.

Parameter	**Setting**
Source lamp	Perkin Elmer hollow cathode lamp
Wavelength	193.8 nm
Slit width	0.7 nm
Lamp current	10 mA
Integration time	0.5 s
Quartz cell temperature	700-1,000 ^{o}C
Air flow rate	8 ml min^{-1}
Nitrogen flow rate	100 ml min^{-1}

Arsenate standard solutions were used to optimize the system within the 0 to 100 parts per billion (µg L^{-1}) concentration ranges. The sensitivity is shown in Figure 2.

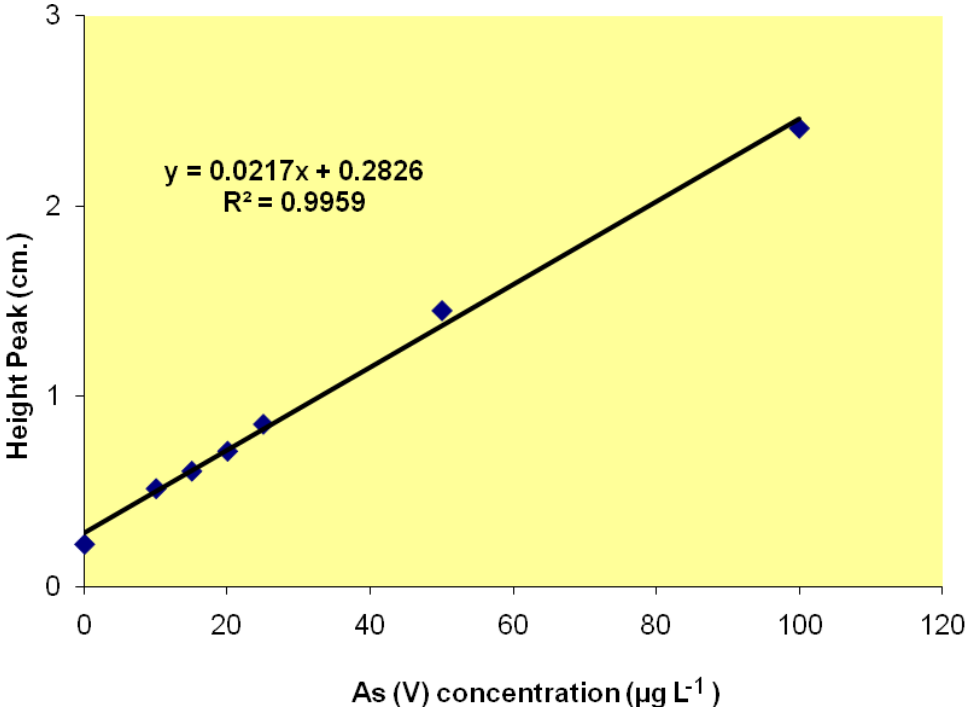

Figure 2 Calibration curve for arsenate standard solutions over the 0-100 µg l^{-1} concentration range

appendix B) Cryogenic trap techniques

i) Overview of the system

The HG-AAS technique described previously (appendix A) is not sufficiently sensitive to measure the arsenic levels in most natural waters. The investigation of natural colloid-bound arsenic will require a more sensitive analysis approach. One of the most commonly used techniques for overcoming the sensitively problem is for a cryogenic trap to be used for the concentration of the arsine gases formed by the HG technique. This cryogenic trap approach can be traced back to early studies by Braman et al.[8] in the early 1970s.

A cryogenic trap was incorporated into the HG-AAS manifold between the gas/liquid separator and the quartz T-piece atomizer. The operation of the system in overview is described in appendix A. The trap is placed in liquid nitrogen and the sample (1 ml) is pumped into the system and mixed with acid and borohydride (Figure 3). Deionised water is then used to wash the complete sample through the system and after 90 seconds, the liquid nitrogen is removed to allow the arsines to volatilise and be transported by the carrier gas into the detector. The chart recorder was switched on to record the absorbance change over time.

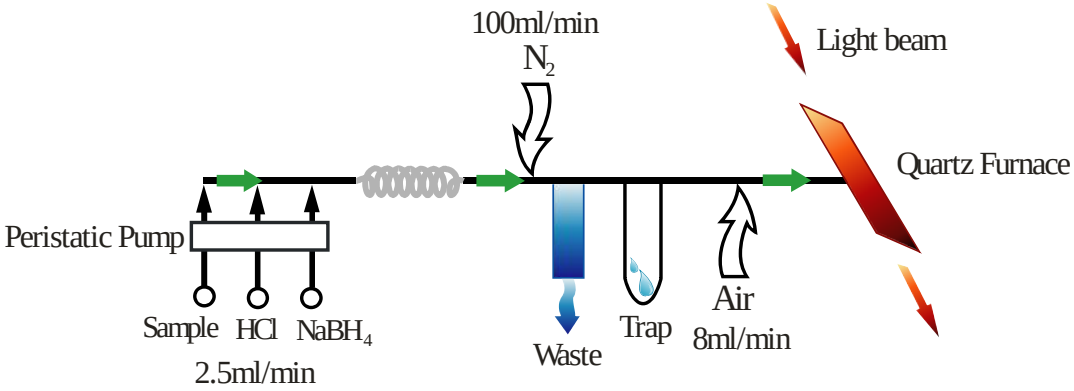

Figure 3 Cryogenic trap hydride atomic absorption spectrometry system.

ii) Calibration curve

Arsenate standard solutions were used to calibrate the system over the 0 to 2,000 parts per trillion (ng L^{-1}) concentration ranges. The calibration curve is shown in Figure 4. Samples of arsenate and arsenite at 300 ng l^{-1}(ppt) were also measured giving concentrations of 298.00 ± 3.50 and 303.00 ± 2.20 ng L^{-1}, respectively. An estimate of the detection limit from the arsenate standard calibration curve is *ca.* 200 ng L^{-1}.

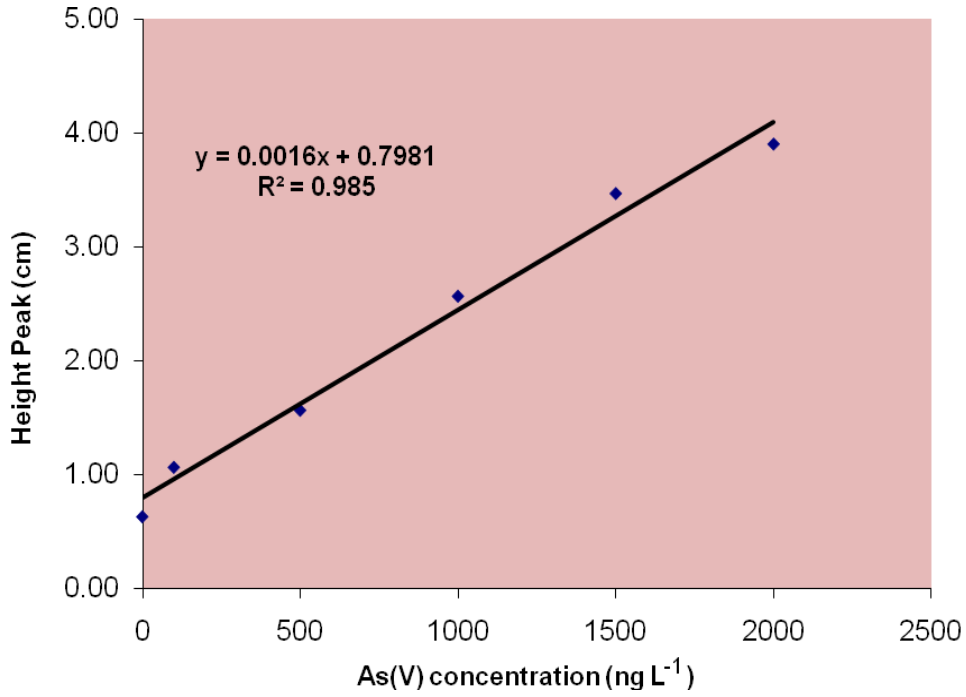

Figure 4 Calibration curve for arsenate standard solutions over the 0-2,000 ng l^{-1} concentration range

appendix C) Analysis of the released arsenic from the labelled-arsenic silicas

i) Equalization the signal of arsenate and arsenite by Potassium iodate

KIO_3 was used to be an oxidizing agent for changing arsenite to arsenate[9]. Air and nitrogen are then introduced into the liquid stream while the mixture flows through the reaction coil (Figure 5). The sample and KIO_3 (50 mmole dm^{-3}) at 1 ml min^{-1} flow rates were merged and then flowed through a time delay reaction coil to permit the oxidation to proceed. 4M hydrochloric cid (HCl) and 2% (w/v) sodium borohydride ($NaBH_4$) were then added. Arsine generated in the HG system is then atomized in a furnace tube (700-1,000 °C) aligned in the light path of the spectrometer.

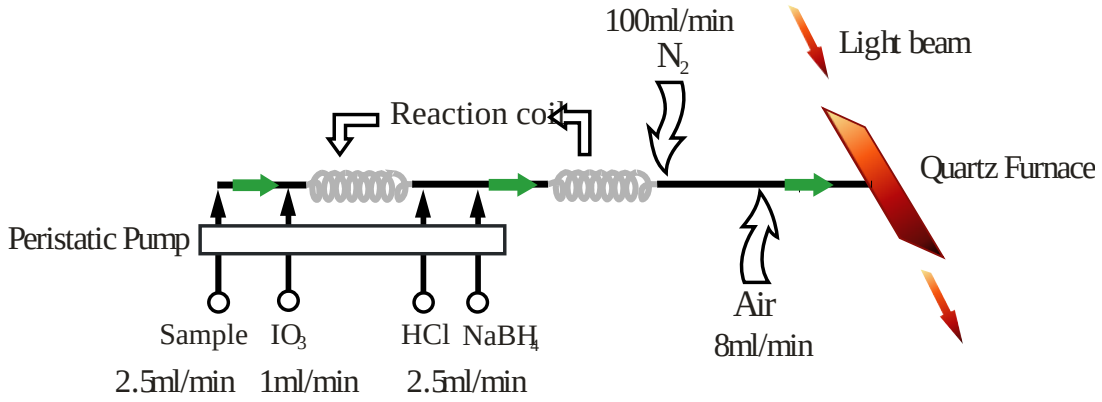

Figure 5 Schematic diagram of a flow HG-AAS system with IO_3

Results and discussion

Arsenate standard solutions were used to calibrate the system. One of the reasons for the iodate was to equalize the signals for arsenite and arsenate. A calibration curve was plotted over the 0 to 50 parts per billion (μg l^{-1}) concentration ranges. The sensitivity is shown in Figure 6.

25 µg l^{-1} arsenate solution generated an arsine signal having the same height peak as a 25 µg l^{-1} arsenite solution, which was *ca.* 3.50 ± 0.14 centimetres. Results found clearly that after converting arsenite to arsenate using oxidation with iodate, the total inorganic arsenic content can be measured.

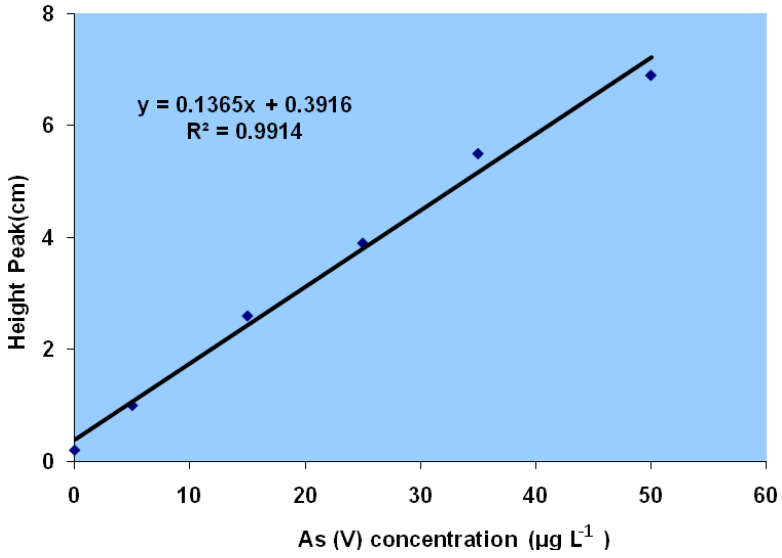

Figure 6 Calibration curve for arsenate standard solutions over the 0-50 µg l^{-1} concentration range

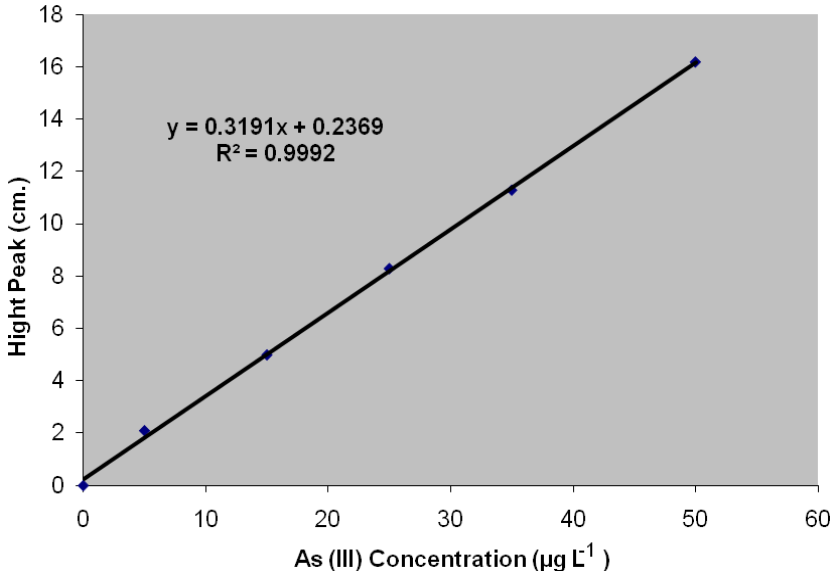

Figure 7 Calibration curve for arsenite standard solutions over the 0-50 µg l^{-1} concentration range

ii) Investigation of whether BH_4^- can release arsenic from silica

Labelled silica had been synthesized with binding arsenic onto the surface of modified silicas. Arsenic was then to be released from the silica by oxidation with iodate and measured by a variant of the AAS continuous-flow hydride generation method (Figure 5) as described in Section 2.4.1.

This experiment was carried out to study whether hydride generation chemistry can release arsine from silica bound arsenic. The experiment was carried out as follows: 50 mg (accurate weight) of modified silica bound arsenic was suspended in 5 ml of water and mixed for 5 mins (portion 1). Portion 2; 5 ml of KIO_3 (2 g l^{-1} in 0.5M HCl) was added into 50 mg of modified silica then left it for 5 mins. 25 ug l^{-1} of arsenate solution was then prepared in order to compare the signal of the arsine. Filtration (Whatman GF/C) has been employed for the experiment and the filtrate was diluted with deionized water to 5 ml in a volumetric flask. The colloidal silica suspension was aspirated into the hydride AAS system that had been calibrated using arsenate standard solutions.

Results and discussion

A result shows that a signal was obtained of arsenate 25 ug l^{-1} similarly to a signal of modified silica with IO_3^- while arsine from modified silica with BH_4^- was no signal. Results indicated that the borohydride may be release arsine signal of the bound arsenic but it could take more time. The analysis of the arsenic loaded silica had found it contained 8.5 μg of arsenic per gram of solid, which would correspond to a concentration of arsenic in the sol of 85 μg l^{-1} (50 mg of arsenic loaded silica was suspended in 5 ml of water). This is significantly higher than the HG-AAS detection limit of *ca.* 3 μg l^{-1}. Hydride generation had therefore produced significant quantity of arsine from the arsenic sol.

appendix D) Fluorescence spectroscopy

i) Method

Fluorescence spectroscopy is a type of electromagnetic spectroscopy which analyse fluorescence from a sample. Fluorescence is a mechanism by which a molecule returns to be the ground state after it has been excited by absorption of radiation. It involves using a beam of light, ultraviolet light, that excites the electrons in molecule and causes them to emit light of a lower energy, typically visible light. The fluorescence is most often measured at a 90^{o} angle relative to the excitation light instead of placing the sensor at the line of excitation light at a 180^{o} angel in order to avoid interference of the transmitted excitation light.

Fluorescence labelling has been developed in this project to identify the impact of particle size colloidal silicas, allowing each sizes to be identified using its unique fluorescence properties. Man-made labelled colloidal particles can be counted by fluorescence spectroscopy, after filtration of water with a fine filter, to track the behavior of each size of colloid.

ii) Rhodamine-labelled silica particles (SiSH-Rh)

The experiments to date have involved comparatively high loadings of silica in the water and greater sensitivity is required to investigate natural water samples if labeled silicas are to be added at concentrations well below those of the natural particles. Fluorescence labeling techniques offer such high sensitivity. Most of the methods used for the preparation of fluorescent particles have been based on physical adsorption or covalent binding to connect to the fluorophores to the solid [10-12]. In theory, fluorescence is detected and identified by changes in the emission and excitation of the spectra. In this experiment, to identify the impact of particle size on filtration efficiencies, different fluorphores will be attached to different size of

colloidal silicas, allowing each size to be identified using its unique fluorescence properties.

Calibration curve of standard Rhodamine

Rhodamine calibration solutions were prepared by dilution of the stock solution in 1.0 M methanolic NaOH. With 543 nm excitation, emission could be measured at 564 nm and calibration was found to linear over the concentration range 0-600 nMolar. Rhodamine concentrations were calculate by linear regression (R^2 = 0.9994) (Figure 8). The concentration of Rhodamine B released into solution therefore reflecting the quantity of labeled silica.

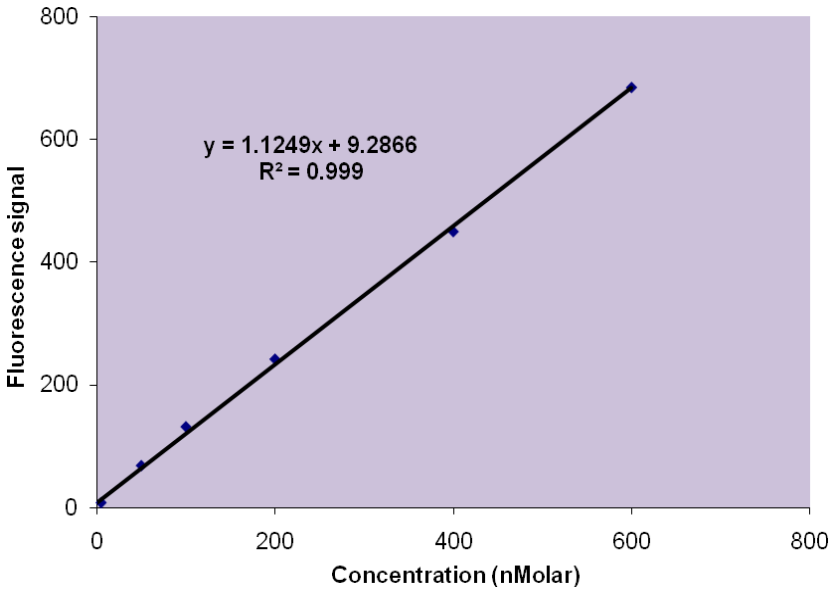

Figure 8 The calibration curve of Rhodamine solutions over the 0-600 nmole dm^{-3} concentration range

appendix E) Quality assurance of the analysis

Spike recovery provides a useful way to check the validity of an analytical method[13]. The digestion and analytical procedures applied to the measurement of arsenic in the colloids were measured using spiked silicas. Two digestion methods; 1) aqua regia and 2) dry ashing with magnesium oxide were examined in this study.

Ca. 20 mg subsamples of mesoporous silica were spiked with 10 μg of arsenic and then digested using the two methods. Samples were analyzed in two or three independent replicates to ascertain reproducibility of analytical results. Assessing spike recovery used EPA method 1632[14]. Sample and spike concentrations were calculated using linear equations ($R^2 = 0.9957$)

$$\% \text{ recovery} = \frac{(\mu g \text{ of spike} - \mu g \text{ of un-spike}) \times 100}{\text{spike}}$$

The spike recoveries were found to be in the range between 80 and 90% for the two methods. Dry ashing with magnesium oxide and wet digestion with aqua regia digestion gave arsenic recoveries on analysis of the resulting digests of 87.44% and 83.32%, respectively. The aqua regia method was therefore used as it more convenient than the dry ashing.

appendix F) Sensitivity and Detection Limit

The word sensitivity is often used in describing an analytical method. The most often used definition of sensitivity is the calibration sensitivity. The calibration sensitivity is the slope of the calibration curve. If the calibration curve is linear, the sensitivity is constant and independent of the concentration. If nonlinear, sensitivity changes with concentration and is not a single value.

The detection limit (DL) is the smallest concentration that can be reported with a certain level of confidence. Every analytical technique has a detection limit. The DL may be expressed as:

$$DL = 3\ SD/slope\ of\ calibration\ curve$$

Linear dynamic range of an analytical method most often refers to the concentration range that can be determined with a linear calibration curve. The lower limit of the dynamic range is generally considered the detection limit.

References

[1] S. Nielsen and E. H. Hansen, *Analytica Chimica Acta* **1997**, *343*, 5-17.

[2] A. G. Howard and C. Salou, *Journal of Analytical Atomic Spectrometry* **1998**, *13*, 683-686.

[3] D. Q. Hung, O. Nekrassova and R. G. Compton, *Talanta* **2004**, *64*, 269-277.

[4] G. Ma, W. B. Xie and R. Feng, *Chinese Journal of Analytical Chemistry* **2006**, *34*, S254-S256.

[5] J. i. M. Bundaleska, T. e. Stafilov and S. Arpadjan, *International Journal of Environmental Analytical Chemistry* **2005**, *85*, 199 - 207.

[6] A. G. Howard, *J. Anal. At. Spectrom.*, **1997**, *12*, 267-272.

[7] Frank L., *Analytical chemical instrumentation, Department of Chemistry*, Umea University, **2003**, p.

[8] R. S. Braman, Foreback, C.C., *Science* **1973**, *182*, 1247.

[9] P. De Kepper, I. R. Epstein and K. Kustin, *Journal of the American Chemical Society* **1981**, *103*, 6121-6127.

[10] R. P. Bagwe, X. J. Zhao and W. H. Tan, *Journal of Dispersion Science and Technology* **2003**, *24*, 453-464.

[11] J. Yan, M. C. Estevez, J. E. Smith, K. Wang, X. He, L. Wang and W. Tan, *Nano Today* **2007**, *2*, 44-50.

[12] Z. Yang, X. S. Kou, W. H. Ni, Z. H. Sun, L. Li and J. F. Wang, *Chemistry of Materials* **2007**, *19*, 6222-6229.

[13] GBC Scientific Equipment Pty Ltd.

[14] E. P. A. 1632, **2001**.